ISSN 1408-7073

RMZ – MATERIALS AND GEOENVIRONMENT

PERIODICAL FOR MINING, METALLURGY AND GEOLOGY

RMZ – MATERIALI IN GEOOKOLJE

REVIJA ZA RUDARSTVO, METALURGIJO IN GEOLOGIJO

RMZ-M&G, Vol. 54, No. 3 pp. 303-438 (2007)
Ljubljana, December 2007

Historical Review

More than 80 years have passed since in 1919 the University Ljubljana in Slovenia was founded. Technical fields were joint in the School of Engineering that included the Geologic and Mining Division while the Metallurgy Division was established in 1939 only. Today the Departments of Geology, Mining and Geotechnology, Materials and Metallurgy are part of the Faculty of Natural Sciences and Engineering, University of Ljubljana.

Before War II the members of the Mining Section together with the Association of Yugoslav Mining and Metallurgy Engineers began to publish the summaries of their research and studies in their technical periodical Rudarski zbornik (Mining Proceedings). Three volumes of Rudarski zbornik (1937, 1938 and 1939) were published. The War interrupted the publication and not until 1952 the first number of the new journal Rudarsko-metalurški zbornik - RMZ (Mining and Metallurgy Quarterly) has been published by the Division of Mining and Metallurgy, University of Ljubljana. Later the journal has been regularly published quarterly by the Departments of Geology, Mining and Geotechnology, Materials and Metallurgy, and the Institute for Mining, Geotechnology and Environment.

On the meeting of the Advisory and the Editorial Board on May 22nd 1998 Rudarsko-metalurški zbornik has been renamed into "RMZ - Materials and Geoenvironment (RMZ -Materiali in Geookolje)" or shortly RMZ - M&G.

RMZ - M&G is managed by an international advisory and editorial board and is exchanged with other world-known periodicals. All the papers are reviewed by the corresponding professionals and experts.

RMZ - M&G is the only scientific and professional periodical in Slovenia, which is published in the same form nearly 50 years. It incorporates the scientific and professional topics in geology, mining, and geotechnology, in materials and in metallurgy.

The wide range of topics inside the geosciences are welcome to be published in the RMZ -Materials and Geoenvironment. Research results in geology, hydrogeology, mining, geotechnology, materials, metallurgy, natural and antropogenic pollution of environment, biogeochemistry are proposed fields of work which the journal will handle. RMZ - M&G is co-issued and co-financed by the Faculty of Natural Sciences and Engineering Ljubljana, and the Institute for Mining, Geotechnology and Environment Ljubljana. In addition it is financially supported also by the Ministry of Higher Education, Science and Technology of Republic of Slovenia.

Editor in chief

Table of Contents – Kazalo

Characterisation of a new dental alloy with high Au content

Karakterizacija nove dentalne zlitine z visoko vsebnostjo Au

Rebeka Rudolf[1], Tjaša Zupančič Hartner[2], Ivan Anžel[1], Primož Mrvar[3], Jožef Medved[3], Dragoslav Stamenković[4]

[1]University of Maribor, Faculty of Mechanical Engineering, Smetanova ulica 17, 2000 Maribor, Slovenia; E-mail: rebeka.rudolf@uni-mb.si, ivan.anzel@uni-mb.si
[2]Zlatarna Celje d.d., Kersnikova ulica 19, 3000 Celje, Slovenia; E-mail: tjasa.zupancic@zlatarnacelje.si
[3]University of Ljubljana, Faculty of Natural Sciences and Engineering, Aškerčeva cesta 12, 1000 Ljubljana, Slovenia; E-mail: primoz.mrvar@ntf.uni-lj.si, jozef.medved@ntf.uni-lj.si
[4]University of Belgrade, Faculty of Stomatology, Rankeova 4, 11000 Belgrade, Serbia; E-mail: dragstam@yubc.net

Received: November 6, 2007 **Accepted:** December 4, 2007

Abstract: The basis for developing a new dental alloy with high Au content is appropriate chemical composition and manufacturing technology. This new Au dental alloy is based on the ternary system of Au-Pt-Zn with a nominal composition of 88.5Au-8.7Pt-1.5Zn-0.5In-0.4Ir-0.3Rh. The alloy was melted and cast in a vacuum-induction melting furnace in Zlatarna Celje. Casting was followed with subsequent thermo-mechanical treatment (procedures of profile and polish milling, thermal treatment) and cutting-off strips to form a regular shape. The heat treatments of Au alloy samples were carried out in a tube furnace under different temperatures, and over different times. Testing of the new Au dental alloy included examining the initial cast, and the different heat treated conditions of the Au alloy. The optical properties of Au-dental alloy were investigated by means of spectrophotometric colourimetry. Finally the test of cytotoxicity of new Au based dental alloys using standard in vitro assays for testing the biocompatibility with establishing new, more sensitive, in vitro tests on cell lines was done.

Izvleček: Osnovo razvoja nove dentalne zlitine z visoko vsebnostjo Au predstavljata pravilna določitev kemijske sestave in tehnologije izdelave. Nova dentalna zlitina temelji na ternarnem sistemu of Au-Pt-Zn z nominalno kemijsko sestavo 88,5Au-8,7Pt-1,5Zn-0,5In-0,4Ir-0,3Rh. Izdelava dentalne zlitine je potekala s pretaljevanjem zelo čistih komponent v vakuumski indukcijski peči v Zlatarni Celje. Temu je sledilo odlivanje taline v ustrezno formo, postopek termo-mehanske obdelave odlitka in razrez zlitine v ustrezno obliko. Toplotna obdelava je bila izvedena pri različnih temperaturah in za različne čase. Testiranje dentalne zlitine je vključevalo določitev lastnosti začetnega stanja in stanja po različnih toplotnih obdelavah. Optične lastnosti dentalne zlitine so bile raziskane s spektro-fotometrično kolorimetrijo. Na novi Au dentalni zlitini so bili narejeni še testi citotoksičnosti z uporabo standarda in vitro analize za testiranje biokompatibilnosti z uvajanjem novih, bolj občutljivih in vitro testov na celični liniji.

Key words: dental alloy, characterisation, microstructure, properties
Ključne besede: dentalna zlitina, karakterizacija, mikrostruktura, lastnosti

INTRODUCTION

Gold alloys have been used in dentistry, not only because their gold colour is preferred, but also because they have extremely high chemical stability in the mouth, plus several desirable mechanical properties such as high strength, ductility and elasticity[1]. They contain five or more elements, the essential components of the alloys being gold and platinum. The main specific physical requirements for those dental alloys used for porcelain fused to metal (PFM) technique are: a) a melting range starting at no less than 1100 °C, b) a coefficient of thermal expansion closely matched to that of high-fusing-point dental porcelain (960-980 °C) developed for the PFM technique – the values for these coefficients should stay within the ranges $12.7\text{-}14.8\times10^{-6}$ K^{-1} for the alloys, and $10.8\text{-}14.6\times10^{-6}$ K^{-1} for porcelain, c) minimal creep or sag when firing the porcelain, d) good wetting of alloy by the porcelain, e) tensile strength about 600 N/mm^2 and yield strength about 550 N/mm^2, f) hardness about 180 HV and g) elongation about 10 %. On the other hand, gold alloy for casting would have a melting range as low as possible whilst an Au alloy for porcelain veneers would have a solidus temperature around 100 °C higher than the firing temperature of the used porcelain, in order to ensure that the cast framework does not sag during firing.

Among various types of alloys for PMF restorations, the Au-Pt-Zn-based high noble alloys have the advantage of being around for some considerable time. They are part of clinical experience and are extremely successful[2]. The bond between the ceramic and the metal, in particular, is very strong and highly reliable[3]. Accordingly for our new Au dental alloy we selected a combination of the following alloying elements: Au, Pt, Zn and traces of: Ir, In, Rh. We wanted to keep all the favourable properties of gold and to improve its inadequate strength and hardness by Pt, Zn and Ir alloying[4]. When considering the formulations of Au-Pt-Zn-based high noble alloys for porcelain bonding, high Au contents are required to ensure biocompatibility and large Pt concentrations are necessary to sufficiently raise the melting range above the porcelain firing temperature to prevent distortion during porcelain application[2],[3]. By the addition of Zn we wanted to lower the surface tension of the liquid alloy, thus enabling the material to be cast into very thin sections. The zinc also serves as a dezoxidant, together with Ir and In. This is because of their affinity to oxygen, being the first to react with it and thus, protect other metals from oxidation. Other micro-alloying metals are added also to form a thin oxide film at the surface of the alloy during the porcelain firing cycle[5],[6]. This new alloy has no Ag which easily reacts with oxygen, gives porous castings, forms sulphur compounds, and can lead to tarnishing and ceramic discoloration (greening). This new Au alloy also has no palladium or copper. Pd reacts with hydrogen; it gives porous castings and can cause allergic reactions. Cu gives reddish colour to an alloy, it reacts with oxygen and forms copper-oxide on the alloy's surface, which can cause ceramic discoloration. These are the reasons for the selected chemical composition of the alloy: about 88.5 w.% Au, 8.7 w.% Pt, 1.5 w.% Zn, and 1.3 w.% of different micro-alloying elements (Ir, In < 0.5 w.%, Rh). Micro-alloying elements are necessary for precipitation hardening; small additions of iridium can reduce the grain size of the alloy, while the presence of rhodium enhance both strength and colour[4].

Testing of our new Au dental alloy included examining the solution treated and heat treated alloy. Measurements of hardness were done according to standard 6507-1:1998, and static tensile testing was performed for determination of the mechanical properties.

Dental alloys used in dentistry must also have good biocompatibility which concerns the biological acceptability and biological performance of those materials used in dentistry. Moreover, biocompatibility has been equated with the lack of a significant interaction between materials and tissues. It has been documented *in vitro* and *in vivo* that metallic dental devices release metal ions, mainly due to corrosion. These metallic components may be locally and systemically distributed and could play a role in the aetiology of oral and systemic pathological conditions. The quality and quantity of the released cations depend upon the type of alloy and various corrosion parameters. Prosthodontic restorations remain in an oral environment for many years and are exposed to the corrosive influences of saliva, temperature changes, pH changes, etc. Metals in electrolyte (saliva) release ions can lead to oxidative processes which tarnish and precipitate the metal in the surrounding tissues[7]. Until now no general correlation has been observed between alloy nobility and corrosion. Dental cast alloys very often cause local adverse tissue reactions such as gingivitis and periodontitis, due to the release of metal ions into the surrounding microenvironment. Their cytotoxic effects are well documented using different *in vitro* and *in vivo* assays. This was the reason why less cytotoxic or non-cytotoxic precisious noble-metal alloys with a high content of gold (Au) and platinum (Pt) although more expensive, are introduced in dental practice.

In this study, only the parts of *in vitro* biocompatibility tests were performed. Within this study we tested the cytotoxicity of our new Au-Pt-Zn dental alloys using standard *in vitro* assays and to establish new, more sensitive, (*in vitro*) tests on cell lines.

In addition to the extremely successful clinical experiments, the attraction of Au-Pt-Zn-based high noble alloys is with the yellow colour. Nowdays it is suggested that colour control must be taken into account as one of the criteria when manufacturing dental gold alloys for crown and bridge metal-ceramic restorations. It has been claimed that a high gold content means that the alloys impart a warm, dentin-like colour to the ceramics. Because of this feature, there is a complete elimination of gingival 'black line disease' associated with traditional metal-ceramic fixed restorations. The optical properties of our new Au-dental alloy were investigated by means of spectro-photometric colourimetry.

EXPERIMENTAL WORK

The meltings of very pure components (Au=99.99 w.%, Pt=99.99 w.%, Zn=99.99 w.%, In=99.99 w.%, Rh=99.99 w.%, Ir=99.99 w.%) were performed at Zlatarna Celje d.d. in vacuum-induction melting furnace at vacuum $p=10^{-2}$ mbar and temperature T=1400 °C. Casting of the melted alloy was performed under argon pressure above 1.03 bar in a metal cast with diameter 8 mm[8]. The alloy ingot was followed with subsequent thermo-mechanical treatment (procedures of profile and polish milling, thermal treatment) and cutting-off the strip to form a regular shape. Alloy specimens were first solution-treated at 950 °C for 30 min and quenched using water. The solution treated samples were then subjected to heat treatments which were carried-out in a tube furnace (Figure 1) at selected temperatures (400 °C, 450 °C and 500 °C) for different times (10 min, 20 min, 30 min)

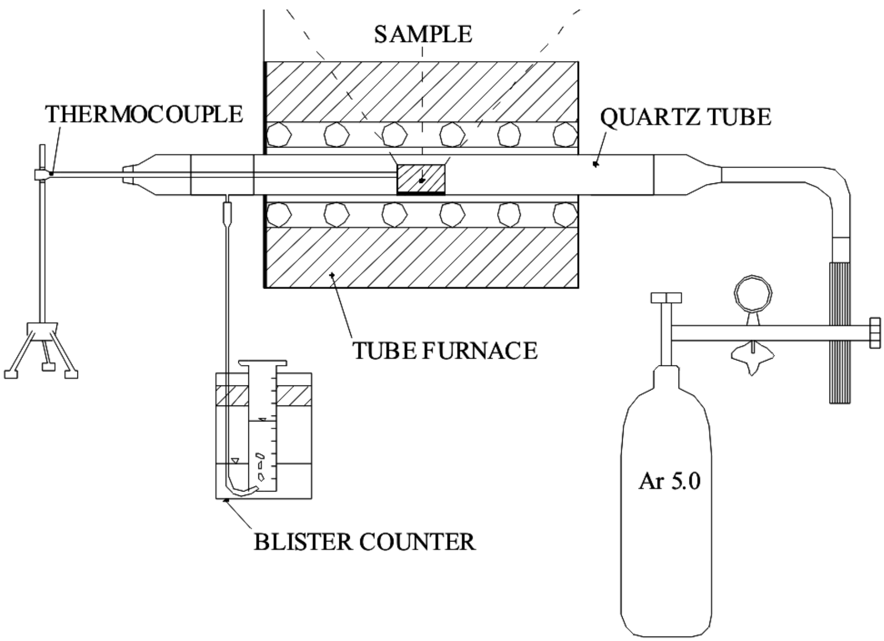

Figure 1. Schematic presentation of appliance
Slika 1. Shematska predstavitev naprave

and, finally, slowly cooled to room temperature.

Testing of the new Au dental alloy included examining the solution treated and heat treated condition. Measurements of hardness were carried out according to standard 6507-1:1998, with the Vickers test on the Zwick 3212 microhardness measurement device. For testing the samples, we used applied load F=49 N, according to standard. For every sample, we performed 12 measurements.

The static tensile testing using tensile device Zwick/Roell ZO 10 was performed for determining the mechanical properties. Measurements of mechanical properties for the all states were performed in one series with 6 samples. The research conditions, as well as the shapes and dimensions of the tensile test tubes were according to standard SIST EN 1562:2000 (chapter 6.2). Tests were performed under constant speed of increasing deformation v=1.5 mm/min. Tensile test tubes were cast and then cut-out from the cylinder shaped casting (diameter 3 mm) - see Figure 2!

Figure 2. Tensile test tube of the dental alloy with high Au content

Slika 2. Natezne epruvete iz dentalne zlitine z visoko vsebnostjo Au

Measurements of the thermal expansion coefficient (CTE) was performed in one series which consisted of 3 samples, on the Mechanical Dilatometry device (at the Chair for Engineering Materials at Faculty of natural sciences and engineering, University of Ljubljana).

For the microscopic analysis, dental alloy plates were ground and then polished using different polish pastes. The samples were, after metallographic preparation, cleaned in an ultrasound vibration cleaning device (medium alcohol). Those specimens for optical microscopy were then etched in H_2O-H_2O_2-$FeCl_3$ solution for 2 min at room temperatures. Concurrently those polished specimens for electron microscopy were put in the chamber of the Sirion NC 400 scanning electron microscope, with vacuum of 10^{-10} mbar. Sirion FEG is a high-resolution scanning electron microscope with field emission gun (FEG) which enables the observation and analysis of nano-scale particles. Microscopic analysis includes examination of the polished surface and qualitative and quantitative micro-chemical analysis at characteristic points on the dental alloy. We observed surfaces using an electron beam voltage at 30 kV, and over different working distances (6.5 mm, 7.2 mm, etc.).

For the biocompatibility (cytotoxicity) test, disk-shaped specimens (4 mm × 4 mm and 10 mm × 10 mm) from Au dental alloys were prepared using a conventional lost - wax technique which simulates the preparation of the cast metal alloy for clinical use. The disks were polished and rinsed in distilled water. After cleaning by sonification for 5 minutes, the samples were autoclaved. Large disks were cultivated in a medium for cell cultures (RPMI medium + 10 % fetal calf serum) for 8 days, in order to test the cytotoxic effect of metals released from alloys (alloy-media), whereas small disks were used for testing the direct cytotoxic effect. Controls consisted of inert glass samples, pre-treated as test samples. Standard cytotoxicity assays were performed on L929 fibroblast cells according to ISO standards: ISO 10993-5; 1992(E) and ISO 7405; 1997(E). These procedures included morphological examinations of cells cultivated with dental alloys for 24h, and quantification of cell death by Tripan blue dye exclusion. In addition, the succinic dehydrogenase (SDH) activity was measured using the MTT assay. Optimization of these assays included prolonged incubation of cells with test samples for 7 days or a combination of direct and indirect (alloy-media) effects. New assays included proliferation of rat spleen lymphocytes in the presence of concanavalin A (Con A), and different concentrations of alloy - media, measured by ^{3}H-thymidine incorporation, and apoptosis of thymocytes and splenocytes using morphological examinations, and staining with propidium iodide or merocyanine 540.

For spectrophotometric colourimetry, the polished samples of new Au dental alloy were mounted on a disk shaped specimen (10 mm × 10 mm × 10 mm), and spectral reflectance data under the CIE standard illuminant D65 were collected at 10 nm intervals (D65/10) in wavelengths ranging from 400 to 700 nm. These measurements were done on a Spectraflash SF 600 Plus spectrophotometer and repeated 3 times, rotating the sample by 120 degree each time. Three-dimensional colour coordinates lightness L^*, chromaticity indices a^* (red green direction) and b^* (yellow-blue direction) in the CIE $L^*a^*b^*$ system, and chroma, C^* and hue angle h in the CIE L^*C^*h system were obtain to specify the

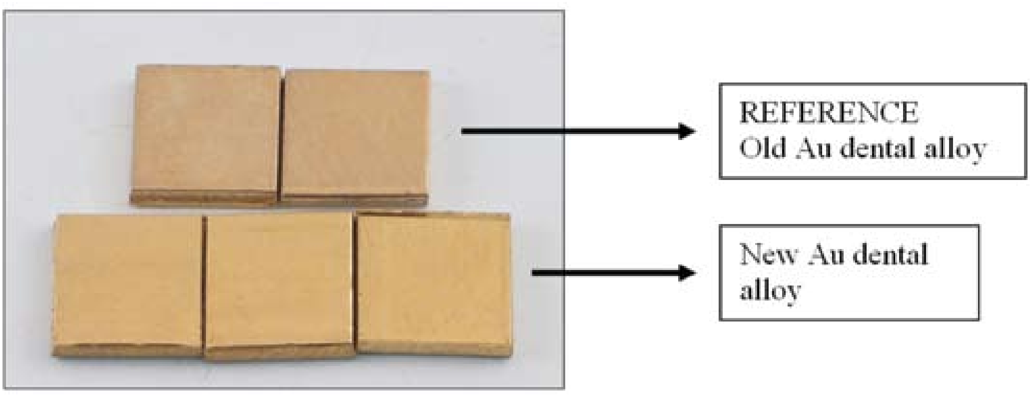

Figure 3. Old and new Au-Pt-Zn alloy specimens for testing optical properties
Slika 3. Vzorci iz stare in nove Au-Pt-Zn zlitine za testiranje optičnih lastnosti

Table 1. Results of hardness measurments [in HV5]
Tabela 1. Rezultati meritev trdot [v HV5]

Solution treated state : **125**		
Heat treated at 400 °C for 10 min: **145**	Heat treated at 400 °C for 20 min: **170**	Heat treated at 400 °C for 30 min: **175**
Heat treated at 450 °C for 10 min: **160**	Heat treated at 450 °C for 20 min: **180**	Heat treated at 450 °C for 30 min: **180**
Heat treated at 500 °C for 10 min: **160**	Heat treated at 500 °C for 20 min: **168**	Heat treated at 500 °C for 30 min: **170**

sample colour. The CIELAB colour difference parameter DE^* between two samples was evaluated. For reference-sample 1 used a comparatively old Au dental alloy with nominal composition Au: 85.9 w.%, Pt: 11.7 w.%, Zn 1.1 w.% and about 1.3 w.% micro-alloying elements (In, Ir, Rh) and for sample 2 a new Au dental alloy with nominal composition was used: about 88.5 w.% Au, 8.7 w.% Pt, 1.5 w.% Zn, and 1.3 w.% of different micro-alloying elements (Ir, In, Rh) see Figure 3.

Results

The average results of the hardness measurement are presented in Table 1 for each alloy state. For the solution-treated specimen, the average hardness value was about 125 HV. It can be concluded that the alloy a solution-treated state had very low hardness. On the other hand there were different heat treated samples where hardness began to increase and reached the maximum value at isothermal holding by 450 °C for 20 min and also 30 min (the results in Table 1 are grey coloured).

The average results of the mechanical properties measurements (yield strength at 0.2 % strain, tensile strength and elongation) for all tensile test tubes are gathered in Table 2. With respect to the results for hardness, we can conclude that this optimal mechanical property also applied the samples of Au dental alloy which had been heat treated at 450 °C for 20 min (grey coloured). These samples fulfil, after heat treatment, all the necessary standards regarding mechanical properties and hardness.

Table 2. The average value of the mechanical properties measurements
Tabela 2. Povprečne vrednosti izmerjenih mehanskih lastnosti

	$R_{p0.2}$ [N/mm²]	R_m [N/mm²]	A [%]
Initial hom. state	340	390	15
HT 400 °C, 10 min	450	520	9
HT 400 °C, 20 min	470	530	13
HT 400 °C, 30 min	500	560	12
HT 450 °C, 10 min	520	580	10
HT 450 °C, 20 min	550	610	9
HT 450 °C, 30 min	550	610	10
HT 500 °C, 10 min	520	570	10
HT 500 °C, 20 min	540	600	10
HT 500 °C, 30 min	550	600	13

Measurements of the thermal expansion (CTE) coefficient have shown that the average value of CTE (25-600 °C) for Au-Pt-Zn alloy is about 14.45×10^{-6} K^{-1}.

The results of the chemical spectral analysis of new Au dental alloy are present in Table 3 in w.% or in at.%.

Standard cytotoxic tests showed that Au-Pt-Zn alloy has not cytotoxicity after short term (24 h) incubation of L929 cells. Prolonged incubation of cells with dental alloys showed that Au-Pt-Zn decreased the SDH activity in L929 cells by only 15.1 ± 6.2 % (the difference was not statistically significant) compared to control glass material. Similar results were obtained using the combination of alloys and alloy-media. The Au-Pt-Zn alloy did not induce apoptosis of rat thymocytes and splenocytes during a 24 h assay. However, alloy - media significantly suppressed the proliferation of rat splenocytes in the culture. Inhibition depended on the concentrations of alloy media. Au-medium was less suppressive (26.3 ± 4.6 %; $p < 0.05$ compared to glass-medium). When examining apoptosis in cultures of Con A-stimulated splenocytes, we observed apoptosis of splenocytes incubated with Au-medium at level 49.1 ± 3.0 % ($p > 0.05$; NS).

Figure 4 shows a spectral-reflectance curve and Figure 5 represents the chromaticity a^*, b^* indices of CIELAB colour space for the new Au-Pt-Zn against comparable old alloys. Table 4 shows the comparison of colour coordinates for the reference old Au-Pt-Zn alloy and the new Au-Pt-Zn alloy, and their colour difference ΔE^*.

Discussion

The present studies of heat treatment's influence on the mechanical properties of a new Au-Pt-Zn alloy show improvement in hardness and tensile strength during processing. The results indicate that the specimen which was heat treated for 20 min at 450 °C after solid solution treatment had maximum hardness and tensile strength. The reasons for these conclusions are the chemical composition of the Au-Pt-Zn alloy, microstructure formation

Table 3. The average value of the chemical spectral analysis of Au-Pt-Zn dental alloy
Tabela 3. Povprečne vrednosti spektralne kemijske analize Au-Pt-Zn dentalne zlitine

Element	**Weight %**	**Atomic %**
Zn K	1.55	4.48
Rh L	0.39	0.63
In L	0.49	0.89
Ir L	0.39	0.39
Pt L	8.67	8.42
Au L	88.51	85.19
Totals	100.00	100.00

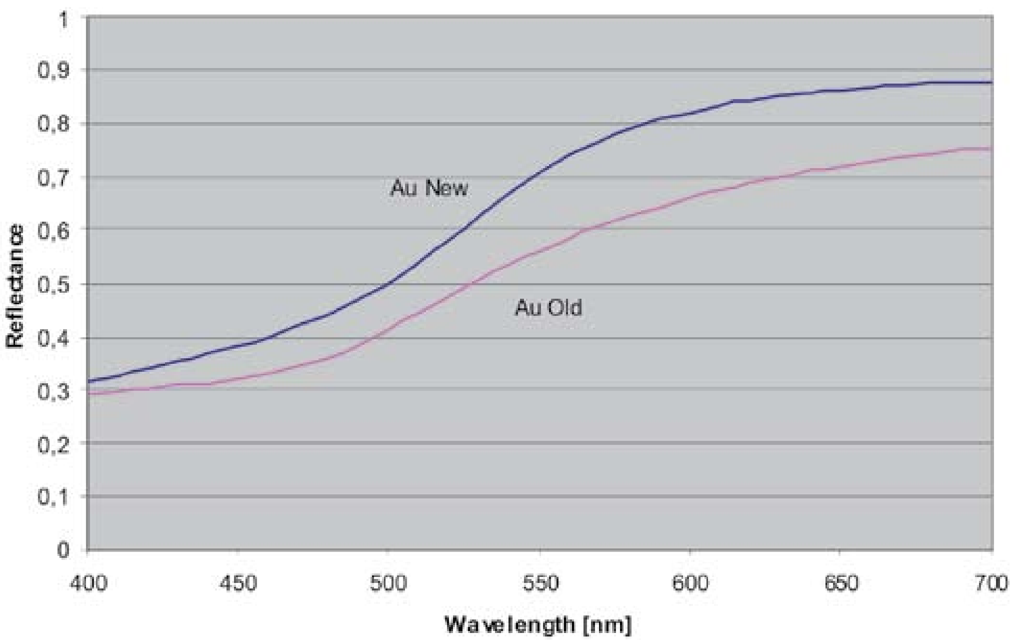

Figure 4. Spectral reflectance curves for both Au-Pt-Zn alloys
Slika 4. Refleksijska krivulja za obe Au-Pt-Zn zlitini

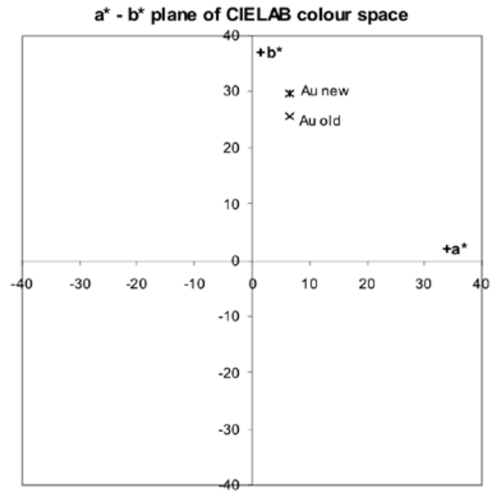

Figure 5. a^* and b^* plane of CIELAB colour space
Slika 5. a^* and b^* ploskvi CIELAB barvnega prostora

Table 4. Colour coordinates (standard illuminant D65/10)
Tabela 4. Barvne koordinate (standardna razsvetljava D65/10)

Alloy	L^*	a^*	b^*	DE^*	Batch is
Reference: old Au-Pt-Zn	78.97	6.64	25.62		
New Au-Pt-Zn	86.06	6.43	29.62	8.137	yellow

and, consequently, the strengthening effect which occurred during heat treatment.

The Au-Pt-Zn alloy is characterized by the ternary Au-Pt-Zn system, which has 5 important marginal phase diagrams: Au-Pt, Au-Zn Pt-Zn Pt-In and Au-In.

The Au-Pt binary phase diagram is characterized by the presence of three metastable phases (Au_3Pt, AuPt and $AuPt_3$)[9]. The existence of Au_3Pt superlattice in alloys is possible up to 40 at.% Pt after severe cold working, followed by annealing at 900 °C. Other diffraction studies[10] of 10 and 25 at.% Pt alloys showed that the Au_3Pt, AuPt and $AuPt_3$ phases materialize as meta-stable phases during the heating of a two-phase mixture of Au and Pt. The Au-Pt system could also contain a miscibility gap (Au) + (Pt), the critical point of which is about 61 at.% Pt and at 1260 °C. Miscibility gap could occur in the solid solution field, as well as the controversial form of the liquidus and solidus boundaries.

The Au-Zn system is characterized by more reactions: five congruent, four peritectoid, three peritectic, two eutectic, and one eutectoid and martensitic. There are four well-known intermediate phases (α_3, α_1, α'_2 and α_2) in the composition range between 10 and 30 at.% Zn, the intermetallic compound Au_5Zn_3 with unknown homogeneity[11], and many other phases. Maximum solid solubility is 33.5 at.% Zn in solid solution of Au and inversely 7.5 at.% Au in solid solution of Zn.

A complete Pt-Zn binary system is unavailable. The assessed diagram is provisional and shows the low-temperature regions[12] with the modifications within the range of the intermediate phase Pt-Zn. The assessed Pt-Zn system is characterized by two peritectoid, two eutectoid, and two peritectic reactions.

The assessed In-Pt phase diagram is based on[13] and showed InPt as line compound, forming peritectoidally at 944 °C and stable down to at least 0 °C. InPt is one of the most conspicuous phases at low temperatures, if it exists, and has peritectoid formation. The In-Pt phase diagram is characterized by many other reactions. Pt_3In[14] which has perictectic formation is important phase for the Au-Pt-Zn system used in dental alloys. The maximum solubility of In in (Pt) is 11 at.% at 1458 °C.

There are many different phases in the binary phase diagram Au-In. The known phase diagram is based on the work of[15]. The maximum solubility of In in Au is of 12.7 at.% at 680 °C, which is only 0.2 at.% more than the solubility of In at the peritectic point. No evidence of solid solubility for Au in (In) was detected.

Detailed microstructural examination of the solution and heat treated of the Au-Pt-Zn alloy revealed the existence of two main components: the base matrix which is identified as an Au-rich α_1-phase, and an other phase, which appears to be small particles (1-8 μm) and is known as a Pt-rich α_2 -phase[6]. These phase assumptions were confirmed by nano EDX analysis (Figure 6). The gained EDX results show

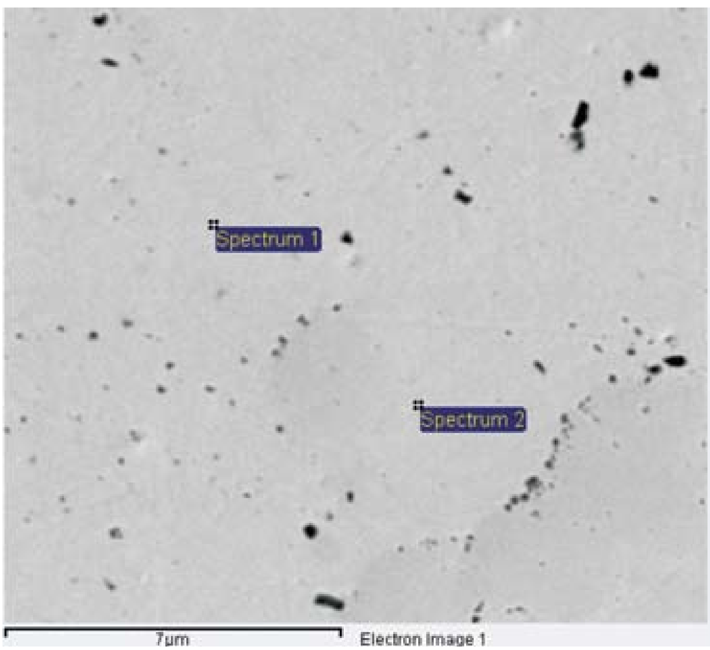

Figure 6. Electron micrograph and the typical places of EDX analysis for the Au-Pt-Zn alloy
Slika 6. Elektronska slika in tipično mesto za EDX analizo Au-Pt-Zn zlitine

that the α_1-phase has about 87-93 w.% Au, 4-8 w.% Pt and approximately 1.2 w.% Zn, 1.22 w.% Ir, In and Rh are traceable (< 1 w.%). On the other hand, the α_2 -phase contains about 60-75 w.% Pt, 20-30 w.% Au, approximately 4.12 w.% Rh, In and Zn are in traceable, while in this phase no Ir was detected.

Optical microscopy shows that the α_1-phase has approximately equal sizes in the solution and heat-treated states (Figure 7). Examinations only showed that the microstructure became homogeneous with the performing of heat treatment. On the other hand, no big difference was found in grain size during the α_2-phase between the two different states. It was only discovered that the number and density of the α_2-phase increased when the performing heat treatment. α_2-phase (in the form of small particles) is located at the grain boundaries and within the grains. We envisage that optimal value was achieved by the Au-Pt-Zn sample which had the best mechanical properties and hardness and was heat treated at T=450 °C for t=20 min after solution treatment.

The immiscibility is well-known[9] for Au-Pt system in a solid state. After casting, a solid solution nucleates from the melt. During cooling the alloy enters the miscibility gap separating into Au-rich and Pt-rich phases. With heat treatment at 950 °C the alloy enters the single phase zone between the miscibility gap and the solidus line. At this temperature, a solid solution

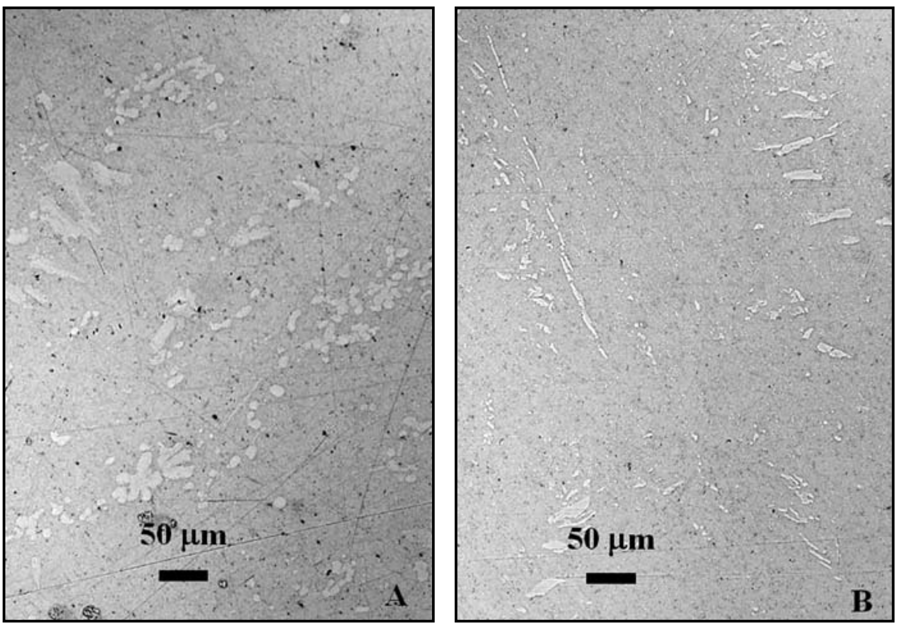

Figure 7. The optical microstructure of Au-Pt-Zn alloy after: A) solution treatment at 950 °C for 30 min and B) heat treatment at 450 °C for 20 min

Slika 7. Optična mikrostruktura Au-Pt-Zn zlitine po: A) raztopinskem žarjenju pri 950 °C za 30 min in B) toplotni obdelavi pri 450 °C za 20 min is thermodynamically stable with random distribution of the atoms within the crystal lattice[6]. The inhomogeneous texture formed after casting therefore is thermodynamically unstable. Owing to the high energy, the atoms could diffuse in the crystal lattice and be forced to distribute randomly on the atomic sites. Subsequently, the alloy became homogeneous. Then during the cooling process, the homogenized microstructure kept in balance. But a small amount of the Pt-rich phase could still precipitate from the solid solution, depending on the cooling rate. Thus, all the specimens showed a microstructure composed of, not only α_1-phase, but some α_2-phase too. In the solution treatment process at 950 °C combined with water quenching, many crystal defects remained and supersaturated solid solution was achieved. After this treatment the alloy was thermodynamically in a metastable state. When metastable, specimens were put under different heat treatment temperature they were subjected to isothermal treatment, precipitation reactions occurred driven by diffusion. Many fine precipitates of α_2-phase appeared within the grains, this lead to hardening of the Au-Pt-Zn alloy.

The optical properties investigations show that our new Au-Pt-Zn alloy has yellow colour compared with the old alloy with less Au content. It seems that the difference of Au at value 2.6 w.% for total chemical composition of the alloy has an influence on the colour difference parameter DE^* cca 8.1. Since the DE^* value of 1.0 is said to be just discernible by the average human eye[16], the colour of the new dental alloys may be very well-distinguished from that of the referenced old alloy. With the analysis of spectral reflectance curves for both Au-Pt-Zn alloy it is shown, that the new Au-Pt-Zn alloy has a higher reflectance of about 10 % in those wavelengths ranging from 400 to 700 nm. On the other hand in the CIE $L^*a^*b^*$ system chromaticity indices a^* for both alloys is equally comparable, while the indice b^* of the new alloy has a higher value for about 4 units. This is the reason that new Au-Pt-Zn alloy is yellower than the old. The yellow colour on the surface plays an important role in developing the restoration aesthetics[17]. Although the alloy is covered with successive layers of porcelain, light travels through the porcelain and is reflected back out. If the surface of the alloy is silver (white) in colour then the entire light spectrum is reflected out. This includes the blue region which, when passing through the pink gum tissue, produces a dark unsightly outline. Au-Pt-Zn dental alloy is opaque and highly reflective, the perceived colour is determined by wavelength distribution of the radiation, which is reflected and not absorbed[16]. Material possessing a much higher reflectivity for the low-energy end of the visible spectrum (red and yellow light) than for the other parts of the spectrum will have a reddish to yellow colour[17].

Conclusions

With the results of our examinations, we can conclude that the new Au-Pt-Zn dental alloy from Zlatarna Celje fulfils all the requested standards in the sense of mechanical properties and hardness, optical properties, and biocompatibility. The obtained results for this alloy are: $R_{p0.2}$=550 N/mm^2, R_m=610 N/mm^2, A=9 %, 180 HV, CTE=14.45×10-6 K^{-1}.

The analyses of different heat-treated states show that the above-mentioned mechanical properties and hardness of the Au-Pt-Zn alloy could be reached with combinations of heat treatment for 20 min at 450 °C and slowly cooling after that, if the alloy was solution treated at 950 °C for 30 min and water quenched.

The microstructure of the Au-Pt-Zn alloy consists of two phases: α_1-phase rich in Au and α_2-phase rich in Pt. It was found that the number and density of α_2-phase increased by the performing of heat treatment.

The α_2-phase, in the form of small particles, is the main factor for the strengthening mechanism in our Au-Pt-Zn alloy.

The optical property investigations show that our new Au-Pt-Zn alloy has yellower colour compared to the old alloy with less content of Au. It seems that the difference of Au at value 2.6 w.% in the total chemical composition of the alloy influences on the colour difference parameter DE* cca 8.1, which may very clearly be distinguished from that of the referenced old alloy.

The Au-Pt-Zn alloy did not show cytotoxicity when using standard short-term *in vitro* assays on L929 cell and prolonged cell incubation did not revealed any adverse effect on the L929 cells manifested by reduced SDH activity. The Au-Pt-Zn alloy did not show any pro-apoptotic effect on rat thymocytes and splenocytes in culture, and significantly decreased Con A - stimulated proliferation of these cells.

Acknowledgments

Zlatarna Celje d.d. is working on the development of a new high Au content dental alloy with the support of associates from the Institute of Materials Technology, Faculty of Mechanical Engineering, University of Maribor; School of Dentistry, University of Belgrade and Zlatarna Celje d.o.o. Belgrade.
This paper is part of a Slovenian applied project no. L2-7096, Bilateral project SLO/SR BI-CS/06-07-031 and EUREKA Programme E!3555 DEN-MAT. The authors gratefully acknowledge the Ministry of Higher Educations, Science and Technology and Slovenian Research Agency.

POVZETEK

Karakterizacija nove dentalne zlitine z visoko vsebnostjo Au

Na osnovi rezultatov naših raziskav lahko zaključimo, da nova Au-Pt-Zn dentalna zlitina Zlatarne Celje ustreza zahtevanim standardom v smislu mehanskih lastnosti in trdote, optičnih lastnosti ter biokompatibilnosti. Dobljeni rezultati za to zlitino so: $R_{p0.2}$=550 N/mm^2, R_m=610 N/mm^2, A=9 %, 180 HV, CTE=14.45×10-6 K^{-1}.

Analiza stanj po različnih vrstah toplotne obdelave Au-Pt-Zn zlitine je pokazala, da zgoraj omenjene mehanske lastnosti in trdoto dosežemo s kombinacijo toplotne obdelave pri 450 °C za 20 minut ter počasnim ohlajanjem do sobne temperature, potem ko je zlitina raztopinsko žarjena pri 950 °C za 30 minut in gašena v vodi.

Mikrostruktura Au-Pt-Zn dentalne zlitine je sestavljena iz dveh faz: α_1-faze bogate z Au in α_2-faze bogate s Pt, pri čemer število in gostota α_2-faze naraščata s toplotno obdelavo.

Delci α_2-faze so v obliki manjših delcev in so odgovorni za mehanizem utrjanja v Au-Pt-Zn zlitini.

Raziskave optičnih lastnosti nove Au-Pt-Zn zlitine so pokazale, da ima bolj rumeno barvo v primerjavi s staro zlitino, ki vsebuje manj Au. Še več, ugotovljeno je bilo, da razlika 2,6 m.% Au v skupni kemijski sestavi bistveno vpliva na razliko v barvnem parametru DE*, ki znaša 8,1 v primerjavi glede na referenčno staro zlitino.

Au-Pt-Zn zlitina ne kaže citotoksičnosti potem, ko je bila v okviru standardnega hitrega *in vitro* testa izpostavljena L929 celicam. Tudi rezultati testov s podaljšano celično inkubacijo niso pokazali nobenega nasprotnega efekta na L929 celicah, ki bi se posledično odražali na zmanjšani SDH aktivnosti. Au-Pt-Zn zlitina tudi nima proaptotičnega efekta na timocitih in splenocitih celičnih kultur podgan in bistveno zmanjšuje Con A stimulirano profileracijo teh kultur.

References

[1] Williams, D. (1990): *Medical & Dental materials*. Oxford OX3, England.

[2] R. van Noort (1994): *Introduction to Dental Materials*. Mosby, London, pp. 219-221.

[3] German, R. M. (1980): *Journal of Dental Research*.;Vol. 59.

[4] Fischer, J. (2002): Effect of small additions of Ir on properties of a binary Au-Ti alloy. *Dental Materials*.; Vol. 18, No. 4, pp. 331-335.

[5] Knosp, H., Holliday, R.J., Corti, C.W. (2003): *Gold Bulletin*.; No. 36, pp. 93-102.

[6] Wang, J. N., Liu, W. B. (2006): A Pd-free high gold dental alloy for porcelain bonding. *Gold Bulletin*.; Vol. 36, No. 3.

[7] Hornez, J. C., Lefvre, A., Joly, D. and Hildebrand H.F. (2002): Multiple parameter citotoxicity on dental alloys and pure metals. *Biomolecular Engineering*.; Vol. 19, pp. 103-117.

[8] Križman, A., Rudolf, R., Albreht, B. (2006): Melting and casting of dental alloys with high Au-content. *Livarski vestnik*.; Vol. 53; No. 1, pp. 19-31.

[9] Grube, G., Schneider, A., Esch, U. (1951): *Festschrift aus Anlass des 100-Jahrigen Jubilaums*. W.C. Heraeus G.m.b.H. pp. 20-42.

[10] Singhal, S. P., Herman, H. and Hirvonen, J.K. (1978): *Appl. Phys*.; Lett. 32(1), pp. 25-26.

[11] Ipser H. and Krachler, R. (1988): *Scr. Metall*.; Vol. 22 (10), pp. 1651-1654.

[12] Khan, Y., Murty, B.V.R. and Schubert, K., (1970): *J. Less-Common*

Met.; Vol. 21, pp. 293-303.

[13] ELLNER, M. (1978): *J. Less-Common Met.*; Vol. 60, P15-P39.

[14] SHIRAISHI, T., OHTA, M. (2002): *J. Mater-Sci. Mater. Med.*; Vol. 13, pp. 979.

[15] ANSARA, I. and NABOT, J. P. (1988): *Thermochim. Acta.*; Vol. 129, pp. 89-97.

[16] CALLISTER, W. D. (1985): *Materials Science and Engineering: An Introduction.* John Willey&Sons, Inc., New York, pp. 535-536.

[17] SAEGER, K. E. and RODIES, J. (1977): *Gold Bulletin.*; Vol. 10.

Characterization of Cu-Al-Ni melt-spun ribbons using a focussed ion beam (FIB)

Karakterizacija hitrostrjenih trakov zlitine Cu-Al-Ni z uporabo fokusiranega ionskega curka

Franc Zupanič[1], Elfriede Unterweger[2], Albert C. Kneissl[2], Ivan Anžel[1], Gorazd Lojen[1]

[1]University of Maribor, Faculty of Mechanical Engineering, Smetanova ulica 17, SI-2000 Maribor, Slovenia; E-mail: franc.zupancic@uni-mb.si, ivan.anzel@uni-mb.si, gorazd.lojen@uni-mb.si
[2]Montanuniversität Leoben, Lehrstuhl für Metallographie, Franz-Josef-Strasse 18, A-8700 Leoben, Austria; E-mail: elfriede.unterweger@unileoben.ac.at, kneissl@unileoben.ac.at

Received: October 1, 2007 **Accepted:** November 26, 2007

Abstract: This work investigates the possibilities for applying a focussed ion beam (FIB) for the metallographic preparation and characterization of Cu-Al-Ni melt-spun ribbons. Two alloys were selected for this reason: CuAl13Ni4 and CuAl15Ni4. The microstructure of the first alloy was fully martensitic and the microstructure of the second consisted of two phases: martensite and γ_2. It was discovered that with FIB-etching the microstructures of both alloys can be clearly revealed on polished cross-sections of the melt-spun ribbons, as well as on their wheel-side and air-side surfaces. However, better results were obtained when the etched surface was smoother, and finer details were visible when using smaller ion currents. In addition, a study was made into the influence of platinum deposition on the quality of 3D-cross sections. It was found that Pt-deposition is necessary when the edge of the trench should be straight and sharp, and the surface of the 3D cross-section smooth. However, in this case, the microstructure of the ribbons free surface cannot be seen.

Izvleček: V tem delu smo raziskali možnosti uporabe fokusiranega ionskega curka (FIB) pri metalografski pripravi in karakterizaciji hitro strjenih zlitin Cu-Al-Ni. Izbrali smo dve zlitini: CuAl13Ni4 in CuAl15Ni4. Mikrostruktura prve zlitine je bila v celoti martenzitna, medtem ko je bila mikrostruktura druge zlitine sestavljena iz dveh faz: martenzita in γ_2. Ugotovljeno je bilo, da lahko pri jedkanju z ionskim curkom odkrijemo mikrostrukturo tako na poliranih prečnih prerezih trakov, kot tudi na obeh prostih površinah hitrostrjenih trakov. Mikrostruktura se je boljše odkrila, če je bila raziskana površina bolj gladka, medtem ko smo lahko razločili drobnejše mikrostrukturne

Scientific paper

sestavine pri uporabi manjših ionskih tokov. Poleg tega smo študirali tudi vpliv nanosa platine na kakovost 3D-prečnih prerezov. Ugotovili smo, da je nanos platine smiselno uporabiti, če želimo zelo ravne in ostre robove reza ter gladko površino prečnega reza, vendar pa v tem primeru ne moremo videti mikrostrukture proste površine.

Key words: focussed ion beam (FIB), metallography, melt-spinning, shape memory alloy, Cu-Al-Ni

Ključne besede: fokusiran ionski curek (FIB), metalografija, litje na vrteče kolo (melt-spinning), zlitina z oblikovnih spominom, Cu-Al-Ni

INTRODUCTION

The traditional metallographic preparation of samples for both light microscopy and scanning electron microscopy (SEM) most frequently consists of hot or cold mounting of a sample, grinding, polishing and, finally, etching. Mounting in resin is unavoidable for small samples such as melt-spun ribbons. Therefore, as a rule, only one surface (or cross-section) of each small sample can be prepared and investigated.

The metallographic preparation of Cu-Al-Ni shape memory alloy (SMA) melt-spun ribbons is usually afflicted with problems from the very start. The as-cast microstructure may already contain the martensitic phase, its fraction being dependent on the exact chemical composition (LOJEN, 2005). Therefore, the alloy might exhibit the shape memory effect when the temperature during hot mounting varies within the range of the alloy's transformation temperatures. As a result, a sample may change its shape or even break-apart as it is held in position by clamps. Cracks in the hot-mounted samples are often observed, especially in Cu-Al-Ni alloys with relatively high Al-content. In the case of cold-mounting, during polymerization, the temperature can also reach the level of the alloy's transformation range. Additionally, gaps between the sample and the resin occur quite frequently, from which the etchant is extremely hard to remove. In our experience good universal etchants which reveal the phase composition, as well as the martensitic pattern, contain quite aggressive and volatile ingredients such as $(NH_4)_2S_2O_8$ and HCl. Consequently, it is very difficult to find the optimal dilution and to obtain reproducible results even within a time period of a few hours. Samples must be examined immediately after etching, otherwise the remnant etchant from the almost always present gaps could damage the sample before examination. All these facts stimulate the search for alternative preparation techniques. One of the most promising methods seems to be preparation using the focussed ion beam (FIB).

The FIB systems, in principle, work in the same way as the electron beam systems. Both consist of an emission source (electron or ion source), lens column, workstage, vacuum unit, and control systems. Ion optics is very much like electron optics. Both, electrons and ions are charged particles and can be focussed into a fine beam using electromagnetic fields. The only difference is that ions can have different masses and charges (Selinger, 1979; Orloff, 2003; Gianuzzi, 2005; Zupanič, 2006).

During the scattering process, ions lose their energy and stop in the surface region of the sample. Elastic scattering changes the direction of the incident ion without a loss of energy. On the other hand, inelastic scattering causes loss of energy in two ways. One is nuclear loss, i.e. an incident ion collides with an atomic nucleus causing the target atom either to dislocate its position (a recoil atom), or to escape from the solid surface. The phenomenon of knocking atoms out of solid targets is called 'sputtering'. The other type is 'electronic loss', i.e. the incident ion transfers part of its energy to the electrons. These electrons can either be excited to produce secondary electron emission or be stripped of the atom resulting in the ionisation of atoms and secondary ion emission. The penetration depth (stopping range) of incident ions increases with ion energy and decreases with increasing ion-mass and relative atomic mass of atoms in a solid. Some incident ions will, after losing all their energy, become part of the material (implantation), which can modify the material's local chemical composition. If this is done purposely, it is called 'doping'. Scattering in an amorphous target material is a random process. In crystalline materials, ions can penetrate several times deeper along directions with low Miller indices, as in other directions or amorphous targets. This phenomenon is called the 'ion-channelling effect' and decreases the yield of sputtered target atoms and the emission of secondary electrons. Therefore, sputtering rates on polycrystalline surfaces can be different. Ion-bombardment can also result in amorphisation of the surface layer.

It was revealed that ion-sputtering yield has the following features: The sputtering yield rises with the beam incident angle (with respect to the normal to the sample surface) and reaches maximum at about 80 ° (Orloff, 2003). For gallium ions, the sputtering yield increases with increasing ion-energy only up to 30 keV (yield saturation). The number of re-deposited atoms increases with the depth of the sputtered hole and any decrease in scanning speed. An efficient way to reduce the re-deposition rate is to sputter with a fast multiple scan of the ion-beam. Ion-bombardment combined with chemically-active gases can multiply the sputtering rate. A small amount of a chemically active gas is introduced into a chamber, where the gas molecules adhere to the target surface. Ion-bombardment ionises the gas atoms, which then react with the target-atoms to form volatile compounds which are in turn evacuated by the vacuum system. Appropriate reactive gas must be applied for every target material.

If the gas ions and target atoms produce non-volatile compounds, the reaction products will stay on the target surface. The deposition process and the sputtering process coexist and compete, but the deposition rate can be adjusted to be greater than the sputtering rate. Since deposition only takes place where an incident ion impacts, controlling the ion beam scanning can produce arbitrary shaped 3D structures. Commonly used gases are organic metal-compound gases, and the deposited materials are organic compounds (containing Ga in the case of gallium ion-source) of Pt, Al, Au or W. Non-metallic materials such as SiO_2 can also be deposited (ORLOFF, 2003).

Sputtering, deposition and doping can be controlled with nanometre-precision. Therefore, FIB is truly a micro-fabrication tool with many applications. In the serial production of IC (integrated circuit) chips, FIB is applied as a diagnostic tool (cross-sectioning of chips for failure analysis), as well as a tool for repairing of IC chips through sputtering or deposition (ZHENG, 2005). FIB implantation can be used to dope the substrates during transistor production. The ability of sputtering is one of the most frequently used features of FIB that can be used directly as a tool for the micro-milling of electronic components, such as read/write heads for modern high density computer hard discs, production of micro-optic switches (XIE, 2003), production of microsurgical manipulators (VASILE, 1999) and for producing micro-milling tools made of steel, diamond or carbides (VASILE, 1999; PICARD, 2003), etc. One of the earliest and still very important applications of FIB systems is preparation (cutting and thinning) of TEM samples for routine inspections during production (electronics), as well as in different fields of science (ZHENG, 2005; PRESSER, 1997; GIANUZZI, 1999; DE VEINEMAN, 1999; SENNHAUSER, 2004). Also in the field of life science the FIB/SEM system provides more comprehensive microscopy results than any conventional microscopy technique in biomedicine (BURKHARDT, 2004; DROBNE, 2004). In dual-beam instruments (FIB/SEM) secondary electron and secondary ion emission caused by ion-bombardment can be used to produce an image providing much more information than conventional SEM-images. In the case of multi-phase samples, but also onephase polycrystalline materials with random orientation of crystal grains, the sputtering rates are not uniform over the scanned area (channelling effect). Although this phenomenon has been referred to as a drawback when preparing a TEM sample or ion-polishing the surface (ORLOFF, 2003) it can also be applied very usefully as an etching technique to reveal the microstructure.

MATERIALS AND METHODS

To investigate the capability of FIB and avoid difficulties pointed out in Introduction, two Cu-Al-Ni alloys were melt-spun: Cu – 13 wt.% Al – 4 wt.% Ni (CuAl13Ni4) and Cu – 15 wt.% Al – 4 wt.% Ni (CuAl15-Ni4). All investigated samples were in as-cast condition. The melt-spun ribbons of alloy CuAl13Ni4 were fully martensitic, whereas the melt-spun ribbons of alloy CuAl15Ni4 consisted of two phases, martensite and γ_2. The presence of the same phases was also determined by (LOJEN, 2005). Some samples of both alloys were mechanically polished (diamond, ¼ μm), whereas the majority of the samples were in as-received condition. The FIB/SEM system used was a FEI Quanta 200 3D equipped with a gallium liquid ion source and a Pt-gas injection system. The following experiments were carried out:

- FIB-etching of diamond-polished cross-sectioned sample, and both the unprepared wheel- and air-side of the

alloy CuAl13Ni4,
- FIB-etching of diamond-polished cross-sectioned sample, and both the unprepared wheel- and air-side of the alloy CuAl15Ni,
- FIB-cutting, -polishing and -etching of the cross-sectioned samples of both alloys.

The polished samples were firstly dismounted from the resin and then attached to the sample holder using a conductive carbon tape. Before placing into the FIB/SEM chamber, all samples were cleaned with alcohol in an ultrasonic cleaner and dried.

All presented micrographs in this work are ion-induced secondary electron images (ISE images). The only exception is Figure 4a, which is an electron-induced secondary electron image (SE image). The presented images were not electronically edited.

Results and discussion

Surfaces and cross-sections

Figure 1a shows the mechanically-polished cross-section of alloy CuAl13Ni4 with six ion-etched fields in the form of squares: dimensions 5 μm × 5 μm. The ribbon air-side of the same alloy was also treated in the same way (Figure 1b). Etching current and etching times are indicated in both figures. It could be seen that the microstructure could not be resolved outside the squares. However, the contrast between microstructural constituents in etched fields increases progressively with etching time. It was clearly revealed that the microstructure is fully martensitic. The contrast between different martensitic plates is caused by the channelling effect, namely, different plates possess different crystallographic orientation. Some of them have low index directions almost parallel to the ion beam; therefore, ions penetrate

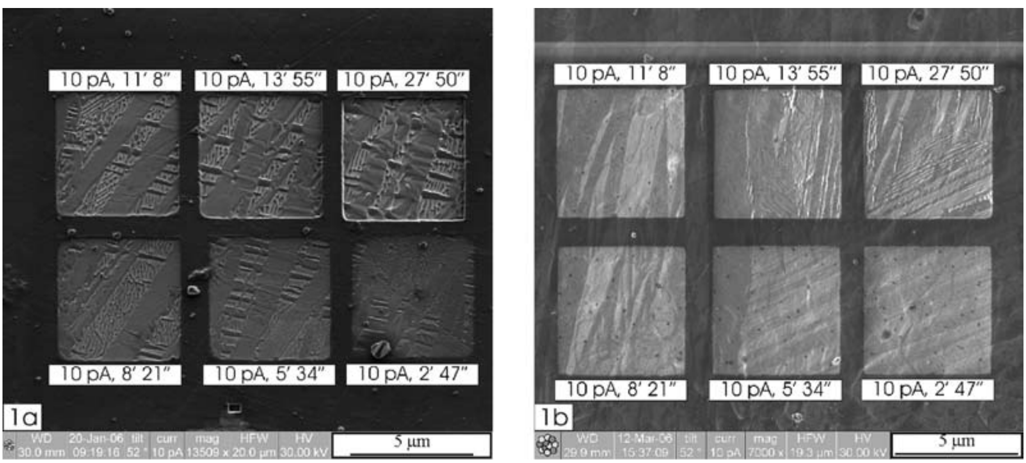

Figure 1. Ion-etched melt-spun ribbon (alloy CuAl13Ni4). a) Mechanically polished cross-sectioned sample; b) as-received air-side of the melt-spun ribbon
Slika 1. Ionsko jedkan hitrostrjen trak zlitine CuAl13Ni4. a) Mehansko poliran prečni prerez, b) metalografsko nepripravljena zunanja površina hitrostrjenega traku

deep into the material. This causes both low scattering yield and low emission of secondary electrons, which finally result in a darker appearance of these plates. It can also be concluded that plates with the same level of greyness have approximately the same orientation to the beam. It seems that in brighter regions the sputtering rate is much higher than elsewhere. In these plates the development of columns can be observed very soon. Such columns are typical FIB-artefacts. Within other plates, which appeared uniform at the beginning of etching, a structure consisting of finer lamellae became visible. By comparing Figure 1a with Figure 1b, it is also obvious that the etching effect is much stronger on the smoother polished sample than on the metallographycally unprepared air-side of the ribbon. Nevertheless, the surface must be clean, without dust or other particles since these particles prevent uniform etching of the surface.

Figure 2 compares images of the same region after mechanical polishing and after 1 hour of FIB-etching with 10 pA (cross-section of a melt-spun ribbon – alloy CuAl15Ni4). As can be expected from Figure 2a, the ribbon consists of two phases, but the contrast is very low. After FIB-etching the two phases can be clearly distinguishable (Figure 2b). It could then be seen that the dendritic γ_2-phase prevails. Two different grey-tones suggest two different crystallographic orientations, and the origin for contrast is the channelling effect. The γ_2-phase on the grain boundary

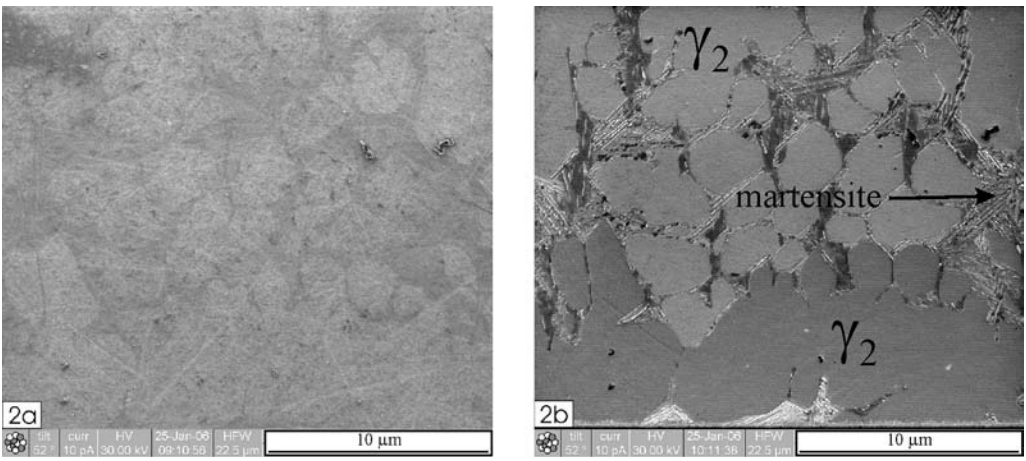

Figure 2. Cross-section of a melt-spun ribbon (alloy CuAl15Ni4). a) ISE-image after mechanical polishing, b) ISE-image of the same area after 1 hour of FIB-etching of the same area, using ion current of 10 pA. Two-phase microstructure is clearly revealed.

Slika 2. Prečni prerez hitrostrjenega traku zlitine CuAl13Ni4. a) Mehansko poliran prečni prerez (slika s sekundarnimi elektroni, ki so jih inducirali ioni), b) mikroposnetek po 1 uri ionskega jedkanja istega mesta s tokom 10 pA (slika s sekundarnimi elektroni, ki so jih inducirali ioni). Dvofazna mikrostruktura je jasno vidna.

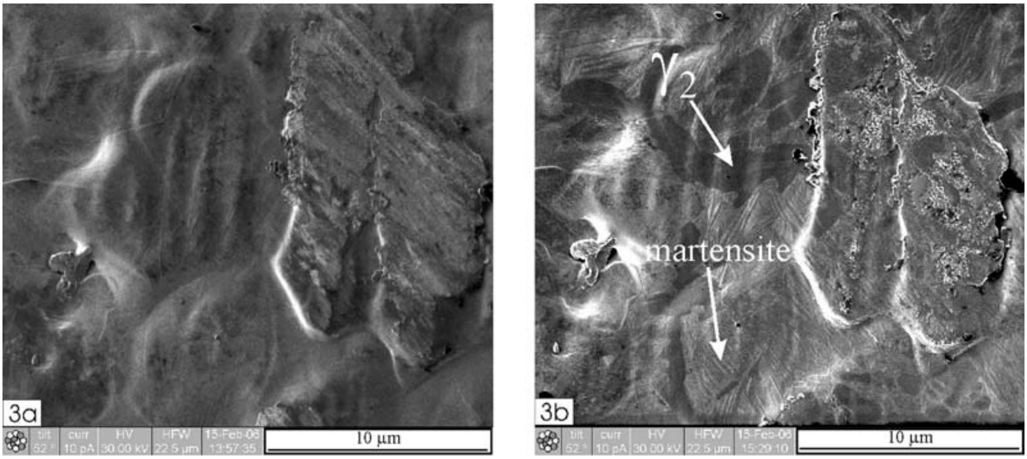

Figure 3. The wheel-side of the melt-spun ribbon (alloy CuAl15Ni4): a) in the as-cast condition; b) after 90 minutes FIB-etching of the same area, using ion current of 10 pA

Slika 3. Površina hitrostrjenega traku, ki je bila pri litju ob kolesu (zlitina CuAl15Ni4): a) v začetnem stanju, b) po 90 minutah ionskega jedkanja istega mesta s tokom 10 pA

appears darker, whilst the intragranular γ_2-phase appears brighter. The characteristic martensitic pattern can be observed in the interdendritic space, consisting of differently-oriented plates.

The unprepared wheel-side surface of the alloy CuAl15Ni4 is shown in Figure 3. The surface is so rough that, besides the surface topography, no microstructural features can be identified (Figure 3a). A comparison with Figure 3b (FIB-etched for 90 min. at 10 pA) makes it obvious that in this case FIB-etching is clearly not as efficient as on smoother surfaces. Although, in Figure 3b, some areas of the martensitic pattern are clearly recognisable and the darker γ_2-phase also distinct, the topographical features cannot be distinguished from the microstructural in many places. It should be stressed that ion-etching means the removal of material by ion-sputtering. Different sputtering rates of differently-oriented grains (plates) and different phases cause the surface to become rough. However, etching is effective when the roughness is only in the order of a few tenths of nanometres. When a larger amount of material is removed, the possibility of introducing different artefacts becomes much more probable. Therefore, if the surface roughness is in the order of a micrometre (Figure 3) than it is obvious that any topographic contrast will be much stronger than the orientational one.

3-D microscopy

Additional freedom during the metallographic preparation of samples allows for so-called 3D-microscopy. In this case a larger portion of material is removed from the surface, which does not require any kind of previous metallographic preparation. We used 3D-microscopy for imaging

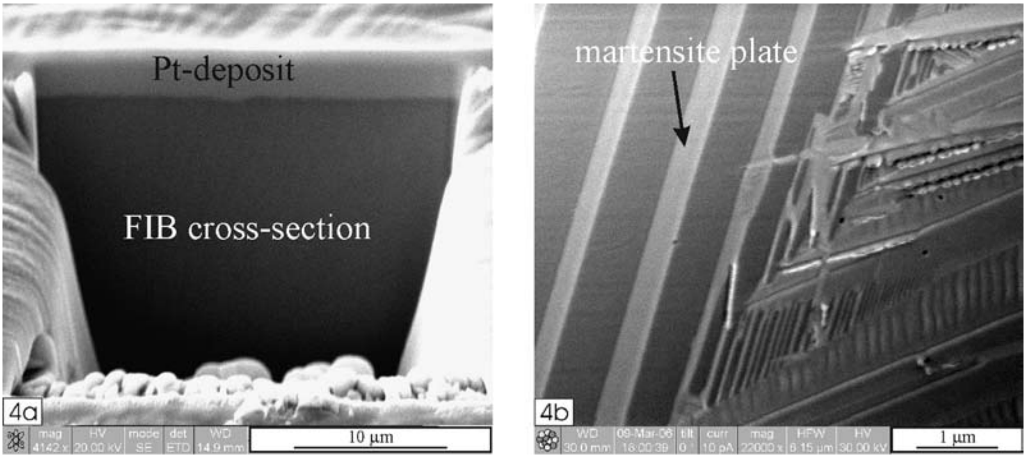

Figure 4. 3D-microscopy of a melt-spun ribbon (CuAl13Ni4 alloy); a) SE image after sputtering and ion-polishing; b) ion induced SE image after 75 min of FIB-etching at 10 pA

Slika 4. 3D-mikroskopija hitrostrjenega traku zlitine CuAl13Ni4; a) posnetek s sekundarnimi elektroni po grobem rezanju in ionskem poliranju površine, b) mikroposnetek po 75 min ionskega jedkanja z ioni (sekundarni elektroni, ki so jih vzbudili ioni)

fully martensitic CuAl13Ni4 alloy (Figure 4). In order to prepare a very smooth cross-section, with a straight and sharp trench edge, a 2 µm thick protective Pt-layer was deposited on the surface (FIB-CVD; FIB chemical vapour deposition). The trench was sputtered with an ion current of 5 nA over two hours. The cross-section surface was then polished with 0.5 nA for an additional hour. The FIB-polished 3-D cross-section is shown in Figure 4a. The brighter layer on the top of the cross-section is the Pt-rich protective layer. The surface below is so smooth, that the contrast of the SE image (Figure 4a is an electron induced SE image) is too poor to reveal the microstructure. On the ion induced SE image the characteristic martensitic pattern can, although with a poor contrast, be recognised without prior FIB-etching (micrograph not shown). After FIB-etching of the cross-section area for 75 minutes with an ion current of 10 pA a contrast rich ion induced SE image can be obtained as shown in Figure 4b.

The 3D cross-section of alloy CuAl15Ni4 was made without a Pt-protective layer. For sputtering the trench and polishing the 3D cross-section shown in Figure 5a the same parameters were selected as in the case of alloy 1 (Figure 4a). When Pt-protection was not used, the free surface surrounding the trench was intensively FIB-etched and the two-phase structure was well revealed (Figure 5a). But in this case the edge of the trench is not as straight as that in Figure 4a and, on the cross-section itself vertical ribs (bright vertical lines in Figure 5b) are present - the so-called ‘curtains’. Except for these curtains an indistinctive image of the two-phase structure can already be seen prior to FIB-etching. The phase-contrast increases over the etching-time. The micrograph in Figure 5b was taken after 38 minutes of FIB-etching at 10 pA. However, several artefacts may appear over prolonged etching times.

Conclusions

FIB is an adequate tool for performing the metallographic preparation of melt-spun Cu-Al-Ni ribbons. Most of the difficulties can be avoided when coupled with conventional metallographic preparation. The major disadvantage of in-situ FIB preparation lies in the fact that it is impossible to cut, polish and etch large areas in reasonable time.

According to the results, smaller ion-currents should be preferred for FIB-etching when revealing fine microstructural details. During the preparation of melt-spun Cu-Al-Ni ribbons, a current of 10 pA turned-out to be a good compromise between the revealed details and the necessary etching time for areas within the range 25 μm^2 to 100 μm^2. But, as the etching area increases, the time required to obtain a satisfactory result increases enormously.

It was clearly determined that the efficiency of FIB-etching is higher on smooth surfaces. If the surface was too rough, microstructural features can be overlapped by the surface topography.

In 3D microscopy, application of FIB-deposited Pt-compound protective layer brings advantages as well as disadvantages. If the edge is straight and sharp and the surface of the 3D cross-section smooth, then the protective layer is unavoidable. If applied, the free surface of the sample cannot be seen. However, if we want to observe both the microstructure of the free

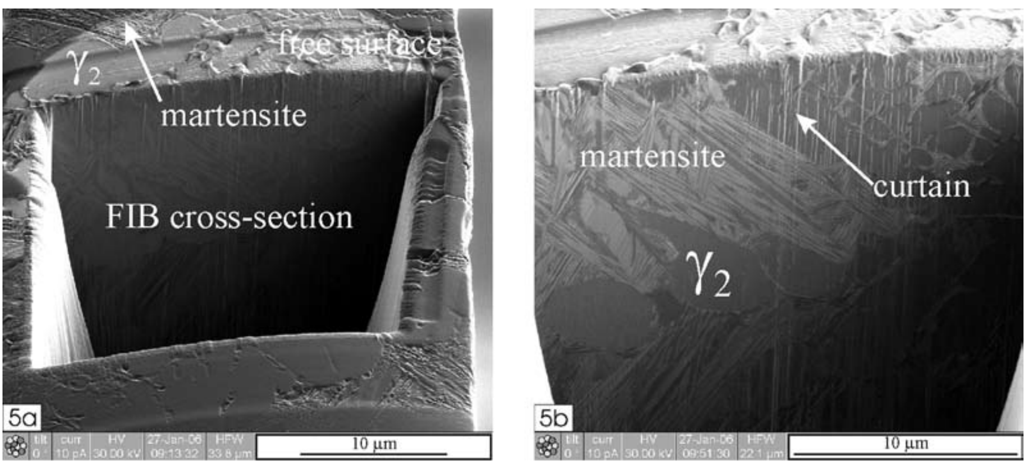

Figure 5. 3D-microscopy of a melt-spun ribbon (CuAl15Ni4 alloy): a) 3D cross-section after sputtering and FIB-polishing; b) After 38 min FIB-etching at 10 pA

Slika 5. 3D-mikroskopija hitrostrjenega traku zlitine CuAl15Ni4. a) 3D-prerez po grobem rezanju in ionskem poliranju, b) mikroposnetek po 38 minutah jedkanja z ioni s tokom 10 pA surface and the microstructure of the FIB cross-section at the same time, then the presence of FIB-artefacts is almost unavoidable.

POVZETEK

Karakterizacija hitrostrjenih trakov zlitine Cu-Al-Ni z uporabo fokusiranega ionskega curka

Vrstični elektronski mikroskop, ki je opremljen s fokusiranim ionskim curkom (FIB), se uporablja za najrazličnejše namene. Naprava FIB uporablja pospešene galijeve ione za odstranjevanje materiala (mikro- in nanoobdelava), izdelavo prečnih rezov (3D-mikroskopija), pripravo TEM-vzorcev, ionsko mikroskopijo, ipd. Trki težkih galijevih ionov z atomi vzorca sprožijo kaskado najrazličnejših procesov, ki povzročijo razprševanje atomov s površine, implantacijo galijevih atomov v vzorec, nastanek najrazličnejših kristalnih napak, deloma pa lahko postane obstreljevana površina tudi amorfna. V polikristalnih in/ali heterogenih materialih je odstranjevanje površinskih plasti neenakomerno. Hitrosti ionskega jedkanja različnih faz namreč niso enake, poleg tega pa so odvisne od orientacije kristalov. Te značilnosti so lahko koristne pri metalografski pripravi vzorcev. Namreč, neenakomerno razprševanje atomov lahko povzroči primeren kontrast med različnimi fazami in med različno orientiranimi kristalnimi zrni.

Mikrostruktura zlitin z oblikovnim spominom Cu-Al-Ni je lahko po hitrem strjevanju (npr. litju na vrteče kolo) v celoti martenzitna ali pa sestavljena iz dveh faz: martenzita in γ_2. Uporaba standardnih metalografskih postopkov in jedkal lahko povzroči številne težave. Zato smo se odločili, da raziščemo možnosti uporabe FIB pri metalografski pripravi eno- in dvofazne mikrostrukture zlitin Cu-Al-Ni. Glavni cilj je bil optimirati pripravo s FIB izdelanih prečnih prerezov, kot tudi obeh prostih površin hitro strjenih trakov. Ugotovljeno je bilo, da je mogoče z uporabo FIB odkriti mikrostrukturo na vseh površinah, toda najdrobnejše detajle lahko razločimo samo na čistih, mehansko poliranih površinah. Veliki ionski tokovi lahko odkrijejo mikrostrukturo na veliki površini zelo hitro, toda na račun izgube podrobnosti. Zato je potreben kompromis med trajanjem jedkanja, velikostjo raziskovanega področja in ločljivostjo mikrostrukturnih podrobnosti. Najpomembnejši zaključek je: mikrostrukturo hitro strjenih trakov lahko odkrijemo s kombinacijo jedkanja z ioni in 3D-mikroskopijo brez uporabe postopkov klasične metalografske priprave.

References

Burkhardt, C., Nisch, W. (2004): *Praktische Metallographie*.; Vol. 41, No. 4, pp. 190-199.

De Veirman, A., Weaver, L. (1999): *Micron*.; Vol. 30, pp. 213-220.

Drobne, D., Milani, M., Ballerini, A., Zrimec, A., Berden-Zrimec, M., Tatti, F., Drašlar, K. (2004): *J. Biomed. Opt*. pp. 1238-1243.

Drobne, D., Milani, M., Zrimec, A., Lešer, V., Berden-Zrimec, M. (2005): *Journal of microscopy*.; Vol. 219, pp. 29-35.

Giannuzzi, L. A., Stevie, F. A. (2005): *Introduction to Focused Ion Beams; Instrumentation, Theory, Techniques and Practice*. Springer-Science + Business Media LLC.

Giannuzzi, L. A., Stevie, F. A. (1999): *Micron*.; Vol. 30 pp. 197-204.

Lojen, G., Anžel, I., Kneissl, A.C., Unterweger, E., Kosec, B., Bizjak, M. (2005): *Journal of Materials processing technology*.; Vol. 162/163 pp. 220-229.

Orloff, J., Utlant, M., Swanson, L. (2003): *High Resolution Focused Ion Beams, FIB and Its Applications*. Kluwer Academic/Plenum Publishers, New York.

Picard, Y.N., Adams, D.P., Vasile, M.J., Ritchey, M.B. (2003): *Precission engineering*.; Vol. 27, pp. 59-69.

Presser, N., Hilton, M.R. (1997): *Thin Solid Films*.; Vol. 308-309, pp. 369-374.

Selinger, R. L., Ward, J. W., Wang, V., Kubena, R. L. (1979): A high-intensity scanning ion probe with submicrometer spot size. *Appl. Phys*. Lett. 34, p. 310.

Sennhauser, U., Jacob, P., Gasser, P. (2004): *Praktische Metallographie*.; Vol. 41.

Vasile, M.J., Nassar, R., Xie, J., Guo, H. (1999): *Micron*.; Vol. 30, pp. 235-244.

Xie, D.Z., Ngoi, B.K.A., Ong, A.S., Fu, Y.Q., Lim, B.H. (2003): *Nuclear Instruments and Methods in Physics Research, B 211*. pp. 363-368.

Zheng, C. (2005): *Micro-Nanofabrication Technologies and applications*. Beijing, Higher education press, Springer-Verlag, Chapter 4, pp. 139-167.

Zupanič, F (2006): Tehnologija fokusiranega ionskega curka (FIB). *Vakuumist*.; letn. 26, št. 4, str. 4-9.

The effect of annealing on properties of AISI 316L base and weld metals

Vpliv žarjenja na lastnosti osnovnega materiala in vara jekla AISI 316L

Stjepan Kožuh[1], Mirko Gojić[1], Ladislav Kosec[2]

[1]University of Zagreb, Faculty of Metallurgy, Aleja narodnih heroja 3, 44103 Sisak, Croatia; E-mail: kozuh@simet.hr, gojic@simet.hr
[2]University of Ljubljana, Faculty of Natural Sciences and Engineering, Aškerčeva cesta 12, SI-1000 Ljubljana, Slovenia; E-mail: kosec@ntf.uni-lj.si

Received: November 14, 2007 **Accepted:** December 4, 2007

Abstract: Results of mechanical testing and of microstructural analysis of AISI 316L austenitic stainless steel carried out before and after welding and post-weld heat treatment are presented. Steel plates of 15 mm thickness were welded by manual electric arc welding process. Heat treatment consisted of annealing at 600, 700, 800, and 900 °C for two hours, and was followed by cooling in the air. For microstructure examination an optical microscope and a scanning electron microscope were used. The weld metal microstructure demonstrated the presence of austenite, ferrite, and microslag inclusions before annealing, and of sigma phase after annealing. The tensile strength increased and impact energy values decreased with the increasing annealing temperature. Complex Mn-Cr-Si-Ti inclusions in the dimples were observed in the tensile and Charpy tested specimens.

Izvleček: V članku so opisani rezultati preiskav mehanskih lastnosti in analiza mikrostrukture avstentnega jekla AISI 316L pred in po varjenju ter toplotni obdelavi zvarov. 15 mm debele jeklene plošče so bile zvarjene ročno elektro obločno. Zvari so bili žarjeni dve uri na temperaturah 600, 700, 800 in 900 °C ter nato ohlajeni na zraku. Mikrostrukturne raziskave smo opravili z optičnim in vrstičnim elektronskim mikroskopom. V mikrostrukturi vara so značilne sestavine avstenit, ferit in vključki žlindre, po žarjenju pa faza σ. S temperaturo žarjenja raste natezna trdnost, obratno pa se zmanjšuje žilavost varov. Na prelomnih površinah obeh vrst epruvet smo v jamicah žilavega preloma opazili kompleksne nekovinske vključke z glavnimi kovinskimi sestavinami Mn-Cr-Si-Ti.

Key words: stainless steel, austenite, welding, microstructure, mechanical properties, sigma phase

Ključne besede: nerjavno jeklo, avstenit, varjenje, mikrostruktura, mehanske lastnosti, faza σ

Scientific paper

Introduction

Stainless steels constitute a group of high-alloyed steels based on the Fe-Cr, Fe-Cr-Ni, and Fe-Cr-C systems. To be classified as stainless, the steels must contain a minimum of 11 % chromium, but less than 30 % [1]. Austenitic stainless steels are an important class of stainless materials that have been used widely in a variety of industries and environments. The basic austenitic composition is the familiar 18 % chromium and 8 % nickel alloy. The increased chromium and nickel contents can improve corrosion resistance, and addition of other elements (most commonly molybdenum in AISI 316L) can enhance it further. For stainless steels welding is an important fabrication technique. In general, stainless steels are considered to be weldable materials, but there is a number of rules to be observed to ensure that they are readily fabricated free from defects, and that they perform as expected in their intended service[2]. Almost certainly, welding will bring about a major microstructural alteration in the weld metal and in the heat-affected zone with respect to the base metal. Weld solidification and liquation cracking will depend on the composition of the base and filler metals, and on the level of impurities, particularly of sulphur and phosphorus.

The complexity of the weld metal microstructure is attributable to the mode of solidification and to subsequent solid-state phase transformation. Depending on the alloy composition, austenite may originate in two ways: from a eutectic reaction and partial solid-state transformation of ferrite, or as a result of ferrite decomposition during postsolidification cooling. Austenitic steels may undergo microstructural changes during short- or long-term exposure to high temperature[3]. Heino et al.[4] reported that during heat treatment of austenitic stainless steels at 600-900 °C, short-time precipitation from austenite (<60 s) was typically associated with the formation of $M_{23}C_6$ carbide. In the case of longer ageing times, other precipitates such as intermetallic phases are formed, which are usually accompanied by dissolution of carbides. The intermetallic precipitations are of great interest not only because they exert influence on the mechanical properties but also because of their strong effect on the corrosive properties. There have been many studies into the microstructure and the precipitation behaviour of stainless steels during welding and in exposure to elevated temperatures[5-9].

The two intermetallic phases most commonly found in austenitic stainless steels are sigma phase and χ phase[10]. Sigma phase is an intermetallic compound with a complex tetragonal crystalline structure. Its composition varies fairly widely and is difficult to describe by means of a formula. Thus, according to literature[11] a typical sigma phase composition for the AISI 316L steel type is 44 % Fe - 29 % Cr - 8 % Mo. At room temperature sigma phase is hard, brittle and nonmagnetic. Its promotion elements are molybdenum, silicon, vanadium, tungsten and columbium, whereas carbon, nitrogen and nickel retard sigma formation. Sigma phase is responsible for reduction in toughness at room temperature. Embrittlement, if it occurs, can be removed by dissolving sigma at temperatures above 1000 °C. Rapid cooling is recommended to avoid brittleness at 475 °C. In contrast to sigma phase, the precipitation of the χ phase in austenitic stainless steels is thermodynamically unstable. With the onset of sigma precipitation, the χ phase vanishes in its favour.

This work is focussed on the effect of post-weld heat treatment of the base and weld metals on their mechanical properties and microstructures. It aims to find out how mechanical properties and impact energy are affected by the sigma phase precipitation, and to determine, by EDX analysis, the sigma phase composition. On the other hand, interpretation of the fracture mechanism can provide valuable evidence for the cause of failure.

Experimental

The austenitic stainless steel in this experiment was AISI 316L. Its chemical composition is given in Table 1. Welding of a steel sheet of 15 mm thickness was carried out by the manual electric arc welding process using solid electrodes 2.5 and 3.25 mm in diameter. Before welding the sheet surfaces were thoroughly cleaned and then brushed. The V-joints were prepared with the Böhler FOX SAS-4A electrodes. Immediately after welding the welded joint was subjected to post-weld heat treatment at 600-900 °C for two hours, and was then cooled in the air.

Tensile testing was carried out in conformity with ASTM standards[12]. It was done with an Instron tensile machine, type 1196, on nonwelded and as-welded specimens at room temperature. Hardness was measured by the Vickers test (HV_{30}). Impact tests were performed on Charpy V-notch specimens (10×10×55 mm) at room temperature. A V-notch of 2 mm depth was machined in the middle of a weld metal sample.

Microstructural analysis of the base and weld metals was carried out by optical microscopy and scanning electron microscopy. Samples for microstructural analysis were subsequently ground, polished and electrolytically etched. To expose austenite boundaries 60 ml HNO_3 and 40 ml water solution was used at 1V DC for 20 s. Sigma phase and ferrite were identified with 56 g KOH in 100 ml water at 2V DC for 10 s.

Fractographic analysis was carried out after both tensile and impact energy testing. Surface fractures were tested with a SEM JEOL JSM-5610 Model 500 Analyser operating at 20 kV and equipped with EDAX and XRF systems. The delta ferrite number in the base and weld metals was determined by means of a ferritoscope. The method takes advantage of the fact that ferrite is magnetic and austenite is not.

Table 1. Chemical composition of the base (BM) and weld metals (WM) [wt.%]
Tabela 1. Kemična sestava osnovnega materiala (BM) in vara (WM) [m.%]

	C	Mn	Si	Cu	V	Mo	Al	Cr	Ni	W	Ti	Nb
BM	0.026	1.49	0.45	0.35	0.060	2.04	0.008	16.75	10.80	0.066	0.081	0.016
WM	0.024	0.85	0.74	0.11	0.074	2.44	0.004	19.15	10.86	0.048	0.009	0.289

Table 2. Mechanical properties of the base and weld metals before post-weld heat treatment
Tabela 2. Mehanske lastnosti osnovnega materiala in vara pred toplotno obdelavo

	Yield strength, [N/mm²]	Tensile strength, [N/mm²]	Reduction of area, [%]	Impact energy, [J]
Base metal	270.7	606.3	75.1	238.3
Weld metal	-	732.7	52.1	83.3

Results and discussion

Table 2 and Figure 1 show results of tensile and impact testing of the base and weld metals before annealing and after it. The values are expressed as the means of three measurements. The tensile strength of the weld metal was higher than that of the base metal. The area reduction for the base metal (about 75 %) was higher than for the weld metal (52 %), and decreased with a rise in the annealing temperature. Elevated annealing temperature produced a remarkable drop in impact energy of either metal (Figure 1). The most likely reason for this was the precipitation of the sigma phase particles which improved strength and reduced plasticity and toughness.

Figure 2 shows Vickers hardness distribution and the effect of annealing temperature on the hardness of the base metal, heat-affected zone and weld metal. The weld metal exibited remarkably higher hardness values than the base metal (Table 3). This could be accounted for by the weld metal chromium content of about 19.0 wt.%, which was higher than that of the base metal (Table 1). It is generally believed that the elevated chromium content of the weld metal, along with the presence of niobium, increases steel hardenability[1]. This is in agreement with the results of Ohkubo et al.[13] who investigated the effect of alloying elements on the mechanical properties of austenitic stainless steel. Elevated weld metal hardness could also be due

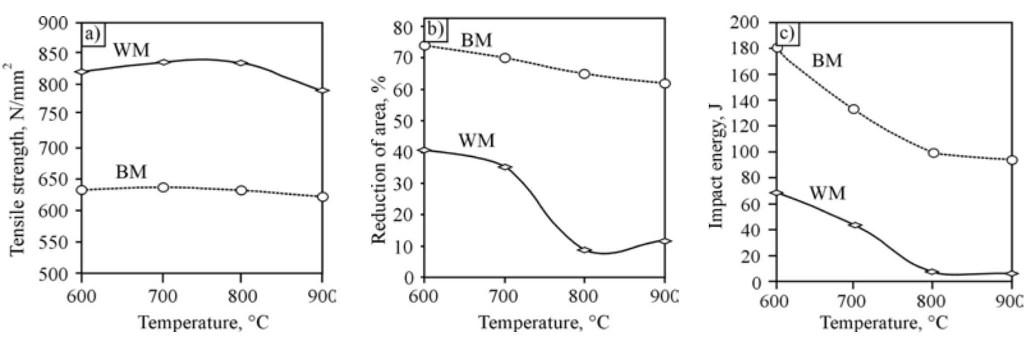

Figure 1. Effect of annealing temperature on tensile strength (a), on area reduction (b), and on impact energy (c) of the base (BM) and weld metals (WM)
Slika 1. Vpliv temperature žarjenja na trdnost (a), kontrakcijo (b) in udarno žilavost (c) osnovnega materiala (BM) in vara (WM)

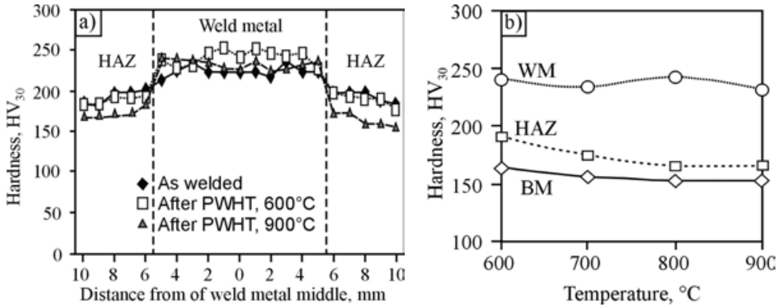

Figure 2. Distribution of Vickers hardness HV_{30} in the welded sections after welding and after post-weld heat treatment (a) and the effect of annealing temperature on hardness (b)

Slika 2. Potek trdote v varu in coni toplotnega vpliva po varjenju in po toplotni obdelavi (a) in učinek toplotne obdelave na trdoto v osnovnih področjih zvara (b)

to heat input during welding, melting and solidification of the area. After annealing, hardness values diminished for the base metal. This could be attributed to a lower stress level and to a change in microstructure.

The microstructure that evolves in a weldment is heterogeneous owing to the temperature gradient associated with the welding process, and the chemical gradient which is generated during that process. As a result of microstructural inhomogeneity gradients in mechanical properties may become noticeable across the weldment.

The microstructure of AISI 316L steel before post-weld heat treatment was austenitic without grain boundary precipitation, as shown in Figures 3 and 4. Ideally, austenitic stainless steels will exibit a single phase that is maintained over a wide temperature range. However, a fully austenitic microstructure is more crack sensitive than the one containing a small amount of ferrite. Figure 3a shows austenitic polygonal grains of AISI 316L stainless steel base metal with a low delta ferrite content. Grain size was G=7.58, and average grain area 679 μm^2 with 1496 grains/unit area. Stringers of delta ferrite can be seen elongated in the rolling direction. The beneficial effect of delta ferrite, which is manifested as decreased susceptibility to hot cracking, stems from its capacity to dissolve harmful impurities such as sulphur, phosphorus, and boron[14].

Table 3. Hardness test results for the base and weld metals before post-weld heat treatment and after it

Tabela 3. Trdote v osnovnem materialu in varu pred in po toplotnih obdelavah zvara

	Hardness, HV_{30}				
	Before annealing	Temperature of annealing [°C]			
		600	700	800	900
Base metal	167.3	164.3	155.6	152.3	153.3
Weld metal	224.2	240.9	233.7	241.5	232.2

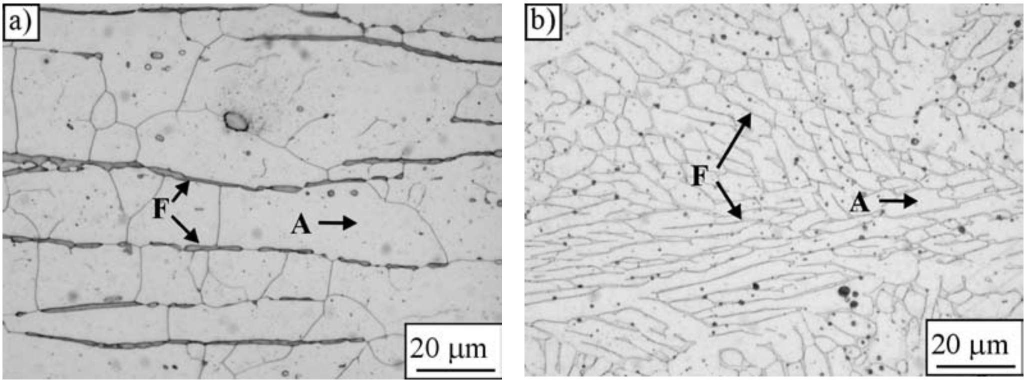

Figure 3. Optical micrograph of AISI 316L stainless steel base metal (a) and weld metal (b) before post-weld heat treatment; A - austenite, F - ferrite
Slika 3. Optično mikroskopska slika mikrostrukture osnovnega materiala (nerjavno jeklo AISI 316L) (a) in vara (b) pred toplotno obdelavo; A - avstenit, F- ferit

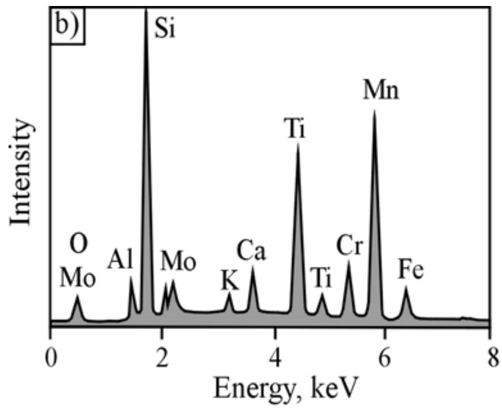

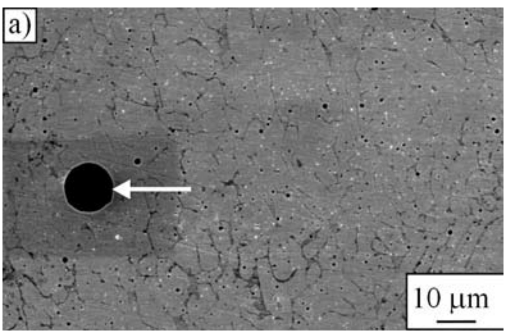

Element	Line	Intensity (c/s)	Concentration (wt.%)
O	K_α	23.20	3.92
Al	K_α	41.33	2.31
Si	K_α	383.71	19.58
K	K_α	30.56	1.50
Ca	K_α	66.37	3.34
Ti	K_α	284.95	18.39
Cr	K_α	95.70	8.39
Mn	K_α	364.57	37.01
Fe	K_α	14.57	1.68
Mo	L_α	30.29	3.01
Other			0.87

Figure 4. SEM micrograph of the weld metal (a) with the corresponding nonmetallic inclusion (b)
Slika 4. Elektronsko mikroskopski (SEM) posnetek mikrostrukture vara (a) s kvalitativno in kvantitativno kemično mikroanalizo nekovinskega vključka (b)

Phase transformations in austenitic stainless steels can be determined with the help of chromium and nickel equivalencies[15]. For the AISI 316L steel base metal in this work, the Cr_{eq}/Ni_{eq} ratio was 1.59, and the final microstructure consisted of austenite and 3.4 % delta ferrite. It is generally held that a 4-8 % delta ferrite content of the base metal is an effective means of offseting a grain boundary weakness that develops in austenite at high temperatures and leads to fissuring. However, high ferrite has been reported to reduce corrosion resistance drastically, and to promote high-temperature embrittlement[16].

In this work the base metal microstructure differed from the microstructure of the weld metal (Figure 3b). The Cr_{eq}/Ni_{eq} ratio was 1.91, and the final weld metal microstructure consisted of austenite and 14.2 % delta ferrite. At room temperature the microstructure of the austenitic stainless steel weld metal is dependent on the solidification behaviour and on subsequent solid-state transformation. Austenitic stainless steels may solidify as primary ferrite or primary austenite i.e. solidification behaviour of the weld metal can be classified into four modes (A, AF, FA, and F). The A and AF solidification modes are associated with primary austenite solidification, whereby austenite is the first phase to form upon solidification. The FA and F solidification types have delta ferrite as the primary phase. The sequence of primary delta ferrite solidification is as follows[17]:

$$L \rightarrow L+\delta \rightarrow L+\delta+\gamma \rightarrow \gamma+\delta \qquad (1)$$

According to literature[18],[19] for commercial 300-series stainless steels the weld metal solidification mode for $Cr_{eq}/Ni_{eq} = 1.91$ is FA (FA mode: $1.48 \leq Cr_{eq}/Ni_{eq} \leq 1.95$). If some austenite forms at the end of solidification, it is termed Type FA. This austenite is result of a peritectic-eutectic reaction and can be found at the ferrite solidification boundaries. With this solidification mode, the potential for cracking will be effectively nil. The presence of intermetallic sigma phase in the weld metal before post-weld heat treatment was not observed (Figure 4). In the weld metal microstructure sporadic complex Fe-Mn-Si-Ti-Cr inclusions were present. During tensile testing, the impurity particles fractured or broke off.

The weld metal microstructure after post-weld heat treatment consisted of austenite grains with sigma phase particles (Figures 5 and 6). Figures 5a and 6a show the microstructure of the precipitated sigma phase, and Figures 5b and 6b the compositions of the precipitated phases as determined by EDX using a SEM JEOL JSM-5610. It is well known that in low-carbon austenitic stainless steel the grain boundary precipitation involves mainly nitrides, carbides and intermetallic phases. Thus, after the solution annealing treatments at different temperatures, the intermetallic sigma phase initially precipitates along the delta ferrite/austenite interface. With increase in the annealing temperature the sigma phase precipitation intensifies. Its original composition is iron and chromium based. Sigma phase has a tetragonal crystallographic structure with an elemental cell of 32 atoms and five crystallographically different atom sites[20]. As seen in Figure 5a the sigma phase particles could be observed at the ferrite/austenite grain boundaries. The sigma phase morphology was usually equiaxed. It changed with the precipitation temperature. At lower precipitation temperatures (600 and 700 °C), a coral-like sigma phase structure could be found. At higher temperatures (800 and 900 °C) the sigma phase was larger and more compact. The presence of sigma precipitates in microstructure can lead to degradation of corrosion resistance, localized stresses at the interfaces between the sigma particles and the matrix, altered crack propagation behaviour, and reduced fracture toughness.

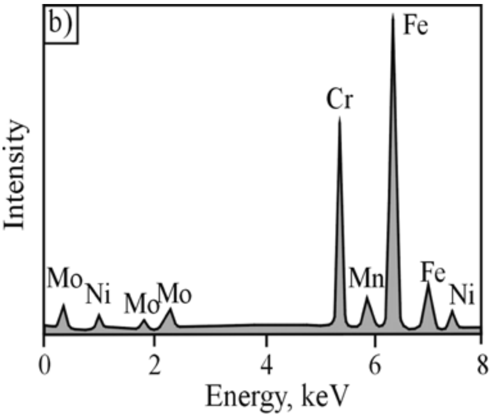

Element	Line	Intensity (c/s)	Concentration (wt.%)
Cr	K_{α}	395.63	24.37
Mn	K_{α}	10.29	0.84
Fe	K_{α}	677.60	67.49
Ni	K_{α}	36.90	5.42
Mo	L_{α}	21.78	1.87

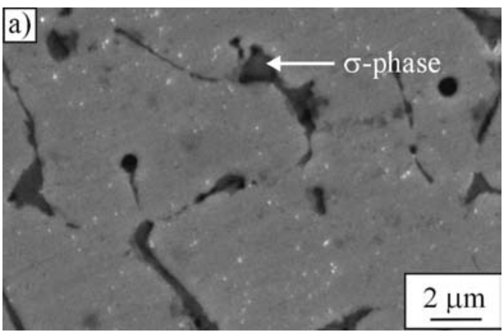

Figure 5. SEM micrograph of AISI 316L steel weld metal (a) with the corresponding EDX spectrum of sigma phase (b) after post-weld heat treatment at 700 °C

Slika 5. Elektronsko mikroskopski (SEM) posnetek mikrostrukture vara jekla AISI 316L (a) s kvalitativno in kvantitativno kemično mikroanalizo delca faze σ (b) po žarjenju na 700 °C

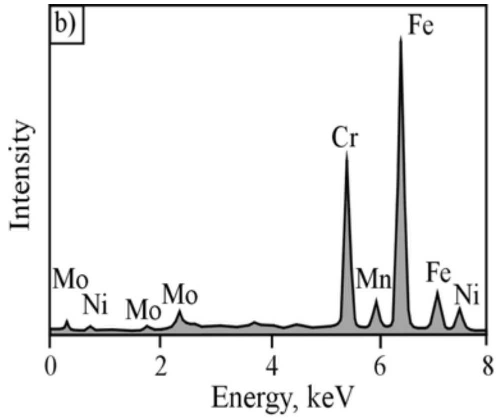

Element	Line	Intensity (c/s)	Concentration (wt.%)
Cr	K_{α}	400.75	22.72
Mn	K_{α}	12.73	0.96
Fe	K_{α}	729.34	66.65
Ni	K_{α}	55.10	7.45
Mo	L_{α}	27.79	2.22

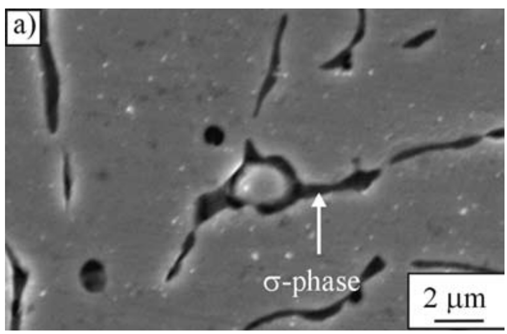

Figure 6. SEM micrograph of AISI 316L steel weld metal (a) with the corresponding EDX spectrum of sigma phase (b) after post-weld heat treatment at 900 °C

Slika 6. Elektronsko mikroskopski (SEM) posnetek mikrostrukture vara jekla AISI 316L (a) s kvalitativno in kvanitativno kemično mikroanalizo mikrostrukturne sestavine faze σ (b) po žarjenju na 900 °C

The EDX analysis showed iron, chromium, and nickel to be dominant sigma phase elements (Figures 5b and 6b). In this work the sigma phase composition was 65-67 % Fe, 22-26 % Cr, 5-7 % Ni, and about 2 % Mo (in wt.). It was slightly different from the typical sigma phase composition of AISI 316 or 316L steels which is 55 % Fe, 29 % Cr, 5 % Ni, and 11 % Mo (in wt.)[21]. As the sigma phase composition tends to vary it is difficult to define it by a formula. The sigma phase precipitation tends to deplete the adjacent chromium matrix. The presence of the chromium depleted zones, which are possible pitting sites, can enhance embrittlement in pitting resistance. After heat treatment the precipitation of the brittle sigma phase produced a considerable drop in impact energy values (Table 3).

The mechanism of sigma phase nucleation is still a matter of controversy and depends on the amount of delta ferrite. The delta ferrite content of the weld metal plays an important role in determining fabrication and service performance of the welded structures. David[22] observed four distinct types of ferrite morphology in stainless steel with a delta ferrite content from 9 to 15 %: vermicular, lacy, acicular, and globular. Variations in ferrite morphology are related to the weld metal composition, ferrite content, and ferrite distribution as a result of thermal cycling during subsequent weld passes. The delta ferrite content of the base and weld metals decreased with the increasing annealing temperature (Table 4). Its transformation was calculated from the values measured before heat treatment and after it. The percentage of delta ferrite decomposition in the weld metal increased from 17.6 % at 600 °C to 96.5 % at 900 °C. It also increased for the base metal, from 23.5 % to 88.2 %. Park et al.[23] investigated fast formation of sigma phase in AISI 304 stainless steel during welding. They suggested that the sigma phase formation could be accelerated by the emergence of delta ferrite at high temperature, and its subsequent decomposition under high strain and recrystallization induced by welding. Kington et al.[7] reported a very rapid sigma phase formation from ferrite in AISI 310 steel at temperatures in excess of 800 °C (complete transformation occurred within 10 minutes at a temperature between 800 and 900 °C). The size, morphology, and distribution of the sigma precipitates and ferrite were sufficiently similar to suggest that the sigma phase had formed by direct ferrite transformation.

Fractographic analysis can describe the fracture process and provide valuable evidence for the cause of failure[14]. In order to determine the fracture mode during tensile and impact energy testing, the failed specimens were examined using a SEM technique. Examination of the fractured specimens demonstrated that the fracture surface was characterized by two fracture modes: a ductile fracture and a cleavage fracture (Figure 7). Dimple morphology dominated on the fracture surface of all samples (Figures 8 and 9). This feature is indicative of a ductile fracture mode. The fracture process is very complex and involves nucleation, growth of micro-voids or cracks, and propagation of these defects. A number of inclusions in small holes were visible on the microfractographs. The EDX analysis demonstrated the presence of complex Mn-Cr-Si-Ti inclusions (Figure 9b).

Table 4. Delta ferrite content of the base and weld metals after post-weld heat treatment [wt.%]
Tabela 4. Delež ferita - δ v osnovnem materialu in varu po žarjenju [m.%]

	Temperature of annealing [°C]	600	700	800	900
Base metal	δ-ferrit, wt.%	2.6	1.2	0.4	0.7
	Decomposition ratio, %	23.5	64.7	88.2	79.4
Weld metal	δ-ferrit, wt.%	11.7	8.0	0.9	0.5
	Decomposition ratio, %	17.6	43.6	93.7	96.5

CONCLUSIONS

Results of investigation into the mechanical properties and microstructure of AISI 316L stainless steel before post-weld heat treatment and after it suggest the following:

- The tensile strength of the weld metal was higher than that of the base metal. The impact energy values and the area reduction decreased drastically with the increasing annealing temperature.
- The hardness test results for the weld metal were remarkably higher than those for the base metal. Comparison of the hardness values measured before post-weld heat treatment and after it showed insignificant variations.
- The base metal consisted of equiaxed austenite grains with some ferrite stringers (3.4 %). The weld metal contained over 14 % of delta ferrite as the result of FA solidification mode during cooling of the welds.
- The delta ferrite content decreased with the increasing annealing temperature. The percentage of delta ferrite decomposition in the weld metal increased from 17.6 % at 600 °C to 96.5 % at 900 °C. It also increased for the base metal, from 23.5 % to 88.2 %.
- Before post-weld heat treatment the weld metal microstructure consisted of austenite and ferrite. Complex micro-slag inclusions were also present. The EDX analysis showed manganese, silicon, titanium, and chromium to be dominant elements in the inclusions.
- After post-weld heat treatment the presence of sigma phase at the ferrite/austenite boundaries was established by EDX analysis as the result of delta ferrite transformation at elevated temperature. Its composition was 65-67 % Fe, 22-26 % Cr, 5-7 % Ni, and about 2 % Mo. The presence of sigma phase was considered to be adverse to impact energy.
- Two distinct fracture modes were

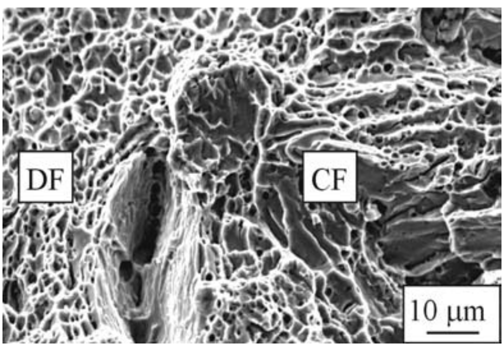

Figure 7. SEM microfractograph of AISI 316L steel weld metal after Charpy impact testing; DF - ductile fracture, CF - cleavage fracture
Slika 7. Mikrofraktografija prelomne površine epruvete za preizkus udarne žilavosti po Charpyju vara jekla AISI 316L; DF duktilni, jamičast prelom; CF - krhki prelom s cepljenjem

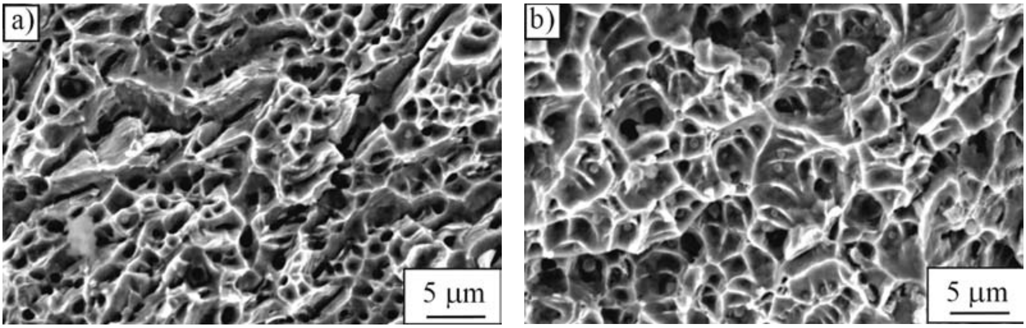

Figure 8. SEM microfractograph of AISI 316L steel weld metal after tensile testing (a) and after Charpy impact testing (b). Specimens annealed at 600 °C.
Slika 8. Mikrofraktografija prelomne površine vara jekla AISI 316L nastale pri nateznem preizkusu (a) in pri epruveti za merjenje udarne žilavosti (b). Epruveti sta bili žarjeni na 600 °C.

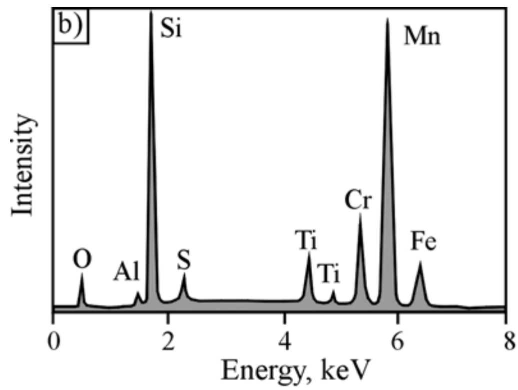

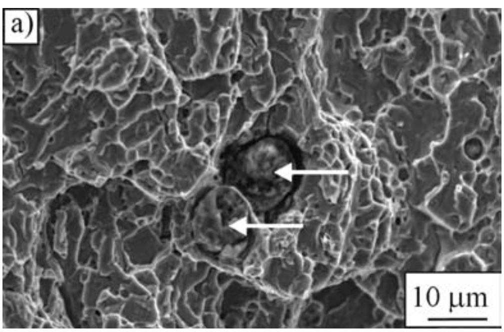

Element	Line	Intensity (c/s)	Concentration (wt.%)
O	K_α	20.49	2.09
Al	K_α	12.34	0.86
Si	K_α	271.44	16.68
S	K_α	21.16	1.18
Ti	K_α	70.80	4.66
Cr	K_α	122.50	11.29
Mn	K_α	534.13	58.54
Fe	K_α	31.19	3.95
Other			0.75

Figure 9. SEM microfractograph of AISI 316L steel weld metal after Charpy impact testing (a) with the corresponding EDX particle spectrum (b). Specimens annealed at 900 °C.
Slika 9. Mikrofraktografija prelomne površine epruvete za preizkus udarne žilavosti vara jekla AISI 316L (a) z mikroanalizo nekovinskega vključka (b). Zvar je bil žarjen na temperaturi 900 °C.

observed, ductile fracture and cleavage fracture. Fracture surfaces of the tensile and impact tested specimens were predominantly ductile with a large number of dimples. The EDX analysis demonstrated the presence of complex Mn-Cr-Si-Ti inclusions in the dimples.

Povzetek

Vpliv žarjenja na lastnosti osnovnega materiala in vara jekla AISI 316L

Iz raziskave mehanskih lastnosti in mikrostrukture osnovnega materiala in varov jekla AISI 316L po varjenju in po naknadni toplotni obdelavi, lahko povzamemo naslednje:

- Natezna trdnost vara je večja od trdnosti osnovnega materiala. Žilavost in kontrakcija padata skokovito s temperaturo žarjenja.
- Trdote v varu so znatno večje od trdote osnovnega materiala. Primerjave trdot pred in po žarjenju kažejo nesignifikantna nihanja.
- Mikrostruktura osnovnega materiala je iz enakoosnih kristalnih zrn avstenita in trakastih delcev ferita δ (3,4 m.%). V varu je več kot 14 m.% ferita δ kot posledica zaporedja strjevanja s primarnim nastankom ferita med ohlajanjem vara.
- Delež ferita δ se zmanjšuje s temperaturo žarjenja. Delež ferita δ v varu, ki razpade pri žarjenju je od 17,6 m.% pri 600 °C do 96,5 m.% pri 900 °C. Pri osnovnem materialu je ta sprememba od 23,5 m.% na 88,2 m.%.
- Po varjenju je mikrostruktura vara iz avstenita in ferita δ. V varu so tudi nekovinski vključki kompleksne kemične sestave v kateri prevladujejo mangan, silicij, titan in krom.
- Po žarjenju zvarov se na faznih mejah ferit δ - avstenit pojavi faza σ kot rezultat transformacije ferita δ.
- Kemična sestava faze σ je v mejah: 65-67 m.% Fe, 22-26 m.% Cr, 5-7 m.% Ni in okoli 2 m.% Mo. Prisotnost faze σ poslabša udarno žilavost.
- Na prelomih smo opazili dve karakteristični morfološki obliki: duktilni, jamičasti in krhki prelom s cepljenjem. Prelomne površine preizkušancev za natezni preizkus udarne žilavosti so pretežno duktilne s številčnimi jamicami v katerih so kompleksni nekovinski vključki.

References

[1] Lula, R. A. (1986): *Stainless Steel*. American Society for Metals, Metals Park, Ohio.

[2] Lippold, J. C., Kotecki, D. J. (2005): *Welding Metallurgy and Weldability of Stainless Steels*. John Wiley&Sons Inc, New Jersey.

[3] Minami, Y., Kimura, H., Ihara, Y. (1986): Microstructural Changes in Austenitic Stainless Steels During Long-Term Aging. *Materials Science and Technology*.; Vol. 2, No. 8, pp. 795-806.

[4] Heino, S., Knutson-Wedel, E. M., Karlsson, B. (1999): Precipitation Behaviour in Heat Affected Zone of Welded Superaustenitic Stainless Steel. *Materials Science and Technology*.; Vol. 15, No. 1, pp. 101-108.

[5] Zhang, W., Debroy, T., Palmer, T. A., Elmer, J. W. (2005): Modeling of Ferrite Formation in a Duplex Stainless Steel Weld Considering Non-uniform Starting Microstructure. *Acta Materialia*.; Vol. 53, No. 16, pp. 4441-4453.

[6] Angella, G., Wynne, B. P., Rainforth, W. M., Beynon, J. H. (2005): Microstructure Evolution of AISI 316L in Torsion at High Temperature. *Acta Materialia*.; Vol. 53, No. 5, pp. 1263-1275.

[7] Kington, A. V., Noble, F. W. (1995): Formation of σ Phase in Wrought 310 Stainless Steel. *Materials Science and Technology*.; Vol. 11, No. 3, pp. 268-275.

[8] Gojić, M., Markotić, A., Kosec, L. (1999): Duplex Stainless Steels in Oil and Petrochemical Industry. *Nafta*.; Vol. 50, No. 7/8, pp. 241-256.

[9] Gojić, M., Kosec, L., Škraba, P., Pinotić, D. (2003): Mikrostrukturna svojstva dupleks nehrđajućeg čelika nakon zavarivanja. *Proceedings International Conference Joining of Corrosion Resistant Materials*. HDTZ, Opatija, pp. 205-212.

[10] Kožuh, S., Gojić, M. (2006): Mikrostruktura austenitnih i dupleks nehrđajućih čelika nakon zavarivanja. *Zavarivanje*.; Vol. 49, No. 5, pp. 177-185.

[11] Sourmail, T. (2001): Precipitation in Creeep Resistant Austenitic Stainless Steels. *Materials Science and Technology*.; Vol. 17, No. 1, pp. 1-14.

[12] ASTM E-370 E8: Tests Methods for Tension Testing of Metallic Materials. ASTM Committee 1994.

[13] Ohkubo, N., Miyakusu, K., Uematsu, Y., Kimura, H. (1994): Effect of Alloying Elements on the Mechanical Properties of the Stable Austenitic Stainless Steel. *ISIJ International*.; Vol. 34, No. 9, pp. 764-772.

[14] Cui, Y., Lundin, C. D., Hariharan, V. (2006): Mechanical Behavior of Austenitic Stainless Steel Weld Metals with Microfissures. *Journal of Materials Processing Technology*.; Vol. 171, No. 1, pp. 150-155.

[15] Gojić, M. (2003): *Tehnike spajanja i razdvajanja materijala*. Metalurški fakultet, Sveučilište u Zagrebu, Sisak.

[16] Farid, M., Molian, P. A. (2000): High-

Brightness Laser Welding of Thin-Sheet 316 Stainless Steel. *Journal of Materials Science*.; Vol. 35, No. 15, pp. 3817-3826.

[17] Tehovnik, F., Vodopivec, F., Kosec, L., Godec, M. (2006): Hot Ductility of Austenite Stainless Steel with a Solidification Structure. *Materiali in Tehnologije*.; Vol. 40, No. 4, pp. 129-137.

[18] Woo, I., Kikuchi, Y. (2002): Weldability of High Nitrogen Stainless Steel. *ISIJ International*.; Vol. 42, No. 12, pp. 1334-1343.

[19] Boothby, R. M. (1986): Solidification and Transformation Behaviour of Niobium-Stabilized Austenitic Stainless Steel Weld Metal. *Materials Science and Technology*.; Vol. 2, No. 1, pp. 78-87.

[20] San Martin, D., Rivera Diaz del Castillo, P. E. J., Peekstok, E., van der Zwaag, S. (2007): A New Etching Route for Revealing the Austenite Grain Boundaries in an 11.4% Cr Precipitation Hardening Semi-Austenitic Stainless Steel. *Materials Characterization*.; Vol. 58, No. 5, pp. 455-460.

[21] Padilha, A. F., Rios, P. R. (2002): Decomposition of Austenite in Austenitic Stainless Steels. *ISIJ International*.; Vol. 42, No. 4, pp. 325-337.

[22] David, S. A. (1981): Ferrite Morphology and Variations in Ferrite Content in Austenitic Stainless Steel Welds. *Welding Journal*.; Vol. 60, pp. 63-71.

[23] Park, S. H. C., Sato, Y. S., Kokawa, H., Okamoto, K., Hirano, S., Inagaki, M. (2003): Rapid Formation of the Sigma Phase in 304 Stainless Steel During Friction Stir Welding. *Scripta Materialia*.; Vol. 49, No. 12, pp. 1175-1180.

Sustainability and aggregates: selected (European) issues and cases

Trajnostni razvoj in mineralne surovine za gradbeništvo: izbrana (evropska) vprašanja in primeri prakse

Slavko Šolar[1], Deborah Shields[2], William Langer[3], Paul Anciaux[4]

[1]Geological Survey of Slovenia, Dimičeva ulica 14, SI-1000 Ljubljana, Slovenia;
E-mail: slavko.solar@geo-zs.si
[2]USDA Forest Service, Rocky Mountain Research Station, Fort Collins, CO 80526, USA;
E-mail: dshields@lamar.colostate.edu
[3]US Geological Survey, Denver, CO 80225-0046, USA; E-mail: blanger@usgs.gov
[4]European Commission, Enterprise and Industry Directorate-General, Unit I/2 - Steel, non-ferrous metals and other materials, B-1049 Brussels, Belgium;
E-mail: paul.anciaux@ec.europa.eu

Received: September 21, 2007 **Accepted:** December 12, 2007

Abstract: Sustainable aggregate resource management (SARM) is based on three pillars of sustainability: environmental, economic and social. The main environmental aspect is preventing or minimizing negative impacts by following these principles: precautionary principle, polluters' pay, and eco-efficiency. Economic aspects are (a) maintaining a viable business environment; (b) encouraging value-added production and employment; (c) embracing full-cost accounting while remaining competitive, and (d) providing for the material requirements of society. Social aspects incorporate: (a) identifying stakeholders' values, interests, goals, furthermore (b) transparency, (c) public participation in decision making, (d) communication and education. In order to provide information, indicators of sustainability for minerals of the European Union and indicators for aggregates for selected countries, including Slovenia are presented.

Povzetek: V članku obravnavamo gospodarjenje z mineralnimi surovinami za gradbeništvo po načelih trajnostnega razvoja, pri čemer so upoštevani okoljski, gospodarski ter družbeni vidiki. Okoljski vidik upošteva preprečevanje oziroma zmanjševanje negativnih vplivov na okolje, pri čemer upošteva načela: previdnosti, onesnaževalec plača ter eko-učinkovitost. Ekonomski vidiki so: ohranjanje gospodarske dejavnosti, povečevanje dodane vrednosti in zaposlenosti, upoštevanje vseh stroškov proizvodnje ter ohranjanje materialne osnove za blaginjo družbe. Družbeni vidiki upoštevajo vrednote in interese udeležene javnosti, transparentnost, sodelovanje javnosti pri odločanju, komunikacijo in izobraževanje. Poleg

Scientific paper

tega obravnavamo tudi kazalce gospodarjenja z mineralnimi surovinami glede na vse tri vidike trajnostnega razvoja, in sicer na nivoju Evropske unije ter posameznih držav, vključno Slovenije.

Key words: aggregates, sustainable development, management, Europe
Ključne besede: mineralne surovine za gradbeništvo, trajnostni razvoj, gospodarjenje, Evropa

INTRODUCTION

Many of the social and environmental problems we face today are complex, urgent, and interconnected across systems. The partial, system-specific solutions used in the past have proven ineffective when applied in such circumstances. The Earth Summit held in Rio de Janeiro in 1992 brought the concept of sustainable development to the attention of the world. The sustainability paradigm is applicable to the types of problems mentioned above because it is both comprehensive and flexible. The overarching goals of sustainability are: economic prosperity, environmental health and social equity. These goals are simple and flexible enough to allow for multiple interpretations and are applicable in a variety of circumstances (ŠOLAR, 2003a).

They are, for example, applicable to mining. The purpose of mining is the extraction and processing of mineral resources. These resources are almost entirely nonrenewable; an individual deposit cannot be recreated except through natural geological processes. Nonetheless, over the past ten years, public discourse on the compatibility of mining and sustainability has progressed from disbelief and rejection, to scepticism, to general acceptance. The basic reason is recognition of the fact that mineral resources are both essential and can be provided in a way that protects the environment and respects the needs and rights of communities. Doing so, however, will require policies that promote and support sustainable behaviors and outcomes.

Policies reflect the values and objectives of the people involved in their creation. That is as true for mineral policies as it is for environmental, monetary or trade policies. According to most general definitions, management deals with the process of planning, organizing, and governing the efforts of co-workers in order to achieve stated goals of an institution. Management therefore about is optimizing the use of human and material resources, together with financial and other contributions, to operationalize policies. The objectives of a sustainable mineral resource policy and associated management plan, and the form they take, will differ between regions and countries due to the interplay of differing value sets, goals and objectives (LANGER et al., 2003).

Differences not withstanding, there are similarities across sustainable mineral policies and management plans. The foundational concepts are: a) facilitating the transformation of natural mineral capital into built physical, economic, environmental or social capital of equal or greater value; b) ensuring that environmental and social impacts of mining are minimized; c) addressing the trade offs that society needs to make, and d) taking all relevant scale hierarchies into consideration.

Aggregate Resources

Mineral resources are classified in many ways. Most commonly they are classified into non-metals, metals and (solid or fluid) energy resources. Non-metals consist of two major groups: industrial minerals, and construction materials. Within the construction materials group aggregates (crushed stone, sand and gravel) are prevailing over others (such as clay, dimension stone, etc.) in terms of volume produced.

Natural aggregate consists of material composed of rock fragments that may be used in their natural state or after mechanical processing such as crushing, washing, and sizing. Natural aggregate consists of gravel and crushed stone. Gravel generally is considered to be material whose particles are about 2.0 to 64.0 millimeters in diameter. Its edges tend to be rounded due to the effects of repeated contact among particles. Crushed stone is of the same size range, but is artificially crushed rock, boulders, or large cobbles. Most or all of its surfaces are produced by crushing, which results in sharp and angular edges. Natural aggregate has hundreds of uses, from chicken grit to the granules on roofing shingles. However, most aggregate is used in concrete, asphalt, and for other construction purposes (Langer & Šolar, 2002).

Natural aggregate extraction is the most important mining industry in the world in terms of production volume (15,000 million tones per annum), and is second only to fossil fuels in terms of production value (70,060 million euros) (Regueiro et al., 2002). The average per capita consumption of aggregate generally ranges from 5 to 15 tons per year (Langer & Šolar, 2002). More than 3 billion tones of sand, gravel and crushed stone are produced annually to meet the demands of the European building and construction industries. Assessment of the actual quantities of construction minerals produced in Europe is difficult because some of the national statistics that are being provided to the European Statistical Office are based on a representative survey of the aggregates sector, which means that not all small and very small quarries are covered by the European statistics.

Aggregate is heavy and bulky. Transportation can add significantly to the cost of aggregate. For example, transporting aggregate 30 to 50 kilometers can double its price. As a result, aggregates have historically had a narrow economic transportation radius, which has led to the presence of extraction near urban areas. While most of the construction minerals continue to be produced close to the major development centers, the establishment of mega-quarries next to the sea in Norway and in Great Britain is a new development that could have important consequences for parts of Europe which can be reached by bulk carriers.

Developing aggregate resources impacts the environment. Most environmental impacts are not serious and can be controlled by employing careful mining practices (environmentally friendly and economically efficient) using available technology. However, there are some geologic situations where mining aggregate may lead to serious environmental impacts, especially with regard to ground water, air, and noise pollution. Environments that are particularly prone to impacts from aggregate extraction include karst and stream channels. One of the most serious environmental problems is the dereliction of abandoned pits or quarries. The reclamation of mined-out land is an important aspect of reducing environmental impacts of aggregate extraction.

In regions with economic growth, the negative public perception of quarrying increases in tandem with demand for aggregates. Operators face serious difficulties in opening new, or maintaining current, quarries or pits. More generally, societies face several dilemmas with regard to aggregate resource management: a) the existence of abundant sites with suitable aggregate that also have conflicting land uses, zoning, regulations, or citizen opposition, and b) conflict between regional demand and local opposition to resource extraction.

Aggregates should be managed similarly as other earth resources / minerals taking into account their specifics (described below).

SUSTAINABLE AGGREGATE RESOURCE MANAGEMENT

A sustainable aggregate resource management (SARM) plan can be organized according to the three main dimensions of sustainability: environmental, economic and social (ŠOLAR et al., 2004).

Environmental aspects of SARM

SARM requires developing aggregate resources in an environmentally responsible manner that does not result in long-term environmental harm, even if short-term environmental impacts are unavoidable. Two main environmental categories should be considered in SARM: reducing negative environmental impacts and resource protection / conservation. These goals are very achievable because the aggregate industry has made, and continues to make, great strides in environmental management.

Three principles inform the forgoing requirements: the precautionary principle, the polluter pays principle, and eco-efficiency. The meaning of the precautionary principle has evolved since its introduction in the 1970's. Initially it stated that actions to protect the environment should not be delayed simply because full information was unavailable. This is the meaning used in the Rio Declaration, which states that the lack of "full scientific certainty shall not be used as a reason for postponing cost-effective measures to prevent environmental degradation"(UN, 1992). The obverse definition is now dominant. We should not take actions in the absence of full information, if those actions have a high probably of causing social, economic, or environmental impacts (FOSTER et al., 2000). Both versions apply to quarrying. The precautionary principle implies the use of environmental impacts assessments, risk analysis and other tools so as to promote the goal of nature conservation.

The polluter pays principle requires funding reclamation / remediation of negative impacts within the quarry and over the mine life cycle including after-care. Eco-efficiency is achieved through the implementation of efficient production practices (with minimal material and energy use and emissions), efficient use of land / space, and the full exploitation of reserves and resources.

Most destructive environmental impacts of aggregates are on the landscape (visual intrusions), air (noise, dust), water (surface, underground water), soil (erosion, pollution), and on biota (loss of biodiversity). Besides type, the nature of impacts (range, timing, duration, ability to prevent /control) should also be considered (Langer & Arbogast, 2002). There are many regulatory and voluntary tools that can be used to identify, reduce and control negative environmental impacts. These include environmental impact assessment, environmental management systems, environmental accounting, environmental reporting, life cycle analysis, ISO 14000 standards. These tools can be applied both on-site (quarry & processing facility) and to transportation routes.

SARM, however, is not just about protecting the environment from the potential negative impacts of aggregate extraction. Reclaiming aggregate operations or orphaned sites has tremendous potential to improve our quality of life, create additional wealth, increase biodiversity, and restore the environment. In the expanding suburban areas of today, mined-out aggregate pits and quarries are converted into second uses that range from home sites to wildlife refuges, from golf courses to watercourses, and from botanical gardens to natural wetlands. Reclamation should be a major consideration in sustaining the environment and in creating biodiversity (Langer, 2003a).

Mineral resource (aggregate) protection includes: a) minimal exploitation of primary aggregates with rational production by introducing the recycling and reuse of construction materials as aggregates; b) exploitation of renewable aggregate and substitute resources; c) increasing the knowledge about aggregate potential, and d) preserving the land access to aggregates in designated areas. The first two of these protection measures are intended to reduce the demand for aggregate that is newly mined or from newly developed sites. The latter two address the long-term need for primary materials (Šolar, 2003).

Economic aspects of SARM

There are four main economic aspects to SARM: a) maintaining a viable business environment; b) encouraging value-added production and employment; c) embracing full-cost accounting while remaining competitive, and d) providing for the material requirements of society. The first two of these are the responsibility of government. The third is the responsibility of the firm. And the fourth is a shared responsibility of government and the firm.

All societies utilize a stream of material inputs for manufacturing and construction. In the case of transition and post-conflict economies, there is particular need for construction materials to support development and rebuilding of infrastructure, industrial capacity, and housing. One aspect of SARM involves ensuring that these resources are available to the marketplace. This is sometimes referred to as secure supply. The main elements of secure supply are creation or maintenance of production capacity, identification of sufficient reserves and resources, provision of land access (extraction and exploration sites / areas), and development of the country's or region's infrastructure capacity (roads, railroads, power). All the foregoing issues are interlinked and need to be balanced by policy makers and resource managers.

A viable business environment exhibits the following characteristics: a) a stable and feasible permitting regime; b) consistent application of rules and regulations; c) functioning capital markets; d) reasonable levels of taxation, and e) well-defined property rights. Under employment and unemployment are serious problems in many parts of the world. Therefore, governments should also consider setting policies that support the availability of a trained workforce and promote employment in the extractive industries. Development of value-added manufacturing is another important issue. Existence of a value-added sector can reduce the need for imported materials while allowing the domestic economy to capture economic benefits (profits, employment, tax revenues) that would otherwise accrue in another country.

Economic realities drive industry activity. Firms need to remain competitive if they are to stay in business. Nonetheless, firms have a responsibility to accept the full cost of doing business, including costs of preventing or remediating environmental damage. Industry must be willing to accept the fact that in some cases, when all the costs are taken into consideration, a quarry will not be a viable economic enterprise and must be either shut down or not developed. Firms can, however, increase competitiveness by modifying production processes, upgrading product quality, and maintaining a well trained workforce. Production process and product quality can be achieved through voluntary quality control procedures such as adherence to ISO 9000 requirements. Quality is an important market element that can be labeled and traded. Research and development (R&D) is another issue that increases the enterprise's overall performance and has a great impact on increasing the added value. Some of R&D's goals include new products, and using BAT (best available technology) in the field. Finally, maintaining or increasing employment is not only governmental issue, because human resources are one of most important driving forces of every enterprise. Corporate culture, knowledge and skills need to be created, maintained, reviewed and revised (if necessary). Special attention with regard to human resources should be put on health and safety of employees.

The issues described above, along with many others, represent the economic aspects of managing aggregates in a manner that would ensure future aggregate supplies and achieve the sustainability goals of different stakeholders. Their various and different goals and linkages among those interests and goals are described within social aspects of SARM (ŠOLAR, 2003).

Social aspects of SARM

Identifying stakeholders' values, interests, goals and the scale at which they apply is the first step in resolving the complex situations that impact a country's ability to maintain a secure material supply and achieve other policy goals. As an example, there may be abundant sites in a region that have suitable aggregate, but the existence of conflicting land uses, zoning, regulations, or citizen opposition can lead to insufficient or more costly supply. Scale of interest is a consideration in such situations due to fact that benefits and costs accrue to different parties in different regions. A third important issue is intra-generational equity, fairness to those living near, or impacted by, quarrying. Equity implies a need for transparency and public participation in decision making, as well as access to information within democratic process (Šolar, 2003).

Broader societal aspects can be described in terms of the legal framework, communication and education. The legal framework should protect the interests not only of country or region, but also investors and all other stakeholders. An effective legal framework needs balance between administrative requirements and flexible, time efficient, inexpensive procedures of licensing. Further, a country or region needs to have the institutional capacity to implement and enforce the legislation (monitoring and control components in particular), to develop and maintain resource information infrastructure, to foster research and development, to use funds from mineral rents (taxes) for the benefit of current and future generations, and facilitate cooperation with other sectors.

In addition to the legal framework, voluntary initiatives from different stakeholders (industry, non-governmental organizations) enrich dialogue and facilitate agreements. Voluntary initiatives include communication, education, partnership, and participation. All stakeholders should have access because increase awareness of the costs and benefits of supplying materials to society will lead to more timely agreements about how to (re)distribute costs and benefits of aggregate extraction and use (Šolar, 2003).

Best practices

To be effective, SARM must be a pragmatic pursuit, not an ideological exercise. It is an iterative process and government, citizens, and industry should all be involved in the pursuit. The process consists of a number of steps, including issuance of policy statements, elaboration of objectives, establishment of actions, identification of indicators, and monitoring (Langer, 2003c).

- Policy statements issued by governments commonly identify the aggregate industry as a key industry contributing to jobs, wealth, and a high quality of life for its citizens, and commit the government to the protection of critical resources and protection of citizens from the unwanted impacts from aggregate extraction. Industry policy statements commonly identify environmental and societal concerns and commit the company to environmental stewardship and interaction with the community.
- Objectives describe what is to be accomplished and commonly are subsets of the social, economic and environmental components of SARM. Typi-

cally objectives will include, but not be limited to: a) ensuring future supplies of aggregate; b) reducing the demand for newly mined aggregate, and c) protecting and restoring the environment (LANGER, 2003b).

- Actions are associated with each objective and describe the steps to reach the objective.
- Indicators deserve special mention. They measure progress as well as the effects of efforts to protect and enhance natural and human systems and will be discussed in more detail below.
- Monitoring, feedback, and the regular reconsideration of requirements as events develop all help to refine the SARM process. The establishment of a joint monitoring process presents an excellent opportunity to forge partnerships with communities and involve citizen groups.

MINERALS INDICATORS

From the steps described above more attention is given only to indicators due to the paper length. First, minerals indicators for European Union are described, and then some aggregate indicators within EU are presented.

There are three basic functions of indicators: simplification, quantification, and communication. Indicators of sustainability should be used as tools for knowledge, information transfer, as integral parts of other initiatives and sets of indicators, and as a solid base for decision making. The selected set of indicators should express a need for balance: (a) among stakeholders; (b) between the process of defining indicators and the set of chosen indicators, and (c) among the dimensions of sustainability (ŠOLAR, 2003).

EU minerals indicators (SHIELDS et al., 2005)

In May 2000, the European Commission published a Communication on "Promoting sustainable development of the EU non-energy extractive industry" (EUROPEAN COMMISSION, 2000). Stakeholder dialogue was one of the important issues mentioned in this Communication that should be improved to achieve a more sustainable minerals industry. Indicators are a useful tool to create a platform for dialogue where different stakeholders are able to define, discuss and evaluate the performance of industry and its contribution to society. The indicators are to serve as a generally understandable means of communication between the different interest groups: (a) the companies, which can represent their economic, ecological and social welfare benefits vis-à-vis other stakeholders, (b) the national, regional and local administrations, which (depending on the legal conditions) examine these performances, and/or give access to land for mineral extraction, (c) the public (local, regional or national population, non-governmental organizations, media), whose interests are affected by existing or new sites.

A Working Group was set up in 2000 as a sub-group of the Raw Materials Supply Group. The Working Group, chaired by the Enterprise and Industry Directorate General, consisted of about 20 experts from industry, Member States, a university and an NGO. It was decided to develop the indicators taking a bottom-up approach and applying the characteristics used for the Global Reporting Initiative (GRI, 2000), i.e., that the indicators should have relevance, reliability, clarity, comparability, timeliness and verifiability. The work on indicators was limited to those phases of the production process that involved the extraction of raw materials, primary refining and the use of secondary raw materials.

Very early in the process a distinction had to be made between indicators at company/ site level and indicators at national (Member State) level.

As a result of indicator creation process the list of minerals' indicators was shortened to provide 13 priority indicators at company level, and 7 indicators at Member State level. They were not developed with a specific policy application in mind, but instead were chosen because they provided a useful picture of the sustainability of the industry, while the data collection requirements were considered to be achievable. The aim was to develop indicators, which can serve at the following scales/ levels as a common basis for dialogue for all involved interest groups: companies and/ or sites, industrial sectors, regional or national, and EU. Current status of the EU Minerals Indicator process is available on internet (http: // ec.europa.eu / enterprise / steel / non-energy-extractive-industry / sd-indicators.htm). Challenges and realities affecting the process are financial realities and difficulties in data collection. Commission's involvement is mainly to costs involving chairing and hosting meetings of the Working Group, some translation costs and hard copy publications. Industry federations and companies have mainly contributed involving people to the process of the Working Group, investing time and money in the data collection process and disseminating the results. The data collection in the SME-dominated sector has proven to be difficult, is further complicated by the business sensitivity of certain data (e.g. lime: energy efficiency), and in general it remains a constant challenge to motivate the companies to participate.

Aggregate Indicators (Langer et al., 2003)

Indicators for aggregates should support public awareness of issues related to sustainable resource management of aggregates and facilitate explicit consideration of the full range of costs and benefits of mineral development of aggregates. Mineral resource development, extraction, use and disposal are complex activities that can be described in many ways. It follows that there are multiple ways to organize mineral indicators. One method is to organize indicators according to the three dimensions of sustainability: economy, environment and society. An alternative is use a life cycle approach.

United Kingdom

In the United Kingdom, natural resource policy, including policies for aggregates, is covered by an overall national development document: "A Better Quality of Life: A Strategy for Sustainable Development for the United Kingdom" (United Kingdom, Department for Environment, Transport and Regions, 1999). In English counties, two levels of plans affect the Mineral Development Plans (Harrison et al., 2002): (1) Structure plans that set out general principles and policies for all forms of development, and (2) Mineral Local Plans that set out detailed policies governing mineral extraction. (See http://www.qpa.org/sus_report01.htm for the UK Quarry Production Association report on SDI's for the aggregate sector).

Every county (minor administrative unit) is required by law to develop, implement and review a Mineral Local Plan. The Durham County Mineral Local Plan (County Durham, 2003) states that provision should be made for at least 82 million tonnes of aggregates per annum, and that part of crushed stone should come from recycling and re-using construction materials. Their stated objectives are to: (1) ensure the efficient use of resources, and (2) minimize the use of non-renewable resources. Each objective has targets and associated indicators. The target of the first objective is to maintain a landbank necessary to meet supply demands. This target is supported by following indicators: (a) the amount of mineral extracted per annum, (b) any changes in the landbank or permissions granted, (c) the viability of the existing landbank, (d) the level and type of employment activity within sector, and (e) changes in the landbank and permissions with Tees Valley. The second objective has a target to increase the production of secondary and recycled materials and implicitly to decrease production of primary materials. This target is observed by two indicators: (a) the amount of materials recycled per annum, and (b) the level and type of employment activity within the sector.

Italy

The Province of Modena, located in the Emilia Romagna Region in northern Italy, recognizes that natural aggregate and clay is necessary to sustain the economic well being of the region (Langer et al., 2003a). Modena Province is preparing a Variant of the Intraregional Plan for Extractive Activities (PIAE) that has been in place in the Province since 1993 (Provincia di Modena, 1995; 1996; 2000; 2001). One objective of the Variant of the PIAE is to minimize the impacts from quarrying and guarantee the reclamation of quarries in a manner consistent with the existing landscape. In order to accomplish that objective, the Emilia Romagna Region, in the 1993 PIAE, developed the innovative concept of the polo estrattivo, (extractive district). The polo estrattivo is not just one or more quarries, but is the whole of the area characterized by the prevalence of quarrying activities including the intervening and surrounding territory that is subject to quarrying impacts (Langer et al., 2003a). A number of draft sustainability indicators were developed to support the Variant of the PIAE (Langer et al., 2003a). Selected indicators for aggregates of the Modena Province are: (1) increase in number of poli from the old 1993 PIAE to the new Variant of PIAE, (2) ratio of area within poli converted to extraction versus area outside poli converted to extraction, (3) volume of aggregate produced per amount of surface area converted to extraction, (4) percentage of aggregate processing plants that have been moved into pits within a poli, (5) percentage of abandoned quarries that have been reclaimed, (6) percentage of perifluvial areas in need of reclamation that have been reclaimed, and (7) percentage of reclaimed quarry area that has been reclaimed as wetland areas.

Slovenia

Mineral resources, including construction materials, should be treated as integral to every country's overall sustainability considerations. Large infrastructure or building projects require substantial material inputs, and their provision should be handled in a manner that is consistent with sustainable development principles. Development of a sustainable mineral resource management plan, and creation of related indicators, will increase the likelihood of this occurring. The 1999 Slovenian Mining Act (partly revised in 2004) mandated the development of a mineral resource programme, the current draft of which is based on sustainability principles.

The indicator resides at the top of an information pyramid that provides a wide range of spatially dispersed information. While useful and informative, the indicator we present here cannot alone tell the complex story of sustainability. Rather it is intended as one of a set of indicators that, when taken together, describe how implementation the national mineral resource management programme is affecting the sustainability of Slovenia.

The case study addresses the sustainable supply of aggregates indicator for Slovenia that is based on policy goals of industry, government and civil society. The indicator is intended as one of a set of indicators that would tell about the trends of implementation the national mineral resource management programme. The latter is required by in 1999 passed mining act.

In Slovenia, the policy goals for aggregates are to secure the aggregate supply, eliminate illegal aggregate extraction, and reduce the overall number of aggregate extraction sites. The latter goal is strongly supported by public opinion on both the local and national scales, as well as by the land use planning and nature conservation authorities. These goals are included in the proposed National Mineral Resource Management Programme (NMRMP), required by the Mining Act. Elimination of illegal quarrying has two aspects: (1) stricter law and regulation implementation to stop the illegal activity, and (2) legalization of those quarries that fulfill land use and mining legal requirements. The mission of the NMRMP is stated to be ensuring minerals supply and land access by following sustainable development principles. One of the most important of those principles is stakeholder involvement; the plan to secure aggregate supply must reflect the objectives of various stakeholders. The desired outcome (included in NMRMP) is for a high number of legal quarry sites to have what are termed acceptable production and enough reserves/resources. For Slovenia, a "proper" quarry would have (acceptable) production annually between 50,000 and 500,000 tonnes, and (enough) reserves for between 10 and 50 years of average production. These levels were chosen so as to address the competing objectives of the stakeholders listed above. In Slovenia, there is so far only one "final" indicator, which resides at the top of a pyramid of primary (raw) and secondary (analysed) data. It is: »Percentage of "proper" quarry sites by administrative unit, across spatial scales, i.e., from municipality to country«.

Annual data needs will include the number of sites, their production, reserves, and resources of aggregates. These data are transformed into an indicator by combining them with land area (on 1,000 km^2, or on administrative, statistical units) and, as a proxy for demand, on population.

The sustainable supply of aggregates indicator is on the top of information pyramid that provides a wide range information that is spatially dispersed information and useful on different levels and to different stakeholders. The information pyramid includes auxiliary indicators, i.e., indicators of I and II. order. All information is stored in suitably organized databases that provide an easy access.

Conclusions

Natural aggregate is the number one non-energy mineral resource in the world in terms of value and volume and is a necessary commodity for sustainable communities. While it is a non-renewable resource, supplies of aggregate are nearly inexhaustible on a global scale. Natural aggregates have characteristics that differentiate them from most other mineral commodities: a high number of potential extraction sites, a high volume to value ratio, and regional importance combined with a narrow economic transportation radius. Because of these and other differences, resource management policies for aggregates should differ from "general" mineral resource policies, even though the end goal is the same for both – ensuring sustainable resource management. Beyond requiring traditional geo-technical, environmental and economic assessments, sustainable policy for aggregates should address: 1) construction material flows and quarry life cycle, 2) the public acceptability of quarries near human habitation, 3) optimizing present and future aggregates supply, including optimal use of current reserves, new locations, recycling, reuse, and substitutions, and 4) stress aggregate-extraction specific environmental and resource pressures. To achieve the goals of sustainable aggregate management each stakeholder – government, industry, the public, and non-governmental organizations – will need to accept certain responsibilities, one of the most important of which is to become informed about natural resource issues. Sustainability is about making trade offs among competing objectives and people disagree about the appropriate balance among the goals of economic prosperity, social equity and environmental health. One of the primary purposes of mineral indicators is to provide information to decision makers and the public so as to ensure that the public debate about policy choices is grounded in fact.

Acknowledgements

This paper was presented as invited lecture at 4.ULUSAL KIRMATAŞ SEMPOZYUMU "Agrega (Beton, Asfalt), Çimento Hammaddeleri Madenciliği" in December 2006 in Istanbul, Turkey.

Povzetek

Trajnostni razvoj in mineralne surovine za gradbeništvo: izbrana (evropska) vprašanja in primeri prakse

Med mineralnimi surovinami so mineralne surovine za gradbeništvo po količini in vrednosti najpomembnejše in predstavljajo del želene prihodnosti človeštva. Kljub temu, da so neobnovljiv vir, je možna skoraj neomejena oskrba z njimi. Mineralne surovine se razlikujejo od večine drugih surovin po velikem številu možnih lokacij pridobivanja, po velikih odkopanih količinah, nizki ceni surovine ter po njenem regionalnem pomenu glede na omejitev z višino transportnih stroškov. Zaradi teh in drugih posebnosti je potrebno, da se tudi usmeritve gospodarjenja z njimi razlikujejo od gospodarjenja z drugimi mineralnimi surovinami, čeprav je za vse enoten cilj: zagotavljanje gospodarjenja po načelih trajnostnega razvoja. Poleg zahtevanih rudarskih, okoljskih in ekonomskih ocen in vrednotenj, naj bi trajnostne usmeritve / politike za mineralne surovine za gradbeništvo obsegale tudi: (a) oblikovanje snovnih tokov materiala in življenjski cikel odkopa, (b) družbeno sprejemljivost odkopov v bližini naselij, (c) optimizirane sedanje in prihodnje oskrbe, vključno z optimalno rabo sedanjih zalog, novih lokacij, recikliranja, ponovne uporabe in zamenjave materialov ter (d) poudarek na specifičnih okoljskih negativnih vplivih. Za dosego želenih ciljev je potrebno, da vsi udeleženci (vlada, industrija, javnost, nevladne organizacije) prevzamejo odgovornost, od katerih je ena najpomembnejših prav zanesljivo in pravočasno informiranje. Trajnostni razvoj vključuje izbiro med več možnostmi glede na vrednote, želje in cilje posameznih vpletenih delov družbe. Zaradi tega je težko doseči ravnotežje med ekonomskim napredkom, družbeno enakostjo ter zdravim okoljem. Osnovna naloga kazalcev je informiranje javnosti, da javna razprava temelji na ustreznih in zanesljivih argumentih.

References

County Durham (2003): *County Durham Minerals Local Plan*. December, 2000. (electronic source: http://www.durham.gov.uk/durhamcc/usp.nsf/pws/Policies+-+County+Durham+Minerals+Local+Plan. Accessed in April 2003 and in May 15 January 2007.

European Commission (2000): *Communication of the Commission (No. 265) 2000: Promoting sustainable development in the EU non-energy extractive industry*. Brussels, 2000, 21 p.

Global Reporting Initiative - GRI (2000): *Sustainability Reporting Guidelines*. London, ICMM, June, 2000, 16 p.

Foster, K., Vecchia, P. & Repacholi, M. (2000): Science and the Precautionary Principle. S*cience*. May 12, 2000, pp. 979-981.

Harrison, D.J., Chapman, G.R., Collins, R., Hillier, J.A., Highley, D.E. & Steadman, E.J. (2002): *Construction Raw Materials Policy and Supply Practices in Northwestern Europe. Facts and Figures*

– *England, Scotland and Wales (Great Britain)*. British Geological Survey, Commissioned Report CR/02/082N, Keyworth, Nottingham.

LANGER, W.H & ARBOGAST, B. (2002): Environmental impacts of mining natural aggregate. *In: Fabbri, A.G. (ed.), Gaal, G. (ed.), McCammon, R. B. (ed.). Deposit and geoenvironmental models for resource exploitation and environmental security*. (NATO science series, Series 2, Environmental security, Vol. 80). Dordrecht, Kluwer, pp. 151-170.

LANGER, W. H. & ŠOLAR, S. V. (2002): Natural aggregate resources - environmental issues and resource management: report of Working Group 5. *In: Fabbri, A.G. (ed.), Gaal, G. (ed.), McCammon, R. B. (ed.). Deposit and geoenvironmental models for resource exploitation and environmental security*. (NATO science series, Series 2, Environmental security, Vol. 80). Dordrecht, Kluwer, pp. 525-532.

LANGER, W. H., ŠOLAR, S. V., SHIELDS, D. J. & GIUSTI, C. (2003): Sustainability indicators for aggregates. *In: Agioutantis, Z. (ed.). Proceedings of the International Conference on Sustainable Development Indicators in the Mineral Industries*. Milos, Milos Conference Center - George Eliopoulos, pp. 251-257.

LANGER, W.H. (2003a): Part 2: Creating a Sustainable Future. Sustainable aggregate resources management is integral to our social, economic, and environmental systems. Department: Carved in Stone. *Aggregates Manager*. October, 2003. http://www.aggman.com/.

LANGER, W.H. 2003b, Part 3: Creating a Sustainable Future. Road trip highlights SARM - efficient aggregate use, resource conservation, and environmental protection. Department: Carved in Stone. *Aggregates Manager*. November, 2003. http://www.aggman.com/.

LANGER, W.H. 2003c, Part 4: How Can We Begin SARM? The process includes policy statements, objectives, action steps, measuring progress, and monitoring. Department: Carved in Stone. *Aggregates Manager*. December, 2003. http://www.aggman.com/.

LANGER, W.H., GIUSTI, C., and BARELLI, G. (2003a): Sustainable development of natural aggregate with examples from Modena Province, Italy. *Society for Mining, Metallurgy, and Exploration Preprint 03-45*. Littleton, Colorado, 9 p.

PROVINCIA DI MODENA (1995): Il Piano Infraregionale per le Attività Estrattive della Provincia di Modena: Quaderni di documentazione ambientale. *Poligrafico Mucchi*. Modena, Italy, 85 p.

______. 1996. P.I.A.E. Piano Infraregionale per le Attività Estrattive (L.R. 17/91 e successive modifiche) Relazione Illustrativa. Modena, Italy, 148 p.

______. 2000. Variante Parziale N°1 al P.I.A.E.-Piano Infraregionale per le attività Estrattive. Modena, Italy, 90 p.

______. 2001. Piano di Azione Operativo

Agenda 21 Locale. Forum Ambiente e Sviluppo Sostenibile. Modena, Italy, 213 p.

Regueiro, M., Martins, L., Feraud, J., & Arvidsson, S. (2002): Aggregate extraction in Europe: the role of the geological surveys. *Raw materials planning in Europe – Change of conditions! New perspectives?* Proceedings, Third European Conference on Mineral Planning, Krefeld, Germany, October 8-10, pp. 187-198.

Shields, D J., Šolar, S. V., Anciaux, P., Villas Boas, R. C. (2005): Regional, national and continental minerals indicators projects: commonalitiesand differences in process and product. *In: MARTENS, Per Nicolay (ed.). Sustainable development indicators in the minerals industry.* Essen, Glückauf, 2005, pp. 95-109 (late ed.).

Šolar, S. V. (2003): *Indicators of Sustainable Development for a Mineral Resource Management Plan: the case of open pits: Doctoral Dissertation*. University of Ljubljana, 182 p., 3 app.

Šolar, S. V. (2003a): Long-term spatial planning and mineral resource management - case study: aggregates in Slovenia. *In: 4th European Congress on Regional Geoscientific Cartography and Information Systems*. Bologna, Italy, pp. 680-682.

Šolar, S. V., Shields, D. J., Langer, W. H. (2004): Important features of sustainable aggregate resource management = Pomembne značilnosti trajnostnega gospodarjenja z mineralnimi surovinami za gradbeništvo. *Geologija*.; Vol. 47, No. 1, pp. 99-108.

United Kingdom, Department for environment, transport and regions (1999): *A better quality of life: a strategy for sustainable development for the United Kingdom*. London, The Stationary Office.

United Nations (1992): *Rio Declaration on Environment and Development*. Rio de Janeiro, June, 1992. (U.N. Doc./CONF.151/5/Rev.1).

Spodnjetriasne plasti na južnovzhodnem obrobju Ljubljanske kotline, osrednja Slovenija

Lower Triassic beds in the southeastern borderland of the Ljubljana depression, central Slovenia

Stevo Dozet[1], Tea Kolar-Jurkovšek[1]

[1]Geološki zavod Slovenije, Dimičeva ulica 14, SI-1000 Ljubljana, Slovenija;
E-mail: stevo.dozet@geo-zs.si, tea.kolar@geo-zs.si

Received: September 6, 2007 **Accepted:** October 17, 2007

Izvleček: Spodnjetriasne plasti na južnovzhodnem obrobju Ljubljanske kotline, ki pripada geotektonski enoti Dolenjsko-Notranjskih mezozojskih grud, so sestavljene iz plastnatih in ploščastih dolomitov in klastičnih kamnin, ki vsebujejo v srednjem delu nekaj deset metrov debel člen oolitnih apnencev, v vrhnjem delu pa člen ploščastih dolomitnih apnencev. Okoli 450 m debelo spodnjetriasno zaporedje sedimentnih kamnin je razdeljeno v 9 litostratigrafskih enot. Konkordantno pod pestro razvitimi pisanimi spodnjetriasnimi sedimenti leže brez vidne prekinitve sedimentacije temne plastnate in ploščaste karbonatne kamnine zgornjega perma s skromno mikrofavno in mikrofloro.

Abstract: The Lower Triassic beds in the southeastern Borderland of the Ljubljana Depression, belonging to the geotectonical unit of the Dolenjska-Notranjska Mesozoic Blocks, are composed of bedded and platy dolomites as well as clastic rocks, comprising in the middle part several ten metres thick gastropod oolite member and in the uppermost part the member of platy dolomitic limestones. About 450 m thick Lower Triassic succession of sedimentary rocks is subdivided in 9 lithostratigraphic units. Concordantly under the variously developed variegated Lower Triassic sediments lie the Upper Permian dark bedded and platy carbonate rocks with scarce microfauna and flora.

Ključne besede: lito- in biostratigrafija, spodnji trias, konodonti, Slovenska karbonatna platforma, Dolenjsko-Notranjske mezozojske grude

Key words: Litho- and biostratigraphy, Lower Triassic, conodonts, Slovenian Carbonate Platform, Dolenjska-Notranjska Mesozoic Blocks

Scientific paper

UVOD

Na ozemlju južnovzhodnega obrobja Ljubljanske kotline, ki v geotektonskem pogledu pripada Dolenjsko-Notranjskim mezozojskim grudam, natančneje pa tektonski enoti Krimsko-Mokrškega hribovja (BUSER,1969;1974), ni nikjer ohranjen popoln profil razvoja skitskih plasti, zato smo vpogled v skitsko sedimentacijo dobili na ta način, da smo sestavili več delnih profilov in sicer: Skopačnik-Sarsko, Klada-Škrilje in Dobravica-Podgozd.

Na območju Skopačnika je ohranjen spodnji in del srednjih skitskih plasti. Ta delni profil je ugoden predvsem zato, ker je pod skitskimi plastmi ohranjen še zgornji del zgornjepermskih plasti. Na širšem območju Sarskega izdanjajo pisani »campilski« klastiti in rdečkasto siv zgornjeskitski dolomit, medtem ko terene okoli Dobravice in Podgozda gradi poleg že omenjenega rdečkastosivega dolomita še rumenkastosivi peščeni zgornjeskitski dolomit ter rdečkastosivi ploščasti in plastnati apnenčev dolomit, dolomitni apnenec in ploščast laporovec, nad katerimi leži konkordantno debelozrnat, svetlosiv do bel srednjetriasni dolomit, ki je močno tektoniziran.

Glavni namen naših raziskav je bil sestaviti, razčleniti in opisati skitsko litološko skladovnico južnovzhodnega obrobja Ljubljanske kotline in ugotoviti uporabnost konodontov pri razčlenjevanju spodnjega dela triasnega sistema.

DOSEDANJE RAZISKAVE

Pri geološkem kartiranju listov Cerknica 1 in 2 je ŠLEBINGER (1953) prišel do zaključka, da se južnejši t.i. slemenski paleozoik nadaljuje konkordantno in neprekinjeno v werfenske sklade.

GERMOVŠEK (1955) je pri kartiranju južnovzhodnega obrobja Ljubljanskega barja pripisal temnosivemu debeloploščastemu dolomitu za senikom Rebolove kmetije in okoli Skopačnika verjetno werfensko starost. Strnjen kompleks sivega in rdečega sljudnega lapornega skrilavca s polami rdečega oolitnega apnenca med Sarskim na severu in Rebolovo kmetijo na jugu je uvrstil med zgornjewerfenske sklade.

GERMOVŠEK (1956) je sklepal, da geološke razmere ob koncu permske dobe niso bile enake po vsem slovenskem ozemlju. Werfenske plasti leže namreč na zgornjepermskem peščenjaku ali na belerofonskem apnencu oziroma dolomitu. Na začetku triasne dobe se pa že povsod odlagajo približno enake usedline.

BUSER (1962, 1976) je menil, da leže skitske plasti pri Skopačniku pri Želimljah normalno na zgornjepermskem dolomitu. Temnosivi permski dolomit prehaja navzgor najprej v rjavosiv skladovit (30-50 cm) dolomit, ki vsebuje na lezikah sljudo in se menjava z do 20 cm debelimi plastmi sivorjavega sljudnatega meljevca in peščenjaka. Sledi okoli 30 m debel paket sljudnatega meljevca in peščenjaka z več debelejšimi plastmi sivega in rožnatega oolitnega apnenca, za katerega je menil, da leži v nižjih delih skitskih plasti in ne v srednjem delu, kakor so ugotavljali poprej.

Na Osnovni geološki karti, list Ribnica 1:100 000 leže skitske plasti diskordantno na permokarbonskih klastičnih kamninah (Buser, 1969).

Zgornjepermske in spodnjetriasne kamnine pri Skopačniku v Želimeljski dolini je nadrobno raziskal Mušič (1992). Opisal je njihove petrografske in paleontološke značilnosti, sedimentacijsko okolje in diagenetske spremembe. Prišel je do zaključka, da predstavljajo te plasti litološki ekvivalent tretje dolomitne enote (zgornje dolomitne plasti) v južnih Karavankah (Tržič). Zgornjepermski del profila je razdelil na tri litološke enote (od spodaj navzgor): 1) - spodnja dolomitna enota, 2) - zgornja dolomitna enota in 3) - prehodna P/T enota.

Kolar-Jurkovšek in Jurkovšek (1996) sta napisala prispevek k poznavanju spodnjetriasne konodontne favne Slovenije. Vzorci spodnjetriasnih oolitnih apnencev v dolini Iške in Drage so vsebovali sledeče konodontne elemente: *Ellisonia* sp., *Foliella gardenae* (Staesche), *Hadrodontina* sp., *Pachycladina obliqua* Staesche in *Parachirognathus ethingtoni* Clark. Preiskani konodontni elementi so značilni za smithijske konodontne združbe.

Materiali in metode

Temeljni podatki, na katerih sloni to delo, so bili pridobljeni pri sistematičnem regionalnem geološkem kartiranju za Geološko karto Slovenije, list Grosuplje 1:50 000, ki ga v tem delu Slovenije izvaja Geološki zavod Slovenije. Geološko kartiranje izvajamo predvsem z metodami opazovanja vseh golic, sledenja kontaktov in stratimetrijskega profiliranja. Najnovejši podatki so zbrani pri stratimetrijskih meritvah skitskih plasti v profilu Skopačnik. Pri sedimentološki obdelavi istega profila smo izvajali vzorčevanje karbonatnih sedimentov za različne laboratorijske raziskave.

Za konodontne analize smo odvzeli skupno 15 vzorcev karbonatnih kamnin iz celotnega profila, pretežno iz nekaj deset metrov debelega paketa z vložki oolitnih apnencev, nekaj vzorcev pa smo nabrali v temnih plasteh karbonatnih kamnin, ki leže v najnižjem delu profila, in za katere menimo, da pripadajo zgornjemu permu in spodnjemu skitu. Vzorčevali smo tudi vrhnje plasti skitske skladovnice, tik pod anizijskim dolomitom, ki sestoje iz ploščastih dolomitnih apnencev. Konodontne elemente vsebujejo le vzorci iz oolitnega dela profila. Trije vzorci iz najnižjega dela profila vključujejo drugo mikrofavno, ki jo sestavljajo foraminifere, ostrakodi in iglokožci.

Pri konodontni analizi je uporabljen postopek za raztapljanje karbonatnih kamnin z uporabo ocetne kisline. Po večkratnem dekantiranju je bil v kislini netopni ostanek ločen v bromoformu. Mikroskopski pregled vzorca je zajel pregled težke in lahke kamninske frakcije.

Karbonatne kamnine so določene po Folk-ovi (1959) in Dunham-ovi (1962) klasifikaciji.

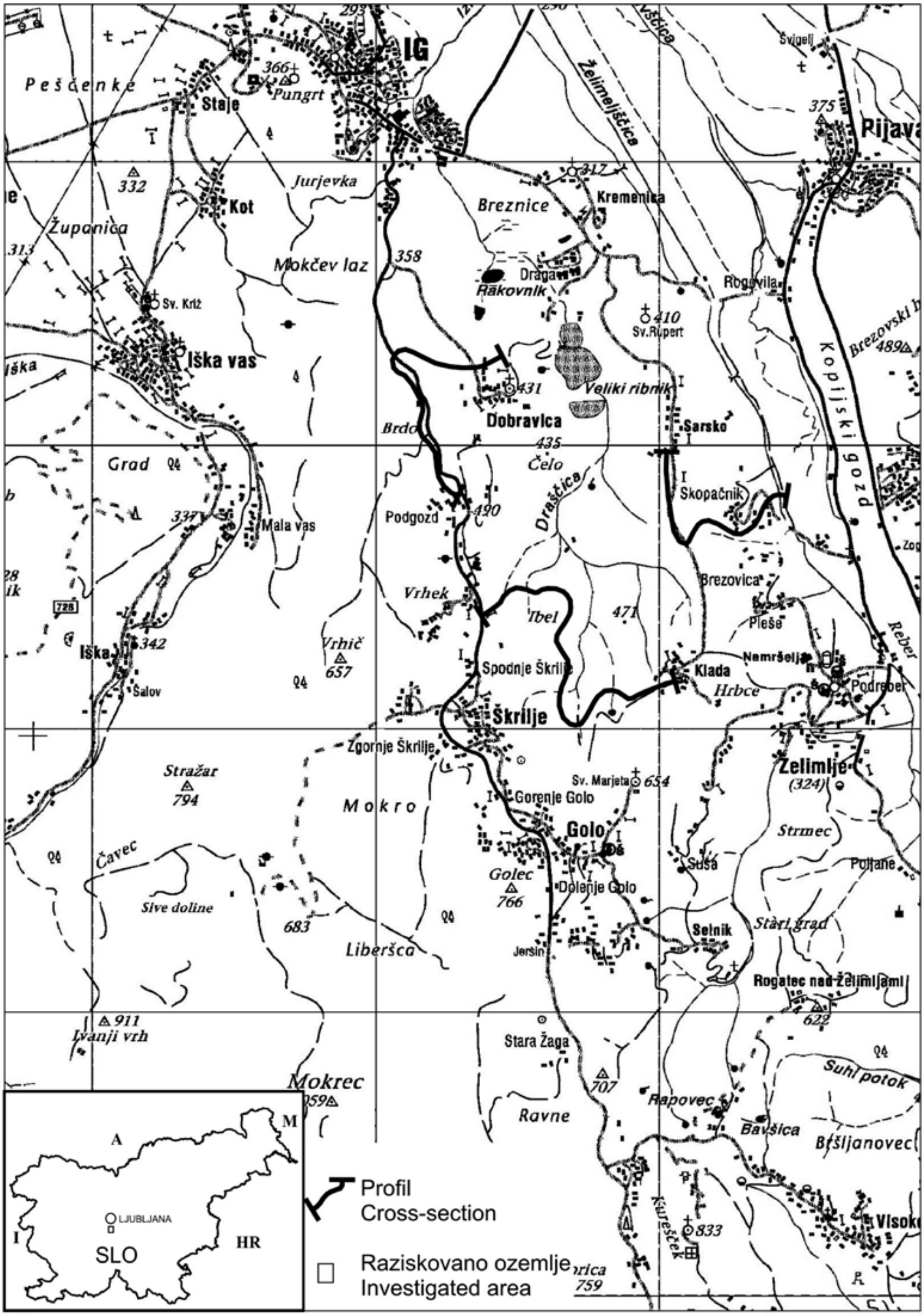

Slika 1. Položajna skica raziskanih profilov
Figure 1. Location sketch map of the examined cross-sections

Rezultati raziskav

V okviru programa Geološke karte in sistematičnega regionalnega kartiranja za izdelavo Geološke karte Slovenije 1:50 000, na listu Grosuplje, je bil raziskan predel na južnovzhodnem obrobju Ljubljanske kotline, ki obsega območja Skopačnika v Želimeljski dolini ter Sarskega, Klade, Škrilja, Dobravice in Podgozda, na območju tektonske enote Krimsko-Mokrškega hribovja (slika 1). Omenjeno ozemlje je zgrajeno iz skitskih, anizijskih, cordevolskih in podrejeno mlajšepaleozojskih sedimentnih kamnin.

Na obravnavanem ozemlju ni nikjer ohranjen celoten presek niti skitskih niti pod njimi ležečih zgornjepermskih plasti, vendar smo z natančno litostratigrafsko analizo sestavili skitski litološki stolpec tega dela Slovenije. Še najbolj je odkrit profil teh plasti na območju Skopačnika, kjer so razgaljene vrhnje zgornjepermske karbonatne kamnine ter spodnji in srednji del skitskega karbonatno-klastičnega zaporedja z debelim horizontom oolitnih apnencev na vrhu. Sicer pa je zgornjepermsko-skitsko zaporedje na spodnji in zgornji strani odsekano s prelomom. Medtem ko je bila skitska skladovnica ob zgornjem prelomu le zamaknjena in jo lahko sledimo ob prelomu v smeri Sarskega in Dobravice, pa pretežni del zgornjepermskih plasti, ki je odsekan s spodnjim prelomom, ni nikjer ohranjen. Na širšem območju Sarskega izdanjajo pisani »campilski« klastiti in rdečkastosivi dolomit, terene okoli Dobravice pa gradijo, poleg že omenjenih rdečkastosivih dolomitov, še rumenkastosivi peščeni zgornjeskitski dolomiti, nad katerimi leži rdečkastosivi ploščasti dolomitni apnenec na njem pa debelozrnat, močno tektoniziran svetlosiv in zelo svetlosiv srednjetriasni dolomit.

Kratek opis zgornjepermskih plasti

Okoli 20 m debel najnižji del obravnavanega sedimentnega zaporedja, ki ga štejemo za zgornji perm, je sestavljen iz temnega ploščastega in plastnatega dolomita z redkimi tankimi vložki dolomitnega laporovca in lapornega glinavca.

Ploščasti dolomikrit, dolomitni laporovec in laporni glinavec.

V najmlajši zgornjepermski litostratigrafski enoti prevladujejo ploščast (5-10 cm), siv, srednje siv in srednje temnosiv gost dolomit oziroma dolomikrit. Mestoma je tankoplastnat (10-20 cm), zrnat in ooličen. Ponekod vsebuje tanke vložke sivega in olivnosivega laporovca in lapornega glinavca, redka zrna pirita in kremena ter ostanke drobnih foraminifer in alg. Pogosto je bolj ali manj rekristaliziran. Vezivo je mikritno ali mikrosparitno. Izmerjena debelina najmlajše zgornjepermske litostratigrafske enote znaša 20 metrov, vendar je v resnici večja, ker je precejšnji del plasti, ki leže spodaj, prekrit s kvartarnimi sedimenti in odsekan s prelomom.

Opis in litostratigrafska razčlenitev skitskega zaporedja sedimentov

Na podlagi stratigrafske lege in glede na litološko sestavo lahko skitsko zaporedje karbonatnih in klastičnih sedimentov razdelimo na sledečih devet enot (od spodaj navzgor):

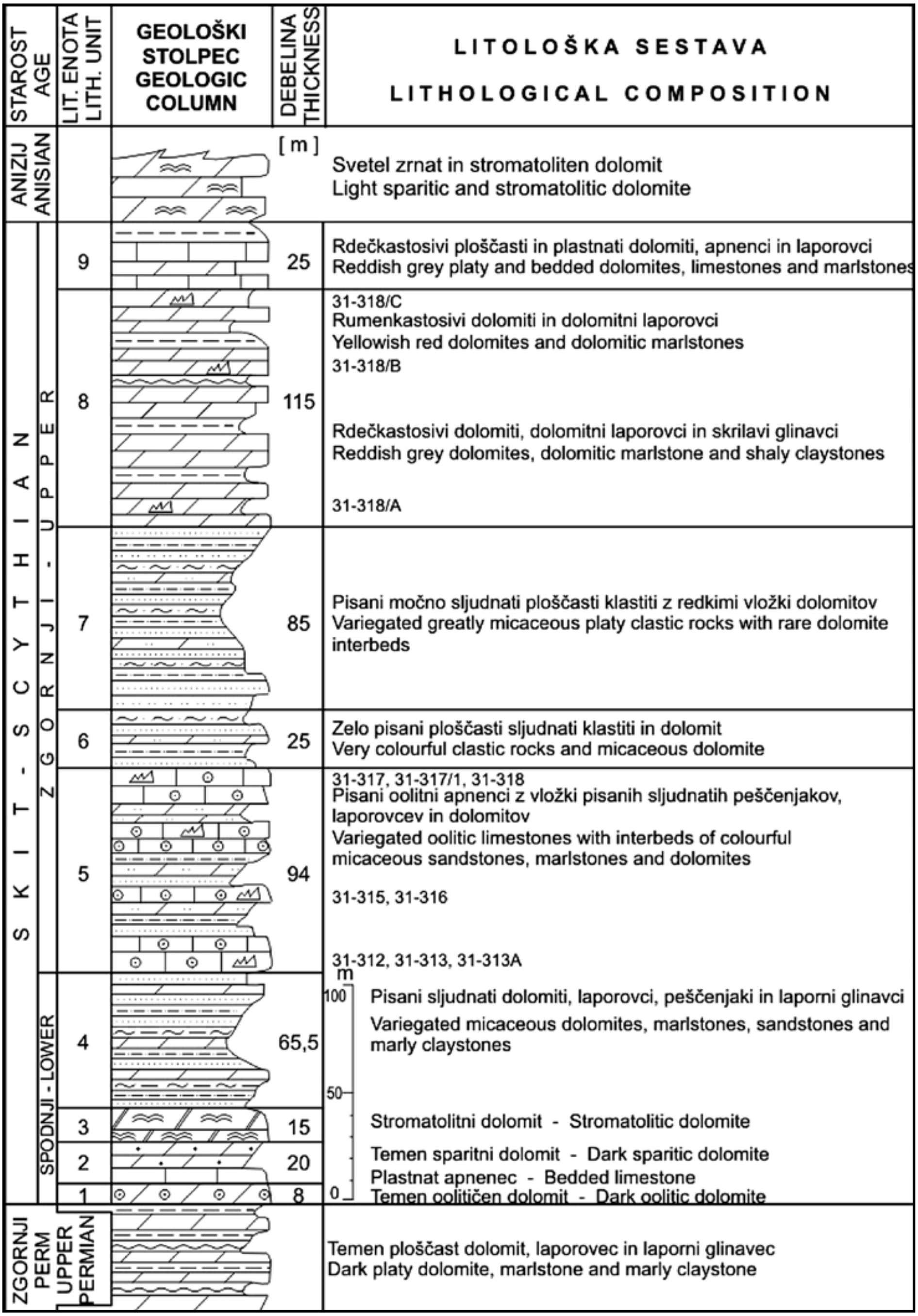

Slika 2. Sestavljeni geološki stolpec skitskih plasti na južnem obrobju Ljubljanskega barja
Figure 2. Composed geologic column of Scythian beds in southern Borderland of Ljubljana Moor

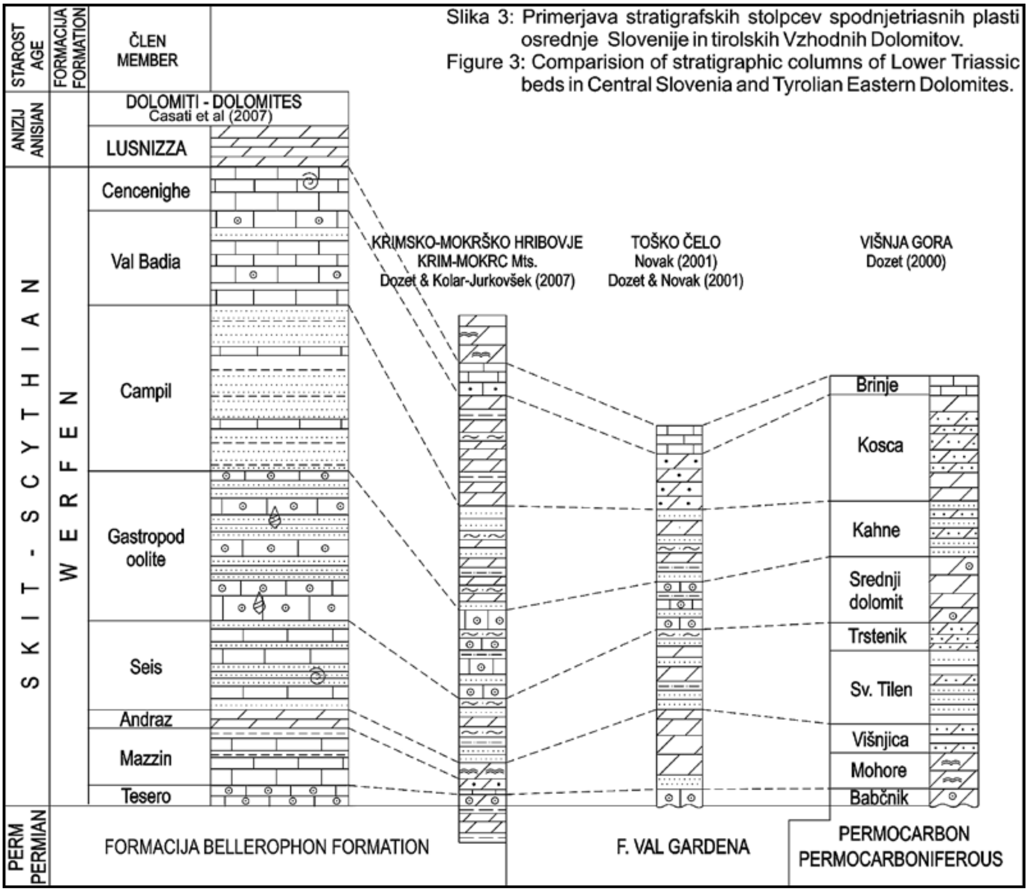

Slika 3. Primerjava stratigrafskih stolpcev spodnjetriasnih plasti osrednje Slovenije in tirolskih Vzhodnih Dolomitov

Figure 3. Comparison of stratigraphic columns of Lower Triassic beds in Central Slovenia and Tyrolian Eastern Dolomites

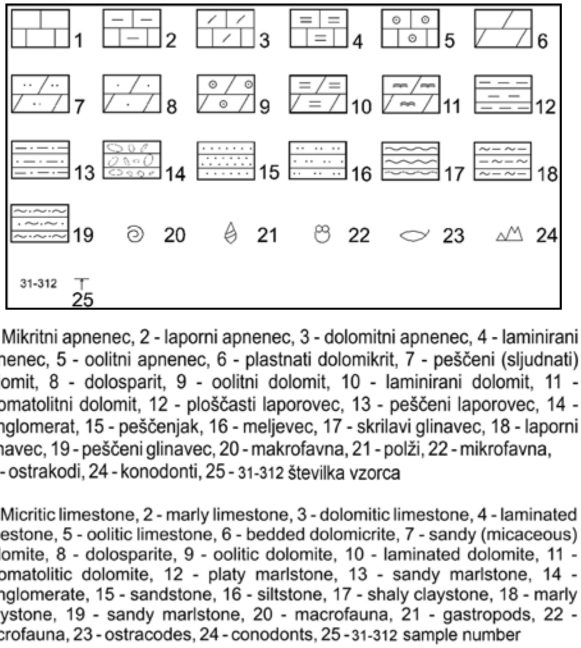

Slika 4. Legenda sestavljenega geološkega stolpca skitskih plasti južnega obrobja Ljubljanskega barja (slika 2) in primerjalne slike stratigrafskih stolpcev spodnjetriasnih plasti osrednje Slovenije in tirolskih Vzhodnih Dolomitov (slika 3)
Figure 4. Legend of composed geologic columns of Lower Triassic beds in Southern Borderland of Ljubljana Moor (Figure 2) and composed figure of stratigraphic columns of Lower Triassic beds in Central Slovenia and Tyrolian Eastern Dolomites (Figure 3)

1) Tesero horizont.
2) Temni plastnati apnenec, dolomitni apnenec, apnenčev laporovec in plastnati sparitni dolomit.
3) Svetli stromatolitni dolomit.
4) Pisani peščeni (sljudni) dolomiti, laporovci, laporni glinavci in peščenjaki (»seiski« člen).
5) Oolitni apnenci s polži (gastropodni ooliti).
6) Horizont izredno pisanih klastičnih sedimentov (Andraz I).
7) Pisani močno sljudnati peščenjaki in meljevci, peščeni dolomiti in laporovci ter laporni glinavci (»campilski« člen).
8) Rdečkastosivi dolomiti, dolomitni laporovci, skrilavi glinavci in rumenkastosivi dolomiti z interkalacijami dolomitnega laporovca.
9) Rdečkastosivi ploščasti do srednje temnosivi apnenčevi dolomiti, dolomitni apnenci in dolomitni laporovci.

1) Tesero horizont

Na južnovzhodnem obrobju Ljubljanske kotline je Tesero horizont slabo razvit. Za bazalne skitske plasti smatramo plastnati in debeloploščasti temnosivi do zelo temnosivi oolitni dolomit. Horizont s slabo ohranjenimi ooidi je debel od 7 do 8 metrov. Struktura celotne kamnine in tudi ooidov je zaradi temeljite dolomitizacije in rekristalizacije tako zabrisana, da je prvotna struktura te karbonatne kamnine prepoznavna šele pod lupo in mikroskopom.

2) Plastnati apnenec, dolomitni apnenec, apnenčev laporovec in sparitni dolomit

Spodnjeskitski apnenec je srednjesiv do sivkastočrn, zelo drobno do drobnozrnat, plastnat (20-45 cm) in redkeje ploščast (5-10 cm) karbonatni sediment. Po strukturi je mikriten (mudstone), redkeje biomikriten (wackestone), zelo redko biospariten ali intrabiospariten (packstone). Vezivo je mikritno in mikrosparitno, redko sparitno. Praviloma je bolj ali manj dolomiten. Vsebuje ostanke foraminifer in alg ter drobne bele kalcitne žilice. Debelina paketa plastnatega apnenca, apnenčevega laporovca in dolomitnega apnenca je 7,5 metrov, posamezne plasti pa so debele 10-30 cm. Kemično je čist, saj vsebuje le nekaj odstotkov detritičnega kremena, sljud in mineralov glin. Mestoma je nekoliko rekristaliziran.

Plastnati sparitni dolomit je temnorjavosiv, bledorjavkastosiv in srednje svetlosiv, plastnat (15-35 cm), pogosto luknjičast srednje in debelozrnat karbonatni sediment s peščenim otipom. V spodnjem delu je debeloplastnat, v zgornjem pa srednje do tankoplastnat. Mestoma vsebuje drobne vključke belega kalcita. Po strukturi je

Slika 5. Spodnjeskitske plasti (sljudnati dolomiti, laporovci in peščenjaki) Skopačnika

Figure 5. Lower Scythian beds (micaceous dolomites, marlestones and sandstones) of Skopačnik

dolosparit, biodolosparit in intrabiodolosparit. Vsebuje zrna pirita ter ostanke foraminifer in alg. Debelina spodnjega dela je 12,5 metrov zgornjega pa 7,5 metrov, skupaj torej 20 metrov. Piritna zrna v opisanih karbonatnih kamninah govore za občasno redukcijsko okolje.

3) Svetli plastnati stromatolitni dolomit
Enoti plastnatega stromatolitnega dolomita pripada okoli 15 metrov debela skladovnica srednje svetlosivega do zelo svetlosivega, plastnatega, v vrhnjem delu debeloploščastega in tankoplastnatega (5-20 cm), izredno kompaktnega in čvrstega, izrazito stromatolitnega dolomita. V stromatolitnem dolomitu ne opazujemo prepokanosti niti paralelepipedske krojitve. Površine plastovnih ploskev so ravne do rahlo valovite.

4) Pisani peščeni (sljudni) dolomiti, laporovci, laporni glinavci in peščenjaki
Vrhnji del spodnjeskitskega zaporedja sedimentov pripada »seiskim« plastem. Gre najprej za okoli 18 metrov debel paket ploščastih rumenkastosivih, oranžnorumenih in oranžnorjavih, pogosto laminiranih ali pasastih peščenih (sljudnih) laporovcev in peščenjakov z interkalacijami in redkeje vložki ploščastega in plastnatega rumenkastosivega bolj ali manj peščenega dolomita. Približno v sredini opisanega karbonatnega zaporedja je 20 do 50 cm debel vložek temnosivega do sivkastočrnega, ploščastega, progastega in pasnatega lapornega glinavca oziroma dolomitnega laporovca.

Nad repernim horizontom temnosivega do črnega ploščastega progastega in pasnatega lapornega glinavca oziroma dolomitnega laporovca je ena do dva metra debel paket ploščastega in tankoplastnatega oolitnega dolomita.

Opisano bazalno »seisko« zaporedje prehaja navzgor postopno najprej v 7,5 m debel paket sivega, ploščastega in tankoplastnatega (3-25 cm), tu in tam laminiranega peščenega dolomita z redkimi interkalacijami dolomitnega laporovca. Nato sledi 15 m debel interval rumenkastosivega in plastnatega (5-20 cm) peščenega dolomita z vložki dolomitnega laporovca. Na vrhu litostratigrafske enote peščenih dolomitov leži 25 m debela skladovnica rožnatorumenega, bledo do rožnatorjavega, ploščastega in tankoplastnatega, močno peščenega (sljudnatega) dolomita z vložki peščenega dolomitnega laporovca, peščenjaka in vložki (20-35 cm) plastnatega peščenega dolomita.

Skupna debelina »seiskega« zaporedja sedimentov znaša 65,5 m.

5) Oolitni apnenci - gastropodni ooliti
Nad enoto pisanih peščenih (sljudnatih) dolomitov leži litostratigrafska enota oolitnih apnencev. Najspodnejši del te enote sestoji iz dveh paketov. V spodnjem 10 metrov debelem paketu se menjavajo sivi in srednje sivi, ploščasti in plastnati zrnati apnenec, laporni apnenec in apnenčev laporovec. Apnenec je tudi oospariten (grainstone) in kaže navzkrižno plastnatost. V zgornjem 7,5 metrov debelem paketu so zelen ploščast laporovec, temnordeč srednjezrnat oolitni apnenec s številnimi preseki polža *Holopella gracilior* (Schauroth) in temnoolivnozelen apnenčev laporovec. Enota, ki smo jo označili kot oolitni apnenec ni tako homogena, kot bi sklepali po

njenem imenu. V tej enoti se pojavljajo namreč različni strukturni tipi apnencev ter vložki dolomitno-klastičnih sedimentov. Tako leži neposredno na sivkastordečem oolitnem apnencu s polži najprej 15 m debel paket ploščastih in redkeje plastnatih pretežno rumenkastosivih močno peščenih dolomitov, dolomitnih laporovcev in lapornih peščenjakov, ki se med seboj ritmično menjavajo. Nato sledi 7,5 metrov debel interval plastnatega srednje sivega do sivega oosparitnega (grainstone) apnenca na katerem leži okoli 15 m debel paket dolomitno-klastičnih sedimentov, ki so podobni tistim, ki leže pod tem apnencem. Zgornji del enote oolitnih apnencev je bolj apnenčev od spodnjega. Debel je okoli 40 metrov, pričenja pa s srednje sivimi do srednje temnosivimi, včasih rdečkastimi, plastnatimi, tu in tam rahlo laminiranimi, lapornimi in zrnatimi, bolj ali manj prekristaljenimi apnenci, kjer je le malo plasti z izrazito biosparitno, intraoosparitno in bioosparitno (grainstone) strukturo. Poznodiagenetske spremembe so v teh apnencih uničile tudi fosilno vsebino, tako da v njih dobimo le redke ostanke moluskov predvsem polžkov rodu *Coelostylina* in odlomke ehinodermov. Homogeno apnenčevo skladovnico prekine v sredini 10 metrov debel interval debeloploščastega in tankoplastnatega (10-20 cm) rumenkastosivega, rumenkastooranžnega in rožnatordečega sparitnega dolomita z interkalacijami sivkastorjavega mikrosparitnega apnenca. Spremembe v strukturi obeh kamnin kažejo, da je dolomit nastal pri pozni diagenezi (dolomitizaciji) apnenca.

Zgornjo tretjino oolitnega člena zaključuje okoli 15 metrov debel paket plastnatih, srednje temnosivih do sivkastordečih apnencev različnih strukturnih tipov: oosparitni (grainstone), intraoosparitni (grainstone) biointraoosparitni (grainstone-packstone), drobnozrnati, mikritni (mudstone). V naštetih apnencih so ohranjeni le redki preseki mikrogastropodov.

Skupna debelina enote oolitnih apnencev znaša okoli 94 metrov.

6) Pisani klastični sedimenti (»campilski« člen)

Okoli 25 metrov debel člen dolomitno-klastičnih sedimentov, ki leže na enoti oolitnih apnencev s polžki, sestavljajo pogosto laminirani in pasnati peščeni dolomiti, ki se menjavajo z dolomitnimi laporovci, sljudnimi in bolj ali manj lapornimi kremenovimi peščenjaki ter meljastimi in lapornimi glinavci. Glavna značilnost tega ritmičnega zaporedja sedimentov je poleg različnih stratifikacij predvsem izredna pisanost barv. Menjavajo se sivkastordeči, bledordeči, sivkastorjavi, rumenkastooranžni ter zelenkasto in modrikastosivi sedimenti. Laminiranost v sedimentih je posledica različne petrografske sestave, različne velikosti zrn ter povečane vsebnosti hematita ali limonita. Po stratigrafski legi in litoloških posebnostih ustreza ta litostratigrafska enota členu Andraz II južnih Tirolskih Dolomitov.

7) Pisani sljudni peščenjaki in meljevci, peščeni dolomiti in laporovci ter laporni glinavci

Nad členom izredno pisanih dolomitnoklastičnih sedimentov se na območju Sarskega pojavlja okoli 85 metrov debelo zaporedje ploščastih peščenjakov, meljevcev, peščenih laporovcev in lapornih glinavcev s precejšnjo vsebnostjo sljude, ki

Slika 6. Sivi debeloplastnati oolitni apnenec z navzkrižno laminacijo, srednji skit, Skopačnik
Figure 6. Grey thick-bedded oolitic limestone with cross-lamination, Middle Scythian, Skopačnik

se med seboj ritmično menjavajo. Poleg sljude jih karakterizira tudi pisanost barv. Med barvami prevladujejo sivkastorumena, rumenkastooranžna, sivkastordeča, sivkastozelena in zelenkasto modra. Barve so najbolj intenzivne na površinah plasti, ki so temnozelene, tirkiznomodre in črnkastordeče. Tudi sljuda je najbolj nakopičena v lezikah plasti. Med terigenimi zrni prevladujejo kremen in sljude. Naštete klastične kamnine so tu in tam tudi laminirane in pasnate. Po stratigrafski legi, litološki sestavi in analogiji z razvoji na bližnjih področjih odgovarjajo obravnavani sedimenti zaporedju campilskega člena.

8) Rdečkastosivi dolomiti, dolomitni laporovci, skrilavi glinavci ter rumenkastosivi dolomiti in dolomitni laporovci

Nad tipičnim srednjeskitskim klastičnim členom leži na obravnavanem ozemlju okoli 50 metrov debela skladovnica plastnatih in ploščastih pretežno rdečkastosivih sicer pa tudi opekastordečih in rožnatordečih karbonatnih kamnin t.j. apnenčevih dolomitov, dolomitnih laporovcev in skrilavih glinavcev, ki vsebujejo drobnozrnato sljudo. Prevladujoča rdeča barva izvira od hematita, sljuda pa je nakopičena zlasti na lezikah, ki so črnkastordeče in kovinsko temnomodre.

Na južnovzhodnem obrobju Ljubljanske kotline zaključujejo obravnavano litostratigrafsko enoto plastnati rumenkastosivi do bledorumenkasti zrnati dolomiti, ki vsebujejo mestoma tanke vložke dolomitnih laporovcev in redkeje lapornih peščenjakov. Skupna debelina naštetih sedimentov zgornjeskitskega zaporedja, ki po stratigrafski legi in primerjavi z werfenskim razvojem v južnih Tirolskih Dolomitih odgovarja členu Val Badia, znaša okoli 115 metrov.

9) Rdečkastosivi ploščasti apnenčevi dolomiti, dolomitni apnenci in dolomitni laporovci

Skitsko skladovnico z območja tektonske enote Krimsko-Mokrškega hribovja na južnovzhodnem obrobju Ljubljanske kotline zaključuje okoli 25 m debelo zaporedje ploščastih (1-5 cm in 5-10 cm) ter tankoplastnatih (10-20 cm) apnenčevih dolomitov, dolomitnih apnencev in dolomitnih laporovcev. Naštete kamnine so rdečkasto sive, temno sive, zelo temnosive, sivkastočrne in olivnosive. Dolomiti in apnenci so drobnozrnati ali zelo drobnozrnati (laporni). Mestoma vsebujejo drobne hematitne lamine. Dolomitni laporovci so največkrat olivnosivi in le redko opekastordeči. So tanko do zelo tanko ploščasti. Nad rdečkastosivo najmlajšo skitsko litostratigrafsko enoto leži svetlosivi plastnati (20-45 m) zrnati dolomit, ki pripada po stratigrafski legi in litoloških značilnostih aniziju. Kon-

Slika 7. Rdeči plastnati oolitni apnenec in sivozeleni ploščasti peščeni (sljudnati) apnenčev laporovec, Skopačnik, srednji skit
Figure 7. Red bedded oolitic limestone and greyish green platy sandy (micaceous) limy marlstone, Skopačnik, Middle Scythian

Slika 8. Rdeči, rjavi in sivi, plastnati in ploščasti, peščeni (sljudnati) dolomiti, dolomitni laporovci in peščenjaki pri Dobravici, zgornji skit
Figure 8. Red, brown and grey bedded and platy sandy (micaceous) dolomites, dolomitic marlstones and sandstones at Dobravica, Upper Scythian

takt je precej tektoniziran, plasti pa so ponekod bolj ali manj nagubane.

KONODONTNA FAVNA: BIOFACIES IN STAROST

Za konodontne raziskave smo pregledali fosilno vsebino petnajstih vzorcev. Le trije vzorci iz najnižjega dela profila (št. vzorcev 31-309, 31-310, 31-311) niso vsebovali konodontnih elementov. Njihovo fosilno vsebino predstavljajo predvsem foraminifere, ostrakodi in iglokožci.

Ves fosilni material je shranjen na Geološkem zavodu Slovenije in zaveden pod naslednjimi inventarnimi številkami: 3753-3757, 3929-3933, 3968-3971, 4088-4090. Konodonti iz oolitnega člena so črni (CAI 5), iz mlajšega dela profila pa so svetlejši (CAI 3-4) (EPSTEIN et al., 1977; REJEBIAN et al., 1987). Razširjenost konodontov v raziskanem profilu je podana v tabeli 1. Ohranjenost konodontnih elementov je slaba, njihova pogostnost je relativno nizka. Konodontni biofacies označujejo predvsem plitvovodne evrihaline oblike.

Raziskane vzorce iz oolitnega dela profila označujejo plitvovodni konodontni elementi *Ellisonia, Foliella, Hadrodontina* in *Pachycladina* (tabla 1). Prevladuje rod *Pachycladina*, ki ga ponekod spremljajo elementi *Hadrodontina* (št. vzorcev: 31-

314, 31-318) ali rod *Foliella* (št. vzorca 31-313A). Favno vzorca št. 31-316 označujejo le elementi rodu *Ellisonia*.

Določena vrsta *P. obliqua* je bila prvič najdena v Južnih Alpah (Staesche, 1964), ki se pojavlja le v zgornjem delu werfenske formacije (Perri, 1991). Pomen plitvovodnih in evrihalinih vrst rodov *Ellisonia, Hadrodontina* in *Pachycladina* za stratigrafijo Južnih Alp je poudarila Perrijeva in uvedla konodontno bioconacijo za večji del werfenske formacije (Perri&Andraghetti, 1987; Perri, 1991). Na osnovi novih najdb *Hindeodus-Isarcicella* združbe, je bila bioconacija spodnjega dela werfenske formacije kasneje še podrobneje razčlenjena (Perri&Farabegoli, 2003).

Prvi pojav konodontne vrste *Pachycladina obliqua* v Sloveniji doslej še ni ugotovljen, da bi lahko z gotovostjo ugotovili spodnjo mejo konodontne cone *obliqua.* To konodontno cono smo v Sloveniji lahko izdvojili v tistih lokalitetah, kjer elemente te vrste spremljajo še nekateri drugi rodovi (*Furnishius*, *Parachirognathus* ali *Foliella*), ki omogočajo primerjavo s standardno konodontno conacijo.

S tokratnimi raziskavami smo ugotovili, da sestavljajo konodontno združbo oolitnega člena poleg vrste *P. obliqua* tudi rodovi *Ellisonia, Hadrodontina in Foliella* z

Slika 9. Rožnato, zelenkasto in olivnosivi, ploščasti in plastnati, peščeni (sljudnati) dolomiti, dolomitni apnenci in laporovci ob cesti Ig-Škrilje, zgornji skit
Figure 9. Rosy, greenish and olive grey platy and bedded sandy (micaceous) dolomites, dolomitic limestones and marlstones at the road Ig-Škrilje, Uppermost Scythian

Tabela 1. Razširjenost konodontov v profilu Skopačnik
Table 1. Distribution of conodonts in the Skopačnik cross-section

	31-312	31-313	31-313A	31-314	31-315	31-316	31-317	31-317/1	31-318	31-318A	31-318B	31-318C
Ellisonia sp.						X						
Foliella gardenae			X									
Hadrodontina sp.				X					X			
Pachycladina obliqua			X	X			X		X			
Pachycladina sp.									X			
? *Pachycladina* sp.					X							
Neospathodus sp.												X
Indet. fragm.	X	X						X		X	X	X

vrsto *F. gardenae*. To združbo uvrščamo v smithijsko cono *obliqua*, njen sestav pa omogoča primerjavo z večino doslej znanih enako starih združb iz Slovenije (KOLAR - JURKOVŠEK&JURKOVŠEK, 2001).

Konodontna združba iz višjega dela je slabše ohranjena in ima nižji barvni indeks. V dveh vzorcih (št. vzorcev: 31-318A in 31-318B) smo našli le slabo ohranjene konodontne elemente robustnih oblik, od katerih nekatere verjetno pripadajo rodu *Pachycladina*. V najvišje ležeči plasti s konodonti v raziskanem profilu Skopačnik je opazna sprememba (vzorec št. 31-318 C) v sestavi konodontne mikrofavne, saj se robustne oblike ne pojavljajo več, označuje pa jo združba, v kateri se pojavljajo neospathodidne oblike (*Neospathodus* ex gr. *triangularis*). Najdene oblike kažejo na to, da so sedimenti tega dela raziskanega profila že spathijske starosti.

Primerjava konodontnih združb sosednjih območij

Študij konodontov iz P-T intervala in spodnjetriasnih plasti je predmet številnih raziskav, ki v zadnjih nekaj letih potekajo v različnih delih Dinaridov. Njihov glavni namen je določitev sistemske meje na osnovi biostratigrafskih markerjev. Kot rezultat natančnega mikropaleontološkega študija so bili predstavniki rodu *Hindeodus* najdeni v nekaterih profilih Dinaridov. Iz Jadarske cone Notranjih Dinaridov Srbije je iz najvišjega dela perma opisana združba cone *Hindeodus praeparvus* (SUDAR et al., 2007). Element *Hindeodus parvus* je bil najden v Zunanjih Dinaridih Hrvaške (ALJINOVIĆ et al., 2006). Z najnovejšimi raziskavami je najstarejša triasna združba *Hindeodus-Isarcicella* ugotovljena tudi v Sloveniji (KOLAR-JURKOVŠEK & JURKOVŠEK, 2007). Prvi pojav vrste *Hindeodus parvus* je bil izbran in potrjen za določitev spodnje meje triasnega sistema s strani mednarodnih geoloških institucij (YIN et al., 2001).

Sistematske raziskave konodontnih združb potekajo v Zunanjih Dinaridih Slovenije že več kot desetletje. Oolitni apnenec, ki je značilen spodnjetriasni člen, je zaradi okolja nastanka dolgo časa veljal kot neperspektiven za te raziskave, vendar pa je prisotnost konodontov v njem dokazana v številnih nahajališčih. Raziskave so pokazale, da gastropodni oolit na številnih mestih vsebuje olenekijsko (smithijsko) združbo (Kolar-Jurkovšek, 1990; Kolar-Jurkovšek & Jurkovšek, 1996). Na tem mestu uporabljamo makrotektonsko delitev mejnega področja med Južnimi Alpami in Zunanjimi Dinaridi po Placerju (1999). Pregled o spodnjetriasnih konodontnih združbah sta podala Kolar-Jurkovšek & Jurkovšek (2001). Vse najdene združbe označuje prisotnost vrste *Pachycladina obliqua* Staesche in *Hadrodontina* sp. in/ali *Furnishius triserratus* Clark, *Parachirognathus ethingtoni* Clark in *Foliella gardenae* (Staesche). Ponekod je prisoten še element *Ellisonia* sp. Konodontne združbe iz slovenskega dela Zunanjih Dinaridov so dobro dokumentirane in jih lahko primerjamo z enako starimi združbami, ki so

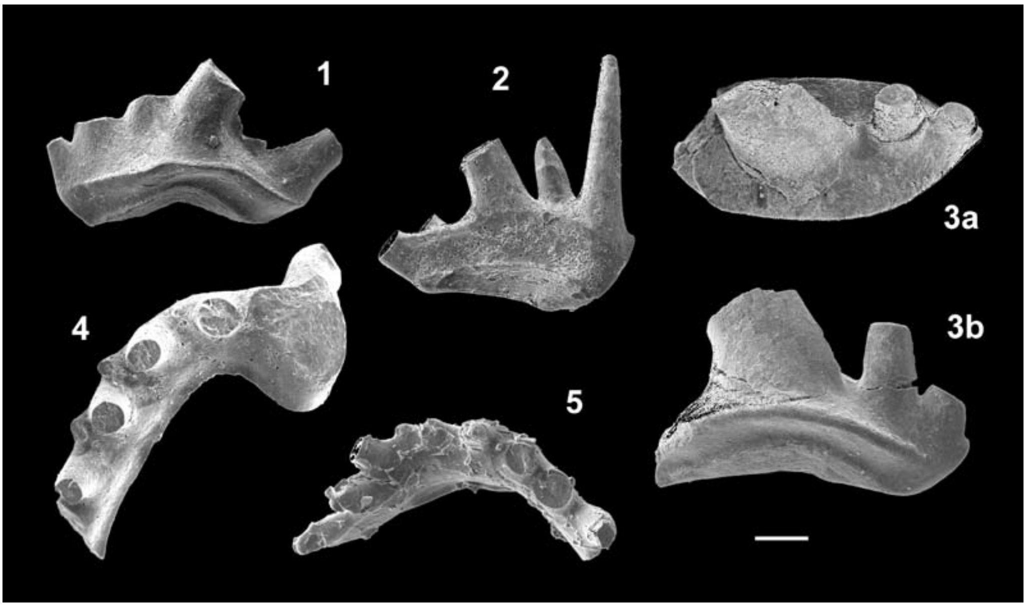

Tabla 1. Konodonti iz profila Skopačnik, smithij, cona *obliqua*. Sl. 1-3: *Pachycladina obliqua* Staesche (1: Pb element, vzorec 31-314 (GeoZS 3754), 2: Sb element, vzorec 31-314 (GeoZS 3754), 3a-b: Pa element, vzorec 31-318 (GeoZS 3757)). Sl. 4-5: *Hadrodontina* sp., Skopačnik, cona *obliqua* (4: M element, vzorec 31-318 (GeoZS 3757), 5: Pa element, vzorec 31-318 (GeoZS 3757)). Merilo je 100 mikronov.

Plate 1. Conodonts from the Skopačnik cross-section, Smithian, *obliqua* Zone. Figs. 1-3: *Pachycladina obliqua* Staesche (1: Pb element, sample 31-314 (GeoZS 3754), 2: Sb element, sample 31-314 (GeoZS 3754), 3a-b: Pa element, sample 31-318 (GeoZS 3757)). Figs. 4-5: *Hadrodontina* sp., Skopačnik, *obliqua* Zone (4: M element, sample 31-318 (GeoZS 3757), 5: Pa element, sample 31-318 (GeoZS 3757)). Scale bar equals 100 microns.

bile doslej najdene drugod po Sloveniji, na primer s favno iz Karavank (Južne Alpe), kjer prevladujoči element *Foliella gardenae* spremljajo drugi tipični plitvovodni konodontni elementi (KOLAR-JURKOVŠEK & JURKOVŠEK, 1995). Sestav smithijskih konodontnih združb iz slovenskih nahajališč je zelo podoben. Primerjali smo jih s spodnjetriasno Cono 7 (cona *Parachirognathus - Furnishius*) (SWEET et al., 1971). Plitvovodni spodnjetriasni rodovi *Foliella, Hadrodontina, Pachycladina* in *Parachirognathus* so pomembni biostratigrafski markerji, ki so uporabni pri konodontni conaciji v Sloveniji.

Najnovejše geološke raziskave v sosednjih delih Zunanjih Dinaridov na Hrvaškem so dale nove paleontološke podatke za Dalmacijo in Gorski Kotar (JELASKA et al., 2003; ALJINOVIĆ et al., 2006) in potrdile podoben sestav ekvivalentnih konodontnih združb na tem območju. Zato lahko zaključimo, da je vrsta *P. obliqua* pomemben biostratigrafski element v Zahodni Tetidi. Izven Zunanjih Dinaridov je bila njegova stratigrafska uporabnost prikazana v Južnih Alpah (PERRI & ANDRAGHETTI, 1987; PERRI, 1991) in v Notranjih Dinaridih Srbije (BUDUROV & PANTIĆ, 1974; SUDAR, 1986).

RAZPRAVA IN PRIMERJAVA

Najbolj podrobno mikrobiofacijalno analizo zgornjega dela zgornjepermskih plasti je na območju Skopačnika naredil MUŠIČ (1992). V zgornjepermskih dolomitih in dolomitnih apnencih navaja foraminifere *Ammodiscus* in *Hemigordius* ter fuzulinidni rod *Stafella*. Poleg foraminifer je našel tudi drobce rdečih alg iz družine Solenoporacea in rodu *Carta*. Ostali fosilni ostanki pripadajo dazikladacejam, problematiki rodu *Tubiphytes*, ehinodermam, mikrogastropodom in briozojem. Sto petdeset metrov debelo skladovnico spodnjetriasnih skladov pri Skopačniku je razdelil v dve litološki enoti. Starost spodnje enote s fosili ni bila dokazana. Prvi fosilni ostanki se pojavijo sorazmerno visoko v lečah apnenca, kjer so nedoločljivi fragmenti moluskov in ehinodermov. V dolomitu so le posamezne hišice foraminifer *Ammodiscus.* Mejo med griesbachijem in »nammalijem« je postavil pod biomikrosparitnim apnencem (packstone) s številnimi polžki rodov *Coleostylina* in *Natica.* V vrhnjem delu profila je našel nekaj presekov polža *Natiria* sp., ki se povsod v Sloveniji pojavlja v vrhnjem delu spodnjega triasa (spathij).

Najdbo polža vrste *Natiria costata* (Münster) v spodnjetriasnih kamninah pri Skopačniku omenja BUSER (1974).

Splošna ugotovitev je, da ima spodnjetriasna sedimentacija južnovzhodnega obrobja Ljubljanske kotline podobne značilnosti kot ostali razvoji spodnjetriasnih plasti na obrobju Ljubljanske kotline, v Posavskih gubah, Škofjeloškem in Polhograjskem hribovju ter Idrijskem in Žirovskem ozemlju, v Julijskih Alpah, Karavankah in na območju južne Slovenije in Gorskega Kotarja. Vendar je stopnja podobnosti lahko precej različna, glede na to kaj pač primerjamo.

Če primerjamo litološko sestavo celotne skitske skladovnice južnovzhodnega obrobja Ljubljanske kotline, v kateri prevladujejo dolomiti z dvema močnima intervaloma klastičnih sedimentov in razmeroma homogenim in debelim horizontom pretežno oolitnih apnencev, potem je le-ta najbolj podobna razvojem na Žirovskem ozemlju, (Grad & Ferjančič, 1976; Grad & Ogorelec, 1980; Ogorelec & Grad, 1986), razvoju na Idrijskem (Mlakar, 1959; Čar et al., 1980; Buser, 1986), v Škofjeloškem hribovju (Demšar & Dozet, 2002), v Polhograjskem hribovju (Premru, 1965; Jurkovšek et al., 1999) in razvoju v Karavankah (Buser, 1980; Dolenec et al., 1981).

Če primerjamo le spodnji in srednji del spodnjetriasne skladovnice potem so obravnavane plasti podobne odgovarjajočim plastem v Julijskih Alpah (Buser, 1980; Jurkovšek, 1987; Ramovš, 1989), v profilu Mišji Dol na Kozjanskem (Ramovš & Aničić, 1995; Ramovš et al., 2001) in na zahodnem obrobju Ljubljanske kotline (Novak, 2001; Dozet & Novak, 2002).

Precejšnjo litološko podobnost kažejo obravnavane plasti tudi z razvoji skitskih plasti na območju Pleš (Dozet, 1985; 2000), Kočevske (Dozet & Silvester, 1979) in Gorskega Kotarja (Babić, 1968; Šćavničar, 1973). Glavna razlika v litologiji med njimi je v tem, da je na jugovzhodnem obrobju Ljubljanske kotline horizont oolitnih apnencev močno poudarjen, v ostalih naštetih razvojih pa je bolj ali manj zakrnel.

Sklepi

Pestro in pisano spodnjetriasno zaporedje karbonatnih in klastičnih sedimentov na območju Skopačnika leži konkordantno in brez vidnih znakov prekinitve sedimentacije na temnih plastnatih in ploščastih karbonatnih kamninah, ki smo jih uvrstili v zgornji perm.

Skitski litološki stolpec karbonatnih in klastičnih kamnin je razdeljen v sledečih devet litostratigrafskih enot (od spodaj navzgor):

1) Tesero horizont, debelina 8 m.
2) Temni plastnati apnenec, dolomitni apnenec, apnenčev laporovec in sparitni dolomit, debelina 20 m.
3) Svetli stromatolitni dolomit, debelina 15 m.
4) Pisani peščeni (sljudni) dolomiti, laporovci, laporni glinavci in peščenjaki, debelina 65,5 metrov (»seiski« člen).
5) Oolitni apnenci s polžki (gastropodni oolit), debelina 94 m.
6) Izredno pisani sedimenti, debelina 25 metrov (Andraz horizont).
7) Pisani sljudnati peščenjaki in meljevci, peščeni dolomit, laporovci ter lapornati glinavci, debelina 85 metrov (»campilski« člen).
8) Rdečkastosivi dolomiti, dolomitni laporovci in skrilavi glinavci, debelina 50 metrov rumenkastosivi dolomiti in dolomitni laporovci, debelina 65 metrov (Val Badia). Skupna debelina osme enote znaša 115 m.
9) Rdečkastosivi do srednje temnosivi ploščasti dolomiti, dolomitni apnenci, dolomitni laporovci, debelina 25 m.

- Prve štiri litostratigrafske enote pripadajo griesbachijski stopnji (spodnji skit) peta, šesta in sedma enota so »nammalijske« (srednji skit), najmlajši litostratigrafski enoti (osma in deveta pa sestavljata spathijsko stopnjo (zgornji skit).

- Spodnjetriasno zaporedje na jugovzhodnem obrobju Ljubljanske kotline lahko stratigrafsko primerjamo z werfenskim razvojem v Vzhodnih Dolomitih Italije, in sicer:

- bazalni oolitični horizont odgovarja Tesero horizontu in predstavlja začetek triasne transgresije,
- temni plastnati apnenec, dolomitni apnenec, apnenčev laporovec in sparitni dolomit druge litostratigrafske enote ustrezajo členu Mazzin Vzhodnih Dolomitov,
- svetli stromatolitni dolomit je ekvivalent horizonta Andraz I in kaže na kratkotrajno šibko regresijo,
- pisani peščeni (sljudni) dolomiti, laporovci, laporni glinavci in peščenjaki odgovarjajo litostratigrafsko in po paleontološki vsebini seiskemu členu,
- oolitni apnenci s polži so ekvivalent gastropodnega oolita v Dolomitih, pomenijo pa novo transgresijo,
- horizont izredno pisanih klastičnih sljudnih sedimentov lahko primerjamo s horizontom Andraz II,
- pisani močno sljudnati peščenjaki in meljevci, peščeni dolomiti ter laporovci in laporni glinavci ustrezajo campilskemu členu Vzhodnih Dolomitov,
- rdečkastosivi plastnati in ploščasti dolomiti, dolomitni laporovci, skrilavi glinavci in rumenkastosivi dolomiti z interkalacijami dolomitnega laporovca predstavljajo člen Val Badia,
- rdečkastosivi do srednje temnosivi ploščasti apnenčevi dolomiti, dolomitni apnenci in laporovci pa ustrezajo členu Cencenighe.

Celotna debelina skitske serije v tektonski enoti Krimsko-Mokrškega hribovja znaša 452,5 m. Pri tem je griesbachijska skladovnica debela 108,5 m, »nammalijska« 204 m, spathijska pa 140 m.

Prve štiri litostratigrafske enote pripadajo griesbachiju (spodnji skit), peta, šesta in sedma stopnja sta »nammalijski« (srednji skit) dve najmlajši litostratigrafski enoti (osma, deveta) pa sestavljata spathijsko (zgornji skit) stopnjo. Zgornja meja skitskega sedimentnega zaporedja je ostra in litološka. Rumenkasto sivi sljudnati plastnati skitski dolomiti z interkalacijami dolomitnih laporovcev prehajajo navzgor v zelo svetlosiv, skoraj bel, masiven ali plastnat, debelozrnat srednjetriasni dolomit.

Sedimenti prvih dveh skitskih enot so nastajali na območju supralitorala in v zelo plitvem litoralnem morju z močnim donosom terigenega materiala s precej zravnanega kopnega. Oolitni apnenci so nastajali v poglobljeni vodi plimskih kanalov in na območju delt, kjer je voda imela večjo energijo in sposobnost turbulence. Sedimentacija v plitvem šelfnem morju in supralitoralu se je nadaljevala tudi v zgornjem skitu in skozi ves anizij s to razliko, da je bil koncem skita donos terigenega materiala s kopnega skoraj popolnoma ustavljen. Prevladujoča karbonatna sedimentacija kaže, da so se skitski sedimenti Skopačnika in širše okolice odlagali na karbonatni platformi, ki je bila sestavni del obsežne

Slovenske karbonatne platforme, ki se ja razvila že v zgornjem permu, zaključila pa koncem anizija.

Zgornja meja skitskega sedimentnega zaporedja je ostra in litološka. Rumenkastosivi sljudni ploščasti in plastnati skitski dolomiti prehajajo navzgor v zelo svetlosiv skoraj bel masiven debelozrnat dolomit srednjega triasa.

Zahvale

Raziskava je bila opravljena v okviru programske skupine »Regionalna geologija« (P1-0011), ki jo finančno omogoča Agencija za raziskovalno dejavnost Republike Slovenije. Laboratorijske raziskave so bile opravljene na Geološkem zavodu Slovenije. Prvi avtor (Stevo Dozet) je odgovoren za geološki in sedimentološki del tega članka, druga avtorica (Tea Kolar-Jurkovšek) je odgovorna za konodontne podatke. Posnetki konodontov z elektronskim mikroskopom so bili narejeni na Paleontološkem inštitutu ZRC-SAZU.

Summary

Lower Triassic beds in the southeastern borderland of the Ljubljana depression, central Slovenia

In the area of the Krim-Mokerc tectonic unit there is nowhere exposed a complete cross-section through the Scythian beds. Therefore, we got an insight into the composition of that series combining several partial cross-sections, namely: Skopačnik-Sarsko, Klada-Škrilje and Dobravica-Podgozd.

A review of stratigraphic, sedimentologic and paleontologic features of rocks adjacent to the Permian-Triassic boundary in the Krim-Mokerc tectonic unit lead us to the conclusion, that the Lower Triassic boundary is concordant, maybe even conformable. It is not possible to evaluate this relation with certainity.

However, the Scythian sedimentation began by an important and pretty widespread Triassic transgression passing upwards concordantly and in some places gradually into the overlying Anisian dolomite.

In the southeastern Borderland of the Ljubljana depression the Scythian series is subdivided in the following nine lithostratigraphic units:

1) Tesero horizon.
2) Dark bedded limestone, dolomitic limestone, limy marl and sparitic dolomite (Mazzin).
3) Light stromatolitic dolomite (Andraz I).
4) Variegated sandy (micaceous) dolomites, marlstones, marly claystones and sandstones (Seis).
5) Oolitic limestone with gastropods (gastropod oolite).
6) Horizon of greatly gay-coloured clastic sediments (Andraz II).
7) Variegated greatly micaceous sandstones and siltstones, sandy dolomites and marlstones as well as marly claystones (Campil).
8) Reddish grey dolomites, dolomitic marlstones, shaly claystones as well as yellowish grey dolomites intercalated by dolomitic marlstones (Val Badia).

9) Reddish grey to medium dark grey platy limy dolomites, dolomitic limestones and dolomitic marlstones (Cencenighe).

The first four lithostratigraphic units belongs to Griesbachian (Lower Scythian), the fifth, sixth and seventh units are of "Nammalian", while the two youngest lithostratigraphic units (eighth, nineth) compose the Spathian stage (Upper Scythian). The upper limit of the Scythian sedimentary succession is sharp, conventional and lithological. The yellowish grey micaceous platy and bedded Scythian dolomites intercalated by dolomitic marlstones pass upwards into the very light grey, almost white, massive or bedded, coarse-grained Middle Triassic (Anisian) dolomite.

The sediments of first two Scythian lithostratigraphic units were formed in the area of supralitoral in a very shallow littoral sea with a strong deposition of terrigenous material. The oolitic limestones were deposited in a deeper water of tidal channels and in a delta area, where the water had a bigger energy and a turbulence capability. Sedimentation in a shallow shelf sea and supralitoral continued also in the Upper Scythian and through the entire Anisian with a distinction, that the deposition of terrigenous material from the land at the end of Scythian epoch was almost completely stopped.

The predominant carbonate sedimentation indicate, the Scythian sediments of Skopačnik and wider surroundings were produced on a carbonate platform, which was a constituent part of the Slovenian Carbonate Platform, developed already in the Upper Permian, and terminated at the end of the Anisian epoch.

Viri

Aljinović, D., Kolar-Jurkovšek, T., Jurkovšek, B. (2006): The Lower Triassic shallow marine succession in Gorski Kotar region (External Dinarides, Croatia): lithofacies and conodont dating. *Riv. Ital. Paleont. Stratigr.*; Vol. 112/1, pp. 35-53, Milano.

Babić, L. (1968): O trijasu Gorskog Kotara i susjednih područja. *Geol. vjesnik.*; Vol. 21, pp. 11-15, Zagreb.

Budurov, K. & Pantić, S. (1974): Die Conodonten der Campiller Schichten von Brassina (Westerbien). I. Stratigraphie und Conodonten-Zonen. *Bull. Geol. Inst.*, *Ser. Paleont.*; Vol. 23, pp. 105-113, Sofia.

Buser, S. (1962): *Geološke razmere na listu Ig-Ribnica 52-25/1*. Geološki zavod Slovenije, 40 pp., Ljubljana.

Buser, S. (1969): *Osnovna geološka karta SFRJ, list Ribnica 1:100 000*. Zvezni geološki zavod, Beograd.

Buser, S. (1974): Tolmač lista Ribnica. *Osnovna geološka karta SFRJ 1:100 000*. Zvezni geološki zavod, 60 pp., Beograd.

Buser, S. (1976): Triasne plasti na listu Ribnica, 1. faza. *Mezozoik v Sloveniji*. Geološki zavod Slovenije, 70 pp., Ljubljana.

Buser, S. (1980): Tolmač lista Celovec (Klagenfurt). *Osnovna geološka karta SFRJ 1:100 000*. Zvezni geološki zavod, 62 pp., Beograd.

Buser, S. (1986): Tolmač listov Tolmin in Videm (Udine). *Osnovna geološka karta SFRJ 1:100 000*. Zvezni geološki zavod, 103 pp., Beograd.

Čar, J., Gregorič, V., Ogorelec, B. & Orehek, S. (1980): Sedimentološki razvoj skitskih plasti v idrijskem rudišču. *Rud. met. zbornik.*; Vol. 27/1, pp. 3-19, Ljubljana.

Demšar, M. & Dozet, S. (2002): Litostratigrafski razvoj skitske serije na Križni gori. *RMZ - Materials and Geoenvironment.*; Vol. 49/2, pp. 145-161, Ljubljana.

Dolenec, T., Ogorelec, B. & Pezdič, J. (1981): Zgornjepermske in skitske plasti pri Tržiču. *Geologija.*; Vol. 24/2, pp. 217-238, Ljubljana.

Dozet, S. (1985): Geološke razmere na območju rudišča Pleše in v širši okolici. *Rud. met. zbornik.*; Vol. 32/1-2, pp. 27-49, Ljubljana.

Dozet, S. (2000): Pleška baritonosna formacija, osrednja Slovenija. Primerjava baritonosnih plasti in baritnih pojavov na območju Zunanjih Dinaridov. *Geologija.*; Vol. 42, pp. 41-68, Ljubljana.

Dozet, S. & Silvester, M. (1979): Skitske in zgornjekarnijske kamenine na Kočevskem. *Geologija.*; Vol. 22/2, pp. 327-336, Ljubljana.

Dozet, S. & Novak, M. (2002): Detailed lithostratigraphic dismembering of the Lower Triassic stratigraphic sequence in the Toško Čelo area. - Comparision with the Višnja gora and Werfen (Southern Tirol Dolomites) formation. *RMZ - Materials and Geoenvironment.*; Vol. 49/2, pp. 163-175, Ljubljana.

Dunham, R.J. (1962): Classification of carbonate rocks according to depositional texture – In Ham W.E (Ed.): Classification of carbonate rocks, a symposium. *Am. Assoc. Petrol.*

Geol. Memoir.; Vol. 1, pp. 108-122, Tulsa.

EPSTEIN, A.G., EPSTEIN, J.B. & HARRIS, L.D. (1977): Conodont Alteration Index - and Index to Organic Metamorphism. *Geol. Surv. Prof. Pap.*; Vol. 995, pp. 1-27, Washington.

FOLK, R. (1959): Practical petrographic classification of limestones. *Bull. Am. Ass. Petrol. Geol.*; Vol. 43/1, pp. 2-38, Tulsa.

GERMOVŠEK, C. (1955): Poročilo o kartiranju južnovzhodnega obrobja Ljubljanskega Barja. *Geologija.*; Vol. 3, pp. 235-239, Ljubljana.

GERMOVŠEK, C. (1956): Razvoj mezozoika v Sloveniji. *Prvi jugosl. geol. kongres.*; Vol. 1, pp. 35-43, Ljubljana.

GRAD, K. & FERJANČIČ, L. (1976): Tolmač za list Kranj. *Osnovna geološka karta SFRJ 1:100 000*. Zvezni geološki zavod, 70 pp., Beograd.

GRAD, K. & OGORELEC, B. (1980): Zgornjepermske, skitske in anizične kamenine na Žirovskem ozemlju. *Geologija.*; Vol. 23, pp. 189-220, Ljubljana.

JELASKA, V., KOLAR-JURKOVŠEK, T., JURKOVŠEK, B. & GUŠIĆ, I. (2003): Triassic beds in the basement of the Adriatic-Dinaric carbonate platform of Mt. Svilaja (Croatia). *Geologija.*; Vol. 46/2, pp. 225-230, Ljubljana.

JURKOVŠEK, B. (1987). *Tolmač listov Beljak in Ponteba*. Zvezni geološki zavod, pp. 56, Beograd.

JURKOVŠEK, B., OGORELEC, B. & KOLAR-JURKOVŠEK, T. (1999): Spodnjetriasne plasti pri Tehovcu (Polhograjsko hribovje). *Geologija.*; Vol. 41, pp. 29-40, Ljubljana.

KOLAR-JURKOVŠEK, T. (1990): Smithian (Lower Triassic) conodonts from Slovenia (NW Yugoslavia). *N.Jb. Geol. Paläont.*; Mh. 9, pp. 536-546, Stuttgart.

KOLAR-JURKOVŠEK, T. & JURKOVŠEK, B. (1995): Lower Triassic conodont fauna, from Tržič (Karavanke Mts., Slovenia*). Eclogae geol Helv.*; Vol. 88/3, pp. 789-801, Basel.

KOLAR-JURKOVŠEK, T. & JURKOVŠEK, B. (1996): Contribution to the knowledge of the Lower Triassic conodont fauna in Slovenia. *Razprave 4. razr. SAZU.*; Vol. 37/1, pp. 3-21, Ljubljana.

KOLAR-JURKOVŠEK, T. & JURKOVŠEK, B. (2001): Conodont researches in the Lower Triassic strata of Slovenia. *Geol. zbor., Povzetki ref., 15. Posvet. slovenskih geol.*; Vol. 16, pp. 46-47, Ljubljana.

KOLAR-JURKOVŠEK, T. & JURKOVŠEK, B. (2007): First record of *Hindeodus–Isarcicella* population in Lower Triassic of Slovenia. *Palaeogeogr., Palaeoclimatol., Palaeoecol.*; Vol. 252, 72-81.

MLAKAR, I. (1959): Geološke razmere idrijskega rudišča in okolice. *Geologija.*; Vol. 5, pp. 64-179, Ljubljana.

MUŠIČ, B. (1992): Zgornjepermske in spodnjetriasne kamnine pri Skopačniku v Želimeljski dolini. *Rud. met. zbornik.*; Vol. 39/1-2, pp. 241-259, Ljubljana.

NOVAK, M. (2001): Skitske plasti Toškega Čela. *Geologija.*; Vol. 44/2, pp. 295-3.3, Ljubljana.

OGORELEC, B. & GRAD, K. (1986): Zgornjepermske, skitske in anizične kamenine na Žirovskem ozemlju. *Sažeci predavanja / V skup sedimentologa Jugoslavije, Brioni 2-5.06.1986*. Hrvat. geol. društvo, pp. 53-56, Brioni.

Perri, M.C. (1991): Conodont biostratigraphy of the Werfen Formation (Lower Triassic), Southern Alps, Italy. *Boll. Soc. Paleont. It.*; Vol. 30, pp. 23-46, Modena.

Perri, M.C. & Andraghetti, M. (1987): Permian-Triassic boundary and Early Triassic conodonts from the Southern Alps, Italy. *Riv. Ital. Paleont. Strat.*; Vol. 93/3, pp. 291-238, Milano.

Perri, M. C. & Farabegoli, E. (2003): Conodonts across the Permian–Triassic boundary in the Southern Alps. *Cour. Forsch.-Inst. Senckenberg*.; Vol. 245, pp. 281-313, Frankfurt.

Placer, L. (1999): Contribution to the macrotectonic subdivision of the border region between Southern Alps and External Dinarides. *Geologija*.; Vol. 41 (1998), pp. 223-255, Ljubljana.

Premru, U. (1965): *Stratigrafski razvoj in tektonska zgradba ozemlja me Polhovim Gradcem in Knapovžami: Diplomsko delo*. Geološki zavod Slovenije, 16 pp. Ljubljana.

Ramovš, A. (1989): Razvoj skitskih plasti (spodnji trias) v severnih Julijskih Alpah. *Rud. met. zbornik*.; Vol. 36/4, pp. 623-636, Ljubljana.

Ramovš, A. & Aničić, B. (1995): Untertrias und Unteranis – Ausbildung in Mišnica-Tal, östlich von Rimske Toplice, Ostslowenien. *Rud. met. zbornik*.; Vol. 42/3-4, pp. 143-145, Ljubljana.

Ramovš, A., Aničić, B. & Dozet, S. (2001): Comparision of Lower Triassic developments in Eastern Sava Folds and Northern Julian Alps (Slovenia). *RMZ - Materials and Geoenvironment*.; Vol. 48/3, pp. 415-432, Ljubljana.

Rejebian, V.A., Harris, A.G. & Huebner, J.S. (1987): Conodont color and textural alteration: An index to regional metamorphism, contact metamorphism and hydrothermal alteration. *Geol. Soc. Am. Bull*.; Vol. *99*, pp. 471-497, Washington.

Staesche, U. (1964): Conodonten aus dem Skyth von Südtirol. *N. Jb. Geol. Paläont*.; Vol. 119/3, pp. 247-306, Stuttgart.

Sudar, M. (1986): Trassic microfossils and biostratigraphy of the Inner Dinarides between Gučevo and Ljubišnja Mts. Yugoslavia. *Geol. an. Balk. Poluos*.; Vol. 50, pp. 151-394 , Beograd.

Sudar, M., Jovanović, D., Kolar-Jurkovšek, T. (2007). Late Permian conodonts from Jadar Block (Vardar Zone, northwestern Serbia). *Geologica Carpathica*.; Vol. 58/2, pp.145-152, Bratislava.

Sweet, W.C., Mosher, L.C., Clark, D.L., Collinson, J.W. & Hasenmueller, W.A. (1971): Conodont biostratigraphy of the Triassic. In: Sweet, W.C. & Borgström, S.M. (eds.): Symposium on conodont biostratigraphy. *Geol. Soc. Am. Mem.*; Vol. 127, pp. 441-465, Boulder.

ŠĆAVNIČAR, B. (1973): Klastiti trijasa u Gorskom Kotaru. *Acta geologica. Jug. akad. znan. umetn.*; Vol. 7/3, pp. 106-160, Zagreb.

ŠLEBINGER, C. (1953): Obvestilo o kartiranju listov Cerknica 1 in 2. *Geologija*.; Vol. 1, pp. 288-292, Ljubljana.

YIN, H., ZHANG, K., TONG, J., YANG, Z. & WU, S. (2001): The Global Stratotype Section and Point (GSSP) of the Permian- Triassic Boundary. *Episodes*.; Vol. 24, pp. 102-114, Ottawa.

Strategija dolgoročne proizvodnje premoga in izvedba procesa prestrukturiranja Premogovnika Velenje

Strategy of the longterm coal production and the restructuring processes execution at Premogovnik Velenje

Evgen Dervarič[1]

[1]Premogovnik Velenje d.d., Partizanska 78, 3320 Velenje, Slovenija;
E-mail: evgen.dervaric@rlv.si

Received: July 26, 2007 **Accepted:** August 20, 2007

Izvleček: Rudarska in premogovniška dejavnost se v obdobju zadnjih petnajstih let v svetu in še posebej v Evropi sooča z obsežnimi procesi zapiranja in prestrukturiranja rudnikov in premogovnikov. Ta proces je zajel tudi Slovenijo, kjer se vsi rudniki in premogovniki zapirajo, dolgoročna proizvodnja premoga do leta 2040 se bo ohranjala le v Premogovniku Velenje. Premogovnik Velenje je pomemben steber Republike Slovenije za proizvodnjo električne energije v Termoelektrarni Šoštanj. V obdobju zadnjih petih let se intenzivno pripravlja na pogoje povsem liberaliziranega trga z električno energijo. Osnovno izhodišče za prilagajanje družbe na nastale spremembe je cenovna in kvalitativna konkurenčnost lignita in dolgoročno naravnano poslovanje podjetja z dobičkom. V Premogovniku Velenje smo se na obdobje, ki prihaja temeljito pripravili in izdelali »Razvojni načrt Premogovnika Velenje za obdobje 2006-2011 (2015)«. V prispevku želim predstaviti strateško načrtovanje, pripravo in izvedbo procesa prestrukturiranja rudarske dejavnosti v Premogovniku Velenje.

Abstract: For the last fifteen years all around the world and especially in Europe mining and coal mining branch is exposed to extensive processes of closing and restructuring mines and coal mines. And Slovenia is no exception in this process. All the mines are in the middle of the closing procedure except Premogovnik Velenje (The Velenje Coal-Mine) where a longterm production is to be continued up to 2040. The Velenje Coal-Mine is very important for Slovenia from the aspect of electric energy supply from Šoštanj Thermal Power Plant. Through the last five years period The Velenje Coal-Mine is intensive focused on new conditions on the market, especially on the opening of the electric energy market. Basic aspects of the company adaptation to the changes are price and quality competitive position and a long term profitable operation of the company. Recognizing the future situation

Review paper

to be faced in the period to come The Velenje Coal-Mine prepared »Strategic Development Plan for The Velenje Coal-mine 2006-2011 (2015)«. So I would like to introduce strategic plans, preparing and execution of the restructuring processes in Velenje Coal-Mine.

Ključne besede: strategija, prestrukturiranje, poslanstvo, vizija, rudarstvo
Key words: strategy, restructuring, mission, vision, mining

Uvod

Delež premoga v energetski bilanci EU-25 znaša 19 %. Danes je EU že 50 % energetsko odvisna, do leta 2030 pa se bo uvozna odvisnost povzpela na 70 %. Proizvodnja premoga v RS (Republiki Sloveniji) pada. Od rekordnih 6,8 milijona ton v začetku 80-tih let je proizvodnja padla na 4,5 milijona ton v letu 2006. Podobni, vendar še izrazitejši trendi se dogajajo tudi v EU (Evropski uniji). Zamenjava premoga z drugimi fosilnimi gorivi (predvidoma s plinom) bo v RS neizogibno poslabšala samozadostnost in povečala uvozno odvisnost tudi pri proizvodnji električne energije. Zaradi tega je tudi v bodoče potrebno ohraniti domačo proizvodnjo lignita in poiskati kompromis med izpolnjevanjem obvez po Kjotskem sporazumu in doseganju konkurenčnih pogojev poslovanja. Uporaba premoga je predvidena samo v Termoelektrarni Šoštanj.

Zmanjševanje proizvodnje domačega premoga bo pomenilo velik pritisk na ceno premoga. V okviru dopuščenih ukrepov evropske energetske zakonodaje (15 % možna zaščita domačih virov, prednostno dispečiranje) ter na podlagi Uredbe Sveta o državnih pomočeh v premogovništvu (EC No 1407/2002) bo treba zagotoviti ustrezno podporo za:

- ohranitev dostopa do potencialnih zalog za bodoče premogovne tehnologije,
- potrebno kadrovsko socialno prestrukturiranje oziroma izvajanje zapiralnih del.

V razvojnem načrtu Premogovnika Velenje od leta 2005 do leta 2014 je predvideno, da bomo zagotavljali proizvodnjo premoga v višini, ki jo predvideva nacionalni energetski program oziroma po potrebah iz letnih energetskih bilanc RS. V letu 2006 smo za zanesljivo oskrbo Slovenije z električno energijo dosegli proizvodnjo 3,94 milijone ton lignita. To je znatno več, kot predvideva nacionalni energetski program. Trendi porabe električne energije pa tudi v prihodnje kažejo le navzgor.

Poslovanje PV (Premogovnik Velenje) temelji na dveh stebrih. Prvi je proces pridobivanja premoga, kjer bomo s stalnimi racionalizacijami poslovanja zmanjšali obseg jame in število zaposlenih iz 1812 v letu 2006 na 1400 do konca leta 2010. Ob tem bo potrebno zapreti del odkopnega polja jame Škale. Stroški zapiranja jame Škale bodo znašali 27 mio EURO. Drugi steber pa predstavlja kadrovsko prestrukturiranje matičnega podjetja in hčerinskih družb. V odvisnih družbah je zaposlenih 1370 delavcev. Osnovni cilj vseh družb je postopno zmanjševanje kapitalske in poslovne odvisnosti od matičnega podjetja. V vseh primerih iščemo za nadaljnjo rast in razvoj odvisnih družb poslovne partnerje z jasno poslovno vizijo in investicijskim potencialom.

Proizvodnjo lignita v Velenju je mogoče zagotoviti z dolgoročnim povezovanjem poslov pridobivanja lignita in proizvodnje električne energije na temelju približevanja konkurenčni ceni 2,25 EURA/GJ do leta 2011, kar zagotavlja zanesljivo delo premogovnika ter optimalno proizvodnjo električne energije (dolgoročna desetletna pogodba o proizvodnji lignita).

Izhodišča pri izdelavi razvojnega načrta

Proizvodnjo lignita v Velenju lahko zagotovimo:

- z dolgoročnim povezovanjem poslov pridobivanja lignita in proizvodnje električne energije na temelju cen, ki zagotavljajo zanesljivo delo premogovnika ter optimalno proizvodnjo električne energije,
- s pridobitvijo dodatnih finančnih sredstev za zapiranje jame Škale. Za del proizvedene električne energije iz velenjskega lignita lahko vlada RS uveljavi mehanizem prednostnega dispečiranja in s tem zagotavlja prodajo električne energije, proizvedene na podlagi domačih virov do največ 15 % primarne energije za pokritje skupnih potreb po električni energiji v Sloveniji,
- z razvojno raziskovalnim delom na področju obstoječih ter novih tehnologij pridobivanja premoga,
- s kompetentnimi zaposlenimi.

Strategija razvoja povezanih podjetij PV je usmerjena:

- v zmanjševanje odvisnosti od internega trga (ciljno pod 20 % PV),
- v zmanjševanje kapitalske odvisnosti od PV, s privatizacijo vseh hčerinskih družb v letu 2007, z izjemo HTZ (največje hčerinsko invalidsko podjetje),
- v invalidskem podjetju HTZ je koncept razvoja usmerjen v izločanje programov, ki so tržno zanimivi in v racionalizacijo ter optimiranje programov, ki podpirajo proces premoga. V podporo konceptu razvoja, je v HTZ ustanovljen center za usposabljanje in izobraževanje ter zaposlovanje.

Nova delovna mesta, zaradi zmanjševanja števila zaposlenih v osnovni dejavnosti in prezaposlovanja presežkov, bomo zagotovili:

- z lastnimi sredstvi - ustanovitev naložbenega podjetja PV Invest d.o.o. z 12.4.2006,
- s strateškimi partnerji z jasno poslovno vizijo, trgom in investicijskim potencialom (delež PV: 30 % ali manj).

Predstavitev podjetja

Premogovnik Velenje je delniška družba, katere osnovna dejavnost je pridobivanje lignita. Premogovnik Velenje sestavljajo poleg matične družbe še družbe, v katerih ima obvladujoča družba na dan 1.1.2007 naslednje dolgoročne naložbe:
Premogovnik Velenje d.d. je povezana družba HSE (Holdinga Slovenske elek-

Slika 1. Premogovnik Velenje in odvisne družbe
Figure 1. The Velenje Coal Mine and Associated Enterprises

trarne). Po končanem procesu privatizacije odvisnih družb, bo PV imel dolgoročne naložbe v naslednjih družbah:

Cilj PV je ohranitev 100-odstotnega lastniškega deleža v podjetjih HTZ IP d.o.o., PV Invest d.o.o. ter v Jama Škale v zapiranju d.o.o. V vseh ostalih odvisnih družbah želimo ohraniti kontrolni delež oziroma 26 % lastniški delež.

POSLANSTVO PODJETJA

Poslanstvo podjetja predstavljajo naslednja izhodišča:

- proizvodnja lignita, s katero bo zagotavljalo nemoteno oskrbo z električno energijo v slovenskem prostoru,
- omogočati tehnično in ekonomsko sprejemljivo poslovanje Premogovnika Velenje,

- zaposlenim zagotavljati največjo stopnjo varnosti in humanosti pri izvajanju delovnega procesa,
- zagotavljati učinkovito reševanje okoljskih problemov, ki nastajajo kot posledica pridobivanja lignita,
- izvajati kadrovsko socialno prestrukturiranje poslovnega sistema, s ciljem ohranjanja sedanjih delovnih mest in ustanavljanja novih.

Vizija podjetja

- Proizvodnja premoga po Dolgoročni pogodbi o nakupu premoga, zakupu moči in nakupu električne energije, podpisane med HSE, TEŠ (Termoelektrarna Šoštanj) in PV (2005 - 2014), v višini 38.500 TJ/leto do leta 2014 (scenarij za naslednje desetletno obdobje 38.500 TJ /leto ± 5 %) in najmanj 30.000 TJ /leto po letu 2014 (skladno s

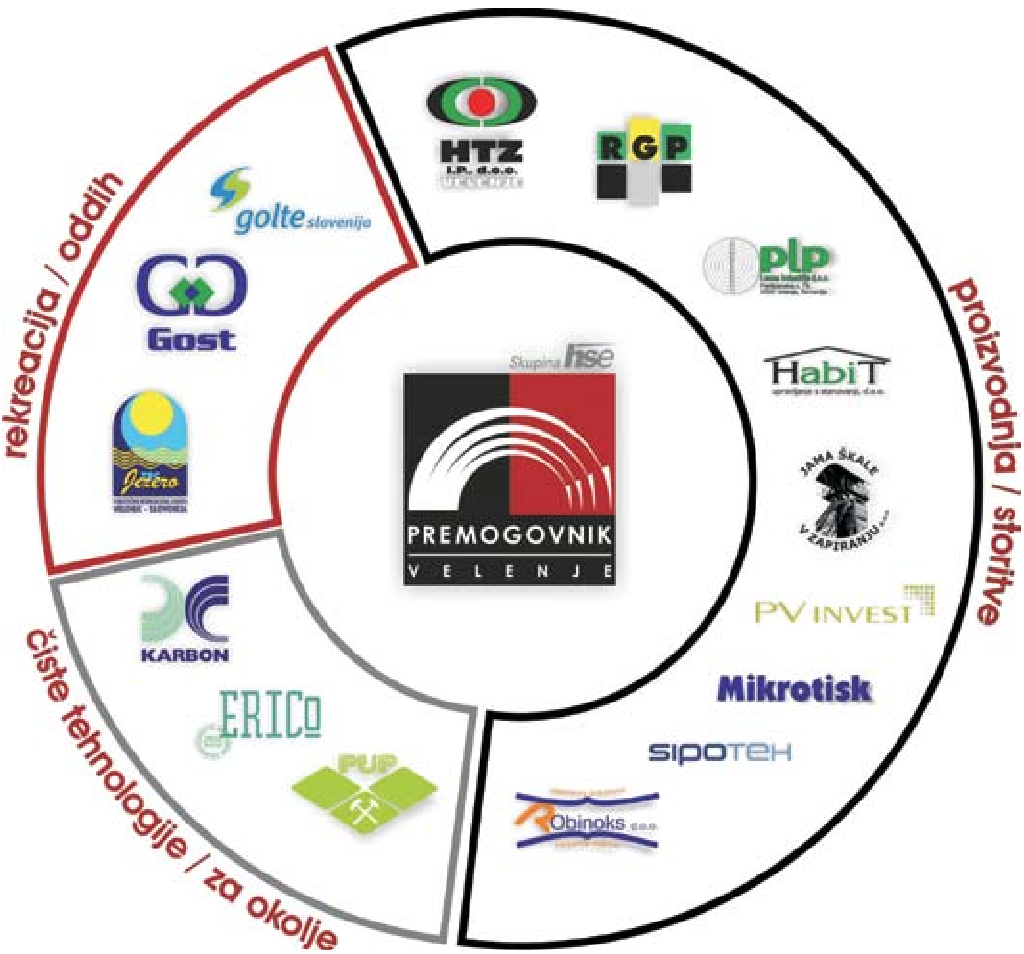

Slika 2. Premogovnik Velenje in odvisne družbe - po privatizaciji
Figure 2. The Velenje Coal Mine and Associated Enterprises after Privatisation

programom razvoja TEŠ).
- Racionalizacija procesa pridobivanja premoga oziroma zmanjšanje obsega jamskih objektov.
- Intenzivno prestrukturiranje Premogovnika Velenje - ohranjanje obstoječih in ustanavljanje novih delovnih mest; postopno zniževanje števila zaposlenih pri procesu premoga in izločanje vseh dejavnosti, ki ne podpirajo osnovne proizvodnje lignita.

VREDNOTE

Vrednote, ki jih bomo spoštovali pri svojem delu, so:
- varnost, humanost in zdravje zaposlenih v procesu dela,
- učinkovitost, gospodarnost in uspešnost pri opravljanju dela,
- odgovoren odnos do naravnega in družbenega okolja,
- znanje, strokovnost, inovativnost,
- skrb za zaposlene in razvoj njihovih potencialov.

MERILA UČINKOVITOSTI, GOSPODARNOSTI IN USPEŠNOSTI

Merila za ugotavljanje doseganja ciljev uspešnosti pri izvajanju poslanstva in vizije podjetja na podlagi razvojnih projektov bodo temeljila na:
- produktivnosti,
- spremljanju delovne uspešnosti obratov, enot in posameznikov,
- dobičku,
- odnosu do okolja,
- zadovoljstvu kupca,
- zadovoljstvu zaposlenih,
- učinkoviti rabi razpoložljivih resursov.

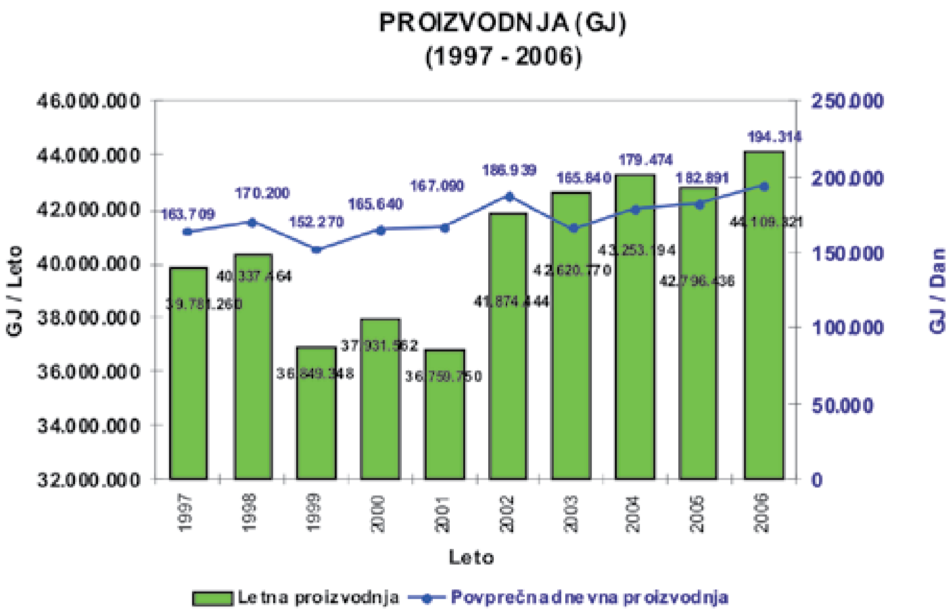

Slika 3. Proizvodnja (GJ)
Figure 3. Production (GJ)

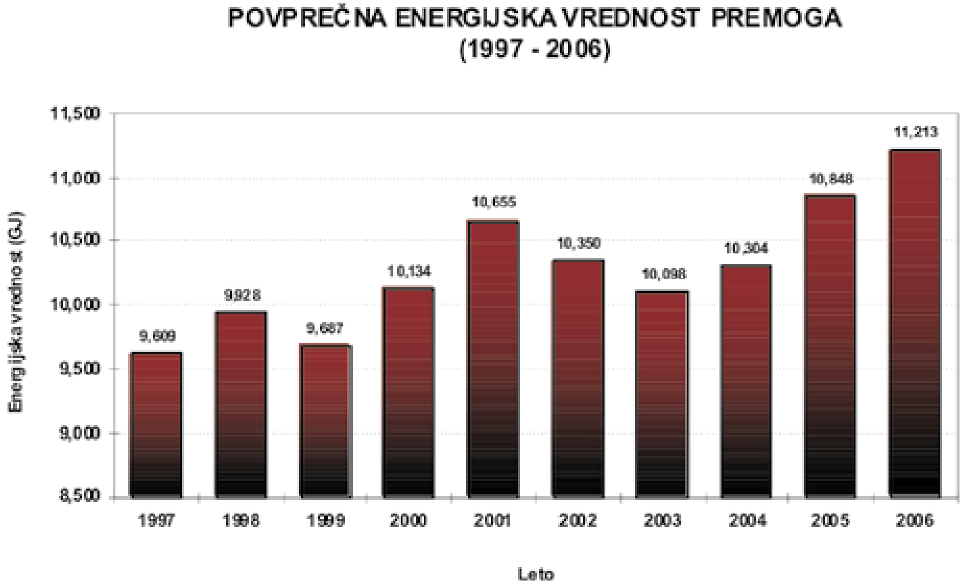

Slika 4. Energijska vrednost premoga
Figure 4. Calorific value of the coal

Analiza stanja

Pomembnejše ugotovitve pri analizi stanja so:

- glavna dejavnost družbe je pridobivanje premoga,
- poslovanje podjetja je bilo v letu 2006 uspešno v smislu izpolnjevanja poslanstva, vizije in strateških ciljev, ki od nas zahtevajo racionalizacijo poslovanja. Podjetje je v letu 2006 poslovalo z dobičkom,
- verificiran je bil dolgoročni načrt odkopavanja velenjskega odkopnega polja glede na investicijo v blok 6 v TEŠ, ki omogoča odkopavanje do leta 2040 (prej do leta 2025),
- v obdobju zadnjih petih let je bila z izboljšanjem tehnoloških procesov pridobivanja premoga znatno povečana njegova kurilna vrednost (več kot 10 %) in s tem ob relativno enaki letni količinski proizvodnji tudi večja energetska vrednost proizvodnje (grafi na slikah 3 in 4),
- nakup sodobne odkopne opreme (povečana varnost zaposlenih, izboljšanje delovnega okolja in večja produktivnost odkopne fronte),
- uvedba frekvenčno reguliranih pogonov v procesu odvoza premoga iz jame (enakomerne obremenitve transportnih sredstev povečujejo zanesljivost obratovanja),
- uvedli smo nov informacijski sistem MFG/PRO,
- pridobili smo standarda OHSAS (varnost pri delu) in USP S-10 (učeče se podjetje),
- prodaja premoga v letu 2006 predstavlja 88,2 % vseh prihodkov, ostala realizacija (prihodki iz prodaje, financiranja, izredni prihodki) pa 11,8 %,
- TEŠ porabi 96,3 % premoga za proi-

zvodnjo elektrike ter 3,7 % premoga za pridobivanje toplote,
- PV zagotavlja dobro četrtino proizvedene električne energije v Sloveniji,
- družba sproti prilagaja svojo organiziranost,
- večina stalnih sredstev podpira glavno dejavnost družbe, to je pridobivanje premoga,
- imamo velik intelektualni kapital in razvite sisteme za njegovo upravljanje.

Analiza okolja

Ugotovitve pri analizi okolja lahko strnemo v naslednjem:
- Posebnost trga energetskega premoga je, da države proizvajalke (razen Indonezije, Južne Afrike, Rusije, Poljske, Avstralije, Kanade, Kitajske, Kolumbije, ZDA, Venezuele) porabijo ves domači premog za proizvodnjo električne energije. Dodatno uvažajo in porabijo za proizvodnjo električne energije cca. 10 % celotne svetovne proizvodnje vseh vrst premoga.
- Cene premoga za proizvodnjo električne energije so v zadnjih desetih letih nihale v zelo širokem razponu. Značilna so nihanja v obliki sinusoide.
- V Sloveniji se letno porabi približno 13.000 GWh električne energije.
- Cena električne energije za posamezno kategorijo kupca je odvisna od namena uporabe in letne količine porabljene električne energije.
- Predvidevanja kažejo, da bo proizvodnja energetskega premoga v svetu naraščala. Na oblikovanje cen bodo še naprej vplivali ponudba in povpraševanje, dogajanja na trgu ostalih fosilnih goriv, politične razmere v svetu in cene transportnih storitev.
- Premogu PV so konkurenčni vsi energetsko primerni premogi, ki predstavljajo v TEŠ nižji strošek goriva kot premog iz PV. Gre za premoge z majhno vsebnostjo žvepla, ki so dražji, in tiste z večjo vsebnostjo žvepla, ki so cenejši. Uporaba tujih premogov je povezana z izgradnjo infrastrukture, potrebne za pretovarjanje, kar njihovo konkurenčnost zmanjšuje. Uvoz energetskega premoga je vezan na strategijo energetske politike Slovenije.
- TEŠ je edini porabnik energetskega premoga iz PV.

Sinteza

Sprejeta pravila igre iz okolja
- Osnovna dejavnost se mora podrejati razmeram na liberaliziranem energetskem trgu v Sloveniji.

Sprejeta interna pravila igre
- Osnovna dejavnost PV se ne bo spremenila in še naprej ostaja pridobivanje premoga.
- Proces pridobivanja premoga bomo optimirali in investicijska vlaganja usmerili v racionalnejšo in varnejšo proizvodnjo.
- PV bo v naslednjem obdobju nadaljeval z organiziranjem dela osnovne dejavnosti v HTZ.
- HTZ bo poleg programov osnovne dejavnosti in programov, ki osnovno dejavnost podpirajo (vzdrževanje opreme v jami), razvijal programe, v katere bo lahko produktivno zaposlil invalide.

- Razpoložljive vire v PV in HTZ bomo prerazporedili v spremljajoče dejavnosti, ki bodo sposobne delo pridobiti tudi izven poslovnega sistema (učinkovito je razmerje 20:80 v korist trga), jih organizirali v samostojna podjetja ter jih poskušali povezati s partnerji izven sistema.
- Povezane družbe PV bomo lastniško preoblikovali (z izjemo HTZ).
- Na trge bomo vstopali tudi prek vezanih poslov.
- Pridobili bomo potrebne licence in koncesije za izvajanje del in storitev.
- V letu 2006 smo pričeli s projektom Prenove organizacijskih procesov, s katerim bomo verificirali organizacijsko strukturo podjetja, zasedenost delovnih mest in opravil ter pretok dokumentov v družbi, s ciljem racionalizacije in poenostavitve vseh procesov.
- Dobre podjetniške zamisli bomo kapitalsko podprli.
- Uveljavili bomo organizacijsko kulturo, ki bo vzpodbujala podjetništvo, inovativnost in timsko delo.
- Razvijali bomo sisteme ravnanja z ljudmi pri delu, izobraževanje za delo, vodenje in razvoj kadrov, motiviranje in nagrajevanje, timsko delo, komuniciranje, letne pogovore, inovativnost, koncept učečega se podjetja.

SWOT analiza za program pridobivanja premoga

PV zagotavlja premog, ki je edini domači fosilni vir energije in je namenjen izključno pretvorbi v električno in toplotno energijo v TEŠ. Velika prednost tovrstne proizvodnje je prilagodljivost in zanesljivost pri oskrbi. PV razpolaga z vsemi potrebnimi viri za dolgoročno pridobivanje premoga. Strošek pridobivanja premoga se bo v prihodnjih 10 letih znižal za 15 %, kar predstavlja osnovo za njegovo konkurenčnost z drugimi energetskimi viri. Slabost PV predstavlja neugodna struktura stroškov (visoki stalni stroški in visok delež stroška dela). Temeljno nevarnost za PV predstavlja sprememba zakonodaje (rudarski zakon, zakon o invalidskih podjetjih, energetski zakon in nacionalni energetski program), zahteve Kyoto protokola (CO_2 takse - toplogredni plini) in zapiranje jame Škale (zagotovitev sredstev). Precej odprtih vprašanj porajajo spremembe, ki jih bo prinesla liberalizacija energetskega trga v Sloveniji.

SWOT analiza za program prestrukturiranja

PV ima postavljen koncept in strategijo prestrukturiranja. Prestrukturiranje oziroma zaposlovanje na nova delovna mesta želimo izpeljati že v aktivni fazi premogovnika in ne v fazi zapiranja le tega. V ta namen bo potrebno zagotoviti lastna sredstva in sredstva strateških poslovnih partnerjev. Osnovne slabosti PV so pretežno netržna usmerjenost, programski portfelji, ki temeljijo na osnovni dejavnosti, neugodna starostna in izobrazbena struktura zaposlenih. Programe, ki so organizirani v povezanih podjetjih, bo potrebno prestrukturirati, saj večinoma ne dosegajo ustrezne rasti in dodane vrednosti na zaposlenega. Osnovna priložnost za povezane družbe so investicijski projekti na avtocestah, železnicah, v energetiki in drugje. Priložnost predstavlja tudi razvoj informacijskih in telekomunikacijskih tehnologij, velik tržni potencial na turističnem področju v regiji ter čistih tehnologijah za okolje.

CILJI, STRATEGIJE, VIRI IN ORGANIZIRANOST

Strateški cilji PS PV

- racionalizacija procesa pridobivanja premoga,
- zagotavljanje varnosti in humanosti pri izvajanju delovnega procesa,
- reševanje okoljskih problemov,
- intenzivno prestrukturiranje povezanih podjetij in strokovnih služb Premogovnika Velenje ter ustanavljanje novih podjetij.

Cilji programa pridobivanja premoga

- proizvodnja in prodaja premoga skladno z 10-letno pogodbo,
- zmanjševati število zaposlenih skladno z rastjo produktivnosti 5,6 % letno (graf na sliki 5) v PV in HTZ,
- pridobiti sredstva za zapiranje Jame Škale v naslednjih letih,
- ohranjati trend zmanjševanja izgubljenih dnin zaradi nesreč pri delu in odsotnosti z dela zaradi bolezni za 3 % na leto,
- zmanjšanje obsega del v delu eksploatacijskega območja, ki je izven vpliva neposrednega odkopavanja,
- prodaja rudarsko tehnološkega znanja, predvsem na tujih trgih bivše Jugoslavije in v povezavi z razvojnimi ambicijami HSE na teh in drugih trgih.

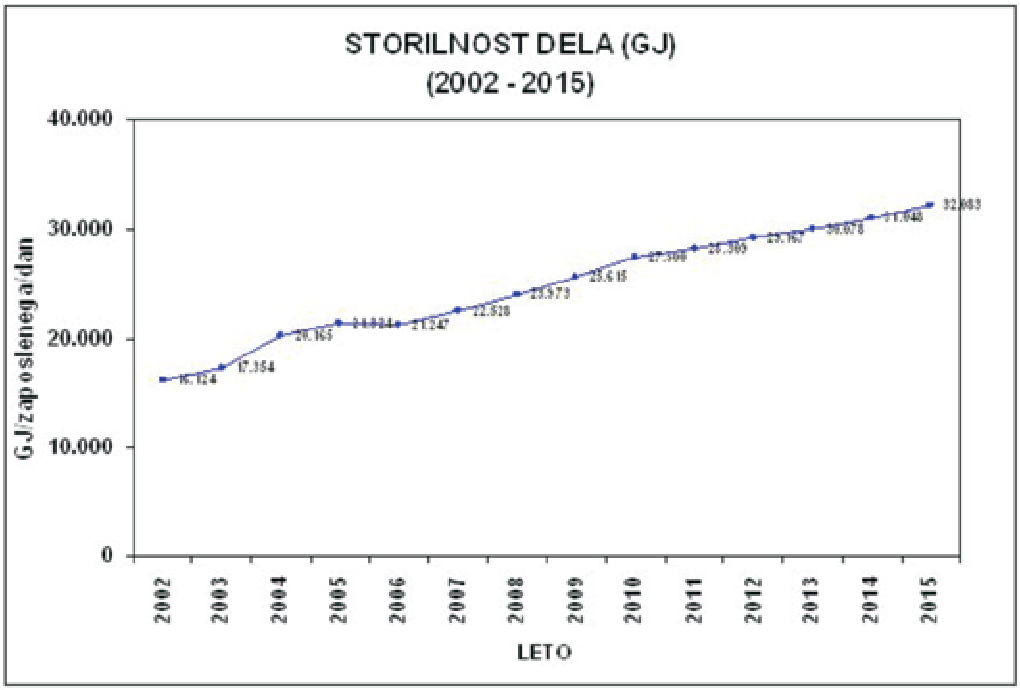

Slika 5. Storilnost dela
Figure 5. Productiveness

Potrebni viri za doseganje ciljev

Kadri

Ob načrtovani proizvodnji smo pripravili kadrovski načrt za obdobje do leta 2015. Število zaposlenih se bo v obeh podjetjih znižalo za 5 % povprečno letno. Do leta 2010 poprečno letno 7,8 %, po tem letu pa za 3 %.

V naslednjih letih bo PV in HTZ predvidoma zapustilo 1460 delavcev:

- pogoj za starostno upokojitev v tem obdobju dosežejo 1304 delavci ali povprečno letno 145 delavcev,
- 160 delavcev bo omenjeni podjetji predvidoma zapustilo zaradi drugih vzrokov (sporazumne razveljavitve pogodb...),
- v obravnavanem obdobju bomo v PV potrebovali povprečno letno 36 novih delavcev, pri zaposlovanju pa težili k optimalni kadrovski strukturi,
- število zaposlenih PV ter HTZ bo določeno z letnim planom in bo odvisno od politike zaposlovanja v invalidskem podjetju, povezane z invalidsko zakonodajo.

Potrebne naložbe

Načrtovane naložbe za proces pridobivanja premoga v naslednjem desetletnem obdobju so v jamske gradbene objekte in izrabljeno ter tehnološko zastarelo opremo. Poleg tega pa bo potrebno vlagati v opremo, ki bo omogočala racionalizacijo proizvodnje. Največja vlaganja bodo potrebna na področju opreme za odkope. V tem obdobju predvidevamo vlaganja med 5 mio EURO in 7 mio EURO letno. Pri opremi za izdelavo prostorov imamo najbolj tehnološko zastarelo in izrabljeno opremo. Glede na to, da izdelava objektov pomeni stroškovno najzahtevnejši proces, bodo v naslednjem obdobju na tem segmentu potrebna intenzivna vlaganja v opremo za izdelavo prostorov in transport premoga iz pripravskih delovišč. V obdobju predvidevamo vlaganja med 1,5 mio EURO in 2,5 mio EURO letno. Oprema za transport in klasiranje ter drobljenje zahteva vlaganja v obnavljanje in s tem podaljševanje življenjske dobe naprav. V obdobju predvidevamo vlaganja med 2 mio EURO in 3 mio EURO letno. Pri opremi za infrastrukturo načrtujemo obnavljanje obstoječe opreme in vlaganja v nove razvode. V obdobju predvidevamo vlaganja med 1 mio EURO in 3 mio EURO letno. Na področju izgradnje jamskih objektov se v naslednjem desetletnem obdobju predvideva zmanjšan obseg del. Vrednost vlaganj v te objekte bo padla s 2,5 mio EURO na 0,7 mio EURO. Na področju opreme za transport materiala, ljudi in premoga načrtujemo obnavljanje iztrošene opreme in s tem zagotavljanje obratovalne zanesljivosti. V obdobju predvidevamo vlaganja med 0,5 mio EURO in 1,5 mio EURO letno. Na področju zunanjih gradbenih objektov ne načrtujemo večjih sanacijskih posegov na infrastrukturnih objektih. V obdobju predvidevamo zmanjšanje vlaganj. Na področju informatike, varnostno tehnološko informacijskega sistema, prenosa podatkov in obdelave informacij načrtujemo vlaganja v zamenjavo zastarele opreme, avtomatizacijo procesov in posodobitev omrežja. V obdobju predvidevamo vlaganja med 0,7 mio EURO in 1 mio EURO letno.

Pri opremi za prezračevanje načrtujemo vlaganja v nove merilnike plinov in ventilatorjev za prezračevanje pripravskih delovišč. V obdobju predvidevamo vlaganja med 0,4 mio EURO in 0,6 mio EURO letno.

Naložbe v alternativne programe
Usmerjene bodo v ustanavljanje novih, tržno naravnanih podjetij z dolgoročno dobičkonosnostjo. Naložbe bodo izvedene s ciljem izločanja vseh dejavnosti, ki ne podpirajo procesa premoga. Pomembnejša naložba v letu 2008 bo investicija v sončno elektrarno z močjo 1 MW, ki bo prva sončna elektrarna v Sloveniji in v tem delu Evrope.

Cilji navedene naložbe so:
- uvedba novega tržnega programa v prestrukturiranje družbe HTZ,
- uporaba prostora, ki poveča vrednost (izkoriščanje degradiranih področij po rudarjenju),
- pridobitev dela sredstev iz EU skladov, iz programa Altener,
- prispevek k trajnostnemu razvoju,
- pridobitev kvot za emisije CO_2.

Razvojni projekti
V smislu racionalizacije procesa pridobivanja premoga smo pripravili razvojne projekte za tista delovna področja, ki nam bodo na osnovi izkušenj iz naše in tujih praks ter možnih sprememb in dopolnitev posameznih procesov in aktivnosti prinesla največje učinke pri realizaciji zastavljenih ciljev.

Razvojni projekti, na katerih temeljijo vse razvojno-raziskovalne aktivnosti, pokrivajo naslednja področja:
- varnost in zdravje pri delu,
- pridobivanje in transport premoga ter ekologijo delovnega okolja,
- optimizacija in avtomatizacija transporta premoga,
- transport in logistika,
- jamske proge,
- jamsko vrtanje,
- elektro področje,
- čiste tehnologije uporabe premogov.

Glede na pričakovane učinke razvojnih projektov bomo za njihovo realizacijo namenili 0,5 mio EURO letno. Za hitrejšo in uspešnejšo realizacijo razvojnih projektov bomo zagotavljali lastna sredstva in še naprej iskali možne oblike sofinanciranja (javni razpisi, državne pomoči, mednarodna sredstva…).

PROGNOZA DELOVANJA DRUŽBE PO LETU 2015

V Nacionalnem energetskem programu je lignit iz Velenja dolgoročno opredeljen vir za zagotavljanje nemotene oskrbe Republike Slovenije z električno energijo. Že v elaboratu: »Koncept odkopavanja od leta 2000 do leta 2025« št. elaborata 9/2000 – MJ smo potrdili, da lahko izkopljemo potrebne količine premoga za nemoteno obratovanje Termoelekrarne Šoštanj v okviru novih investicij in pričakovane dinamike obratovanja posameznih blokov. To potrjujejo tudi naslednji dokumenti:
- koncept izdelave glavnih prog od nivoja k.-44 do dna kadunje in odkopavanja premoga do leta 2025 v Premogovniku Velenje – št. elaborata 16/2003 MJ,
- poročilo o stanju zalog premoga na dan 31.12.2004 ter primerjava z odkopnimi zalogami iz dolgoročnih konceptov odkopavanja,
- dinamika odkopavanja z letno proizvodnjo 3 mio ton premoga po letu 2015

po veljavnih dolgoročnih konceptih odkopavanja v PV,
- dinamika odkopavanja z letno proizvodnjo 4 mio ton premoga.

Letna proizvodnja lignita bo po letu 2015 znašala najmanj 3 milijone ton oziroma glede na potrebe TEŠ. Za investicijski program bloka 6 bomo natančneje načrtovali postopno zmanjševanje proizvodnje PV po letu 2015 oziroma do konca eksploatacije velenjskega odkopnega polja.

Sklepi

Analiza poslovnega sistema kaže veliko paleto programov. Razmerje med notranjim in zunanjim trgom pa se vsako leto povečuje v korist drugega. Za prodor na trg iščemo strateške partnerje z jasno poslovno vizijo, trgom in investicijskim potencialom. Program pridobivanja premoga bomo v naslednjih letih racionalizirali. S procesom prestrukturiranja in z ustanavljanjem novih delovnih mest želimo zmanjšati socialne in razvojne probleme v regiji. Eden izmed pogojev za uspešen in konkurenčen nastop na trgu je racionalno obnašanje posameznih subjektov znotraj poslovnega sistema. To bo mogoče doseči z optimalno izrabo resursov. Z integracijo sistemov razvoja kadrov je potrebno doseči, da bodo zaposleni motivirani za delo, izobraževanje, inovativnost in nove poslovne ideje, saj bomo le tako uspešno in dolgoročno konkurirali na trgu. Sestavni del razvojnega načrta je tudi reševanje okoljskih problemov in rudarskih škod ter realizacija programa zapiranja jame Škale. Z uspešno implementacijo razvojnega načrta bomo bistveno izboljšali svoj finančni položaj in okrepili svojo vlogo pri dolgoročni energetski politiki v Sloveniji.

Summary

Strategy of the longterm coal production and the restructuring processes execution at Premogovnik Velenje

The main purpose of this article is to introduce main strategic restructuring aspects of enterprises which are directly (coalmines) or indirectly (enterprises depending on coalmines) linked with coal mining. And according to that fact, we try to determine principal factors required for a successful execution of a restructuring process as well in enterprises focused on its basic activities (coal mining) as in enterprises which also appear in other branches, but remain tied connected to its basic activities or these enterprises were established through the process of coalmine supporting activities (depending companies) exclusion. Importance of the restructuring process exerts influence upon the whole area, relaying on coal mining activity. So (according to this fact) reconciliation of activities between the government – local community – coalmine is very important. Content of the article is concepted on this base.

Due to the fact of the crisis in coalmining in Europe, shown by decreasing production, number of employees, number of mines, it is important to find out which are the facts of achieving at least conditional competitive position or successful execution of the restructuring process and, as a result, to overcome the crisis. In case of subordinating enterprises the situation is

even more complicated. These enterprises act on other markets under hard competitive conditions. And to be competitive is priority. This way we try to find out what a positive praxis is to be and to point out important aspects for a successful restructuring process execution.

It is intended to analyse the conditions and the main restructuring aspects in Slovenian coalmining. Concerning to the aspects, Slovenian praxis is specific and indicates two possible directions of knowledge development in restructuring process of introvertil systems. And due to good results from the view of successful restructuring process, praxis executed in Velenje Coalmine is very important.

The paper represents the identification of main strategic aspects in restructuring process in coalmine enterprises and explanation of the restructuring process model. Formed model is to be based on positive coalmine restructuring process praxis all over the Europe (accentuation on Slovenia), on knowledge of mastering critical conditions in enterprises and identification of basic districts required for the execution of strategic changes in operation.

This report introduces the system of restructuring at Velenje Coal Mine, the biggest coal mine in Slovenia with yearly extraction about 4 million tonnes of lignite and where the production for next at least 35 years is foreseen.

For several years Velenje Coal Mine has been preparing the strategy of the European Union electricity market liberalisation. The basic strategic goals have been pointed out with an important decision – to carry out these programs without violent interventions in achieving the reduction of employees.

Process of restructuring inside Velenje Coalmine is based on achieving four of the main strategic goals:

- organization and realization of technological process of coal extraction with intention to achieve the highest grade of productivity and the lowest possible coal price,
- the highest grade of safety and humanization of the working process,
- to solve the environment problems which may occur in future as a consequence of an extraction and electric supply,
- new working places as replacement for working places which might be cancelled as a consequence of restructuring.

.

It is very important that Velenje Coal Mine has complete support from unions and employees which take an active part in this process. The results are extremely positive and could be used as a restructuring model and as a good experience as well for subjects which are at the beginning of coal mine accommodation on new, extremely hard conditions for successful business.

Viri

[1] *1., 2. in 3. Strateška konferenca skupine HSE za leti 2003, 2004 in 2005.*

[2] Coal in Europe. *Euracoal.* Brussels, 2005.

[3] Coal Industry across Europe. *Euracoal,* 2003.

[4] *Council Regulation on State Aid to the Coal Industry ECN 1470/2002.*

[5] *Dokumentacija in elaborati o razvoju odkopnih polj in odkopavanja premoga v jamah Premogovnika Velenje.* Premogovnik Velenje, 2005.

[6] *Dolgoročna pogodba o nakupu premoga, zakupni moči in nakupu električne energije.* Velenje, 2004.

[7] *Dolgoročni kadrovski plan Premogovnika Velenje.*

[8] *Druga dokumentacija Premogovnika Velenje.*

[9] *Ekonomski in makroekonomski vidiki dolgoročne pogodbe o nakupu in prodaji premoga za obdobje od 2004 do 2014.* Ekonomski inštitut pravne fakultete v Ljubljani, 2004.

[10] *Elaborat o zapiranju jame Škale Premogovnika Velenje (2000) z rebalansi v letih 2002 in 2004.*

[11] *Energetska bilanca Republike Slovenije za leto 2005.* Ministrstvo za gospodarstvo RS, 2005.

[12] Energetski zakon – EZ. *Ur.l. RS, št. 79/1999 in 51/2004.*

[13] *Koncesijska pogodba št. 354-14-73/01 2002.*

[14] KtatAnnual Report 2005. European *Association for Coal and Lignite.*

[15] *Načrti Vlade RS na področju energetike.* Ministrstvo za gospodarstvo RS, Direktorat za energijo, 2006.

[16] *Poročilo o stanju zalog premoga na dan 31. 12. 2004 ter primerjave z odkopnimi zalogami iz dolgoročnih konceptov odkopavanja.* Premogovnik Velenje, 2005.

[17] *Poslovni načrt Premogovnika Velenje za leto 2007.*

[18] *Poslovno poročilo Premogovnika Velenje za leto 2006.*

[19] *Programi razvojnih projektov v Premogovniku Velenje.*

[20] *Razvojni načrt družbe Premogovnik Velenje za obdobje 2001-2005/2010.* Velenje, 2000.

[21] Resolucija o Nacionalnem energetskem programu. *Ur.l. RS št. 57/2004.*

[22] *Steam Coal Forecaster. Issue 36, McCloskey`s,* 2004.

[23] *Strokovno mnenje - odločanje o odprodaji in nakupu družb hčera oziroma večinskih kapitalskih deležev ter prestrukturiranju lastniškega kapitala.* Inštitut za gospodarsko pravo Maribor, 2005.

[24] *Transparentni postopek prodaje oziroma dokapitalizacije družbe hčere oziroma kapitalske naložbe zaradi restrukturiranja kapitala.* Inštitut za gospodarsko pravo Maribor, 2005.

[25] Zakon o postopnem zapiranju Rudnika Trbovlje-Hrastnik in razvojnem prestrukturiranju regije. *Ur. l. RS, 61/2000 in Ur. l. RS št. 2/6-894/2005.*

Creating new user defined functions for 2D adjustment by parameter variation modelling

Ustvarjanje novih lastnih funkcij za modeliranje 2D posredne izravnave

Milivoj Vulić[1], Dušan Setnikar[2]

[1]University of Ljubljana, Faculty of Natural sciences and Engineering, Department of Geotechnology and Mining Engineering, Aškerčeva cesta 12, SI-1000 Ljubljana, Slovenia;
E-mail: milivoj.vulic@ntf.uni-lj.si
[2]Geodetski zavod Celje d.o.o., Ulica XIV. divizije 10, 3000 Celje, Slovenia;
E-mail: dusan.setnikar@gz-ce.si

Received: September 25, 2007 **Accepted:** December 9, 2007

Abstract: Trigonometric network adjustments are executable with a wide range of programmes. For the modelling of a 2D adjustment by parameter variation[5], Excel was chosen due to its widespread use, accessibility and generally well-known basic use, furthermore also because of the easy scanning, flexibility in procedure determination and UDF support, the use of which adds considerably to the ease of scanning. The user defined functions arranged for an Excel environment that were used in the referred adjustment[1],[5] are presented. Each UDF presentation consists of an overview of terms, directions of use and the simple uniform case. Created UDFs can be downloaded[3],[4] for free as Add-ins for an Excel environment. A new approach, referred to as the "switching off/on of data of single measurements or a group of measurements of the same sort," is also presented. The adjustment of a simple imaginary trigonometric network consisting of five measurement points is also included in the article. As an addition[1] to the latter, a visual review of UDF use, filmed with the programme CamStudio[2] - which enables a beginner to learn how to use these functions - was included.

Izvleček: Izravnavo trigonometrične mreže lahko izvedemo z veliko programi. Za izdelavo modela posredne 2D izravnave[1] je bil izbran Excel, ker je splošno dostopen, osnove uporabe so znane, je pregleden in prilagodljiv pri izvajanju procedure, hkrati pa podpira tudi uporabo lastnih funkcij. Uporaba lastnih funkcij doprinese predvsem k večji preglednosti. V članku so predstavljene funkcije, ki so bile prilagojene za Excelovo okolje in so bile uporabljene pri referenčni izravnavi[1],[5]. Vsaka lastna funkcija je predstavljena z opisom uporabljenih pojmov, navodilom za uporabo in enotnim preprostim primerom. Vse te funkcije so dostopne[3],[4] zastonj v obliki dodatk-

Scientific paper

ov za Excelovo okolje. Predstavljen je nov pristop k izravnavi z možnostjo izključevanja/vključevanja posameznih meritev ali sklopa istovrstnih meritev. Sestavni del članka je tudi preprosta namišljena trigonometrična mreža, sestavljena iz 5 merskih točk. Dodatek[1] k temu članku so vizualni prikazi uporabe lastnih funkcij, narejeni s programom CamStudio[2], tako da se začetnik lahko nauči uporabljati te funkcije.

Key words: adjustment by parameter variation, UDF, MS Excel, switching off/on measurements
Ključne besede: posredna izravnava, UDF, MS Excel, izklop/vklop meritev

INTRODUCTION

When adjusting a trigonometric network, we process a substantial amount of data, which is why the use of any computer programme that performs these calculations without any substantial errors is a reasonable step to take. We can perform a selection from a wide range of specialised programmes (TRIM, GEOS…) as well as programmes that enable the user to adjust an individual procedure to its demands (such as Matlab, Mathematica, Scilab, Maple, Excel, OooCalc…).

Specialised programmes are more user-friendly, but also rather expensive. Besides that, these programmes function on the basis of the "black box," in which data is entered, and from this, the results are returned. However, in such a case, we have no insight into the actual performance and thus cannot check the accuracy other than by a reference calculation. Due to the fact that we know their true function, with proper programming tools, our own customised application can be created. Each programming tool has both advantages and disadvantages. The main factors affecting what our chosen programme is to be are the malleability of the working environment to our demands and calculation process auditing, sometimes even the data processing speed. Programmes such as Matlab, Mathematica - to name a couple of examples - are usually a lot faster; however, they are far less auditable, more expensive and, due to much needed specific previous knowledge, applicable only to a few users. On the other hand, we have programmes such as MS Excel and OOo.Calc, available for a low price or for free, respectively. Their basic use is well-known, they are flexible in procedure determination and can easily be scanned. Specialised programmes are meant to be used in fluent projects by poorly educated users. They are intended for users who adopt results as optimal or accurate enough for their needs, remising the presence of eventual larger errors, which could be annulled or reduced to an acceptable range through the use of a proper approach. Individually adjusted programmes are more research-oriented and therefore intended for users wanting to know the influences on calculation accuracy, there due to the acquiring of satisfactory results through the rejection of bad measurements or with simulated measurements, creating a model convenient for the task set. The referred adjustment[1] and the simplified case presented as an attachment to this article offer us this option.

Due to all the stated reasons, and because MS Excel supports creating user defined functions with the help of MS Visual Basic for Applications, MS Excel was chosen to form a model of a 2D adjustment by parameter variation[1]. This is a compromised solution, using both an individual procedure and user defined functions, which are actually specialised sub-programmes for defined calculative operations; the kind that are again part of an adjustment procedure as a whole. UDFs are still small black boxes, but their algorithms are presented further in the continuation of this article and a visual presentation of UDF use is available[1], thus making this model acceptable for a lower level of theoretical knowledge as well. In turn, the model enables the calculation of an extensive trigonometric network:

- in several epochs,
- on optional locations,
- merely by entering field measurements.

Created UDFs can be downloaded[3],[4] for free as Add-ins for Excel environment. Since they can be optionally complemented, the authors would appreciate any forwarded comments, experiences or eventual malfunctions in their use.

Due to a limited printing space, the case enclosed to this article is a hypothetical small-scale application of a referred adjustment model. It consists of five measurement points, four of them known (the visures) and one unknown (the station). The coordinates of the unknown point are calculated when three known points (*T1*, *T2* and *T3*) are used. The calculation is repeated when a new known point (new*) is introduced. The value of m_0 is a reference to evaluate the benefits of introducing a new known point into the adjustment process. Its decreased value (see the enclosed case in Table 15) clearly shows that the accuracy of coordinate determination of the unknown point has been improved. Analogically, we can also conclude that the

Table 1. The imaginary data set for the network adjustment
Tabela 1. Namišljeni podatki za izravnavo mreže (dolžina, smer, stojišče, vizurne točke, meritev, natančnost, utež)

	A	B	C	D	E	F	G	H	I	J
1				measurement			accuracy			ponder
2		station	visure	o	'	"	o	'	"	md[rad],ml[m]
3	direction	T	MT_1	0	0	0	0	0	5	2.42407E-05
4		T	MT_2	270	0	3	0	0	5	2.42407E-05
5		T	MT_3	216	52	10	0	0	5	2.42407E-05
6		T	new*	171	52	11.6	0	0	5	2.42407E-05
7	distance	T	MT_2	499.99			0.005			0.400008
8		T	MT_3	500.01			0.005			0.399992
9		T	new*	707.106			0.005			0.282843025
10		T	MT_1	500.02			0.005			0.399984001

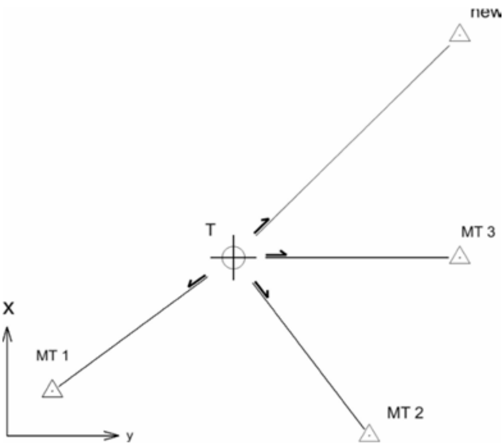

Figure 1. The trigonometric network and points

Slika 1. Trigonometrična mreža s točkami

direction measurement to point new* is more accurate than the distance measurement to the same point.

The enclosed printed case cannot express the dynamic nature of the referred adjustment and moreover doesn't include all the UDFs presented here. For these reasons, the reader is encouraged to visit the NTF site[1] and download the large-scale adjustment model including all of the UDFs presented in the article at hand.

WHAT IS A UDF?

A user defined function (referred to simply as a "UDF" further on in the article) functions as an add-in in the MS Excel programme tools platform. It is virtually a part of MS Excel and is simply summoned from the function line. This additional function enables faster work and adds to table transparency. An optional number of UDFs can be added, although it is recommended to add only those used in the specific task in order to achieve a higher processing speed. UDFs are similar to macros, but with a less complex code. Their benefits are:

- creating a complex or custom math function,
- simplifying formulas that would otherwise be extremely long "mega formulas",
- custom text manipulation,
- advanced array formulas and matrix functions,
- a UDF's programme code can be locked, preventing its unauthorised alteration,
- an add-in is available without the need to open new worksheet.

ADJUSTMENT BY PARAMETER VARIATION WITH THE USE OF A UDF

The basis for the calculations is presented by the adjustment theory. The setting out method is used and distances and directions are measured. Field measurements or their simulations are used in UDFs in order to acquire matrices of equation coefficients; to eliminate z through Gaussian elimination in order to get residuals equations.

The adjustment consists of two separate parts. First we acquire the design matrix of the equation coefficients by assuming the sought-for coordinates. In the second part, we use the field measurements and perform a Gaussian elimination. The matrix of normal equation coefficients, as well as the matrix of unknowns, is formed. The result is the residuals equation:

$$v = Ax + f \quad (1)$$

where v is the vector of the residuals, A is the design matrix of observation equations, x is a vector of unknowns and f is a vector of absolute terms.

The weighed least square method is used. When the product of $v^T Pv$ (v is a vector of residuals, P a matrix of weights, acquired in the base of expected measurements accuracy) is the smallest, the result is optimal for the data entered. A vector of unknown parameters is then added to the assumed coordinate data, thus iterating its value until we reach satisfactory results, but of course always according to the accuracy of our field measurements.

How to use a UDF?

Furthermore, the way we use our own - personally written - functions is presented. We have carried out the adjustment with the use of following functions[6].

dLine

This function returns the coefficient values for the direction station_visure, thus giving us its angle towards the oriented direction, Δz and normalizing all the coefficients.

Syntax: dLine (yStation;xStation;yVisure;xVisure;grade;minute;second)

Legend:
yStation - [m] is the y coordinate of the station
xStation - [m] is the x coordinate of the station
yVisure - [m] is the y coordinate of the visure
xVisure - [m] is the x coordinate of the visure
grade - [°] is the angle between the oriented direction and the visured direction, rounded off to a full number
minute - [’] is the hexadecimal part of the angle between the oriented direction and the visured direction, rounded off to a full number
second - [”] is the hexadecimal part of the minute (see above), rounded off to full a number or to one decimal place

Use:
1. We select a field of size 1×5 (1 row for the direction, 1 column for Δz, 2 columns for the station coefficients, 2 columns for the visure coefficients).
2. From the function line, we select UDF, then **dLine**.
3. In the fields opened, we enter the data listed in the legend. Before closing the window, we confirm the data entered by pressing Ctrl+Shift+Enter.

dLineW

This function returns the matrix of coefficients of the values for all directions of station_visure, thus giving us their angles towards the oriented directions, Δz and normalizing all the coefficients. All the coefficients for the visures are listed in two columns (for y and x).

Syntax: dLine (Station;Visure;to25;grade;minute;second)

Legend:
Station - the name of the station, taken from to25
Visure - the name of the visure, taken from to25
to25 - is the standard geodetical formulary.

Table 2. The initial and calculated points coordinates and mean square error for T point coordinates

Tabela 2. Začetne in izračunane koordinate točk in srednji kvadratni pogrešek določitve koordinat točke T

	A	B	C	D	E	F	G
12	points/	y	x	Dy	Dx	y	x
13	coordinates	[m]	[m]	[m]	[m]	[m]	[m]
14	MT_1	100	100	0	0	100	100
15	MT_2	800	0	0	0	800	0
16	MT_3	1000	400	0	0	1000	400
17	T	500	400	0.0055	0.0013	500.0055	400.0013
18	new*	1000	900	0	0	1000	900
19				X^2= 3.E-05			

Table 3. Calculated coefficient values for directions station_visure and vice versa
Tabela 3. Izračunani smerni koeficienti za smeri stojišče_vizurna točka in obratno

fx {=dLine($B17;$C$17;B16;C16;D5;E5;F5)}

M	N	O	P	Q
	direction koeficients			
z	station/visure (y)	station/visure (x)	visure/station (y)	visure/station (x)
-1	-0	0,002	0	-0,002

Table 4. Calculated matrix of normalized coefficient values for directions station_visure and vice versa and as well for a vector of absolute terms
Tabela 4. Izračun matrike normaliziranih vrednosti smernih koeficientov za smeri stojišče_vizurna točka in obratno ter za vektor popravkov *f*

fx {=dLineW(A17;A16;A14:C18;D5;E5;F5)}

M	N	O	P	Q	R
	direction koeficients				
z	station/visure (y)	station/visure (x)	visure/station (y)	visure/station (x)	f
-1	-0	0,002	0	-0,002	839270

Table 5. Calculated matrix of normalized value for Δz and coefficient values for all directions station_visure and vice versa, for a vector of absolute terms
Tabela 5. Izračun matrike normaliziranih vrednosti Δz in vseh smernih koeficientov za smeri stojišče_vizurna točka in obratno, za vektor popravkov *f*

fx {=dLineWall(B8;C8;A14:C18;D5;E5;F5;M12:X13)}

M	N	O	P	Q	R	S	T	U	V	W	X
	MT_1	MT_1	MT_2	MT_2	MT_3	MT_3	T	T	new*	new*	
z	y	x	y	x	y	x	y	x	y	x	f
-1	0	0	0	0	0	-0.002	-0	0.002	0	0	839270

That is the table of coordinates assigned to all points in a trigonometric network, with which we operate in this function. It consists of one column for point names and two columns for the *y* and *x* values of the point coordinates. Where the coordinates are not known, we simply assume their values. Use of to25 in **dLineW** returns the table of coefficient values assigned to each direction_visure$_{1,2,3,....}$.
grade, minute, second (see previous function)

Use:
1. We select a field of dimensions 1×6 (1 row for the direction, 1 column for Δ*z*, 2 columns for the station coefficients, 2 columns for the visure coefficients, 1 column for the vector of absolute terms).
2. From the function line, we select UDF, then **dLineW**.
3. In the fields opened, we enter the data listed in the legend. Before closing the window, we confirm the data entered by pressing Ctrl+Shift+Enter.

dLineWall

This function returns a matrix of coefficient values for all directions of station_visure, thus giving us their angles towards the oriented directions, Δ*z* as well as normalizing all the coefficients and the vector of residuals. Each coefficient for the station or the visures (the number of visures is *m*) is showed in a separate column and row. One column is reserved for vectors of absolute terms only.

Syntax: dLine (yStation;xStation;yVisure;xVisure;to25;grade;minute;secund;list)

Legend:
yStation, xStation, yVisure, xVisure, grade, minute, second; to25 (see previous function)
listC - is the table of measurement points and their appropriate coordinate names (*y* and *x*)

Use:
1. We select a field of size *n*×(2*m*+4) (*n* rows for *n* directions, 1 column for Δ*z*, 2 columns for the station coefficients, 2*m* columns for the visure coefficients, 1 column for the residuals).
2. From the function line, we select UDF, then **dLineWall**.
3. In the fields opened, we enter the data listed in the legend. Before closing the window, we confirm this data entered by pressing Ctrl+Shift+Enter.

dLineWallZ

This function performs the Gaussian elimination of Δ*z* and returns the matrix of coefficient values for all directions of station_visure, thus giving us their angles towards their oriented directions; Δ*z* is annulled. Each coefficient for the station and all visures is shown in a separate column and row. One column is reserved for the vector of residuals alone.

Syntax: dLine (inputKernel;to25;distant;listC)

Legend:
to25, listC (see previous function)
inputKernel - is a table 5×*n* of the named station and visure points and their belonging measured directions (given in grades, minutes and seconds)
distant - is the distance between the station and visure point, reduced on a Gauss-Krüger projection

Use:
1. We select a field of size *n*×(2*m*+4) (*n*

Table 6. Calculated matrix of reduced coefficient values for all directions station_visure and vice versa and as well for a vector of absolute terms after the Gaussian elimination of *Δz*
Tabela 6. Izračun matrike reduciranih vrednosti vseh smernih koeficientov za smeri stojišče_vizurna točka in obratno ter za popravke *f* po izvedeni Gaussovi eliminaciji *Δz*

fx =dLineWallZ(B3:F6;A14:C18;M12:X13)

L	M	N	O	P	Q	R	S	T	U	V	W
	MT_1	MT_1	MT_2	MT_2	MT_3	MT_3	T	T	new*	new*	
z	y	x	y	x	y	x	y	x	y	x	f
:X13)	-9E-04	0.0012	0.0004	0.0003	0	0.0005	0.0008	-0.0023	-0.0003	0.0003	0.334237
0	0.0003	-0.0004	-0.0012	-0.0009	0	0.0005	0.0012	0.00055	-0.0003	0.0003	-2.665763
0	0.0003	-0.0004	0.0004	0.0003	0	-0.002	-0.0005	0.00135	-0.0003	0.0003	1.965763
0	0.0003	-0.0004	0.0004	0.0003	0	0.0005	-0.0015	0.00035	0.0008	-8E-04	0.365763

Table 7. Calculated coefficients of a residual equation for a distance measurement
Tabela 7. Izračun koeficientov enačbe popravkov za dolžinsko meritev

fx {=dDist(B17;C17;B16;C16;D8)}

Y	Z	AA	AB	AC
	direction koeficients			
	station/visure (y)	station/visure (x)	visure/station (y)	visure/station (x)
	-1	-0	1	0

Table 8. Calculated coefficients of a residual equation for a distance measurement and vector of residuals
Tabela 8. Izračun koeficientov enačbe popravkov za dolžinsko meritev in popravka *f*

fx {=dDistW(A17;A16;A14:C18;D8)}

Y	Z	AA	AB	AC	AD
	direction koeficients				
	station/visure (y)	station/visure (x)	visure/station (y)	visure/station (x)	f
	-1	-0	1	0	-0,01

Table 9. Calculated coefficients of a residual equation for all distance measurements and vector of residuals
Tabela 9. Izračun koeficientov enačbe popravkov za vse dolžinske meritve in popravka *f*

fx =dDistWall(B8;C8;A14:C18;D8;M12:X13)

L	M	N	O	P	Q	R	S	T	U	V	W
	MT_1	MT_1	MT_2	MT_2	MT_3	MT_3	T	T	new*	new*	
	y	x	y	x	y	x	y	x	y	x	f
	2:X13)	0	0	0	1	0	-1	-0	0	0	-0.01

rows for n directions, 1 column for Δz, 2 columns for the station coefficients, $2m$ columns for the visure coefficients, 1 column for absolute terms).
2. From the function line, we select UDF, then **dLineWallZ**.
3. In the fields opened, we enter the data listed in the legend. Before closing the window, we confirm the data entered by pressing Ctrl+Shift+Enter.

dDist

This function returns the coefficients of a residual equation for distance measurement.

Syntax: dDist (yStation;xStation;yVisure; xVisure;distant)

Legend:
yStation, xStation, yVisure, xVisure,distant (see previous functions)

Use:
1. We select a field of size 1×4 (1 row for the distance, 2 columns for the station coefficients, 2 columns for the visure coefficients).
2. From the function line, we select UDF, then **dDist**.
3. In the fields opened, we enter the data listed in the legend. Before closing the window, we confirm this data entered by pressing Ctrl+Shift+Enter.

dDistW

This function returns the coefficients of the residual equation for a distance measurement and the vector of residuals.

Syntax: dDistW (Station; Visure; to25; distant)

Legend:
station, visure, to25, distant (see previous functions)

Use:
1. We select a field of size 1×5 (1 row for the distance, 2 columns for the station coefficients, 2 columns for the visure coefficients, 1 column for the vector of absolute terms).
2. From the function line, we select UDF, then **dDistW**.
3. In the fields opened, we enter the data listed in the legend. Before closing the window, we confirm this data entered by pressing Ctrl+Shift+Enter.

dDistWall

This function returns the coefficients of a residual equation for distance measurements and the vector of residuals. Each coefficient for the station and all the visures (the number of visures is m) are shown in a separate column.

Syntax: dDistW (Station; Visure; to25; distance, ListC)

Legend:
station, visure, to25, distant, ListC (see previous functions)

Use:
1. We select a field of size 1×(2m+3) (1 row for the direction, 2 columns for the station coefficients, $2m$ columns for the visure coefficients, 1 column for the vector of absolute terms).
2. From the function line, we select UDF, then **dDistWall**.
3. In the fields opened, we enter the data listed in the legend. Before closing the window, we confirm this data entered by pressing Ctrl+Shift+Enter.
4. We can expand this field in order to acquire the coefficients and vector of residuals also for the other distance measured in the same network. We

do this simply by selecting the field 1×(2*m*+3) and dragging it down, thus expanding it to as many rows as we have distances measured.

takeDiagMatrix
This function returns the values on a diagonal of a quadratic $n \times n$ matrix as a vector of $1 \times n$ dimensions.

Syntax: takeDiagMatrix(matrix)

Legend:
Matrix - any quadratic matrix

Use:
1. We select a field of size $1 \times n$ (n for the number of rows = the number of columns in a quadratic matrix).
2. From the function line, we select UDF, then **takeDiagMatrix**.
3. In the fields opened, we enter the data by selecting a quadratic matrix. Before closing the window, we confirm the data entered by pressing Ctrl+Shift+Enter.

createListC
This function returns a table of measurement points and their belonging coordinate names (y and x), vectors of absolute terms and, when operating with direction measurements, also with Δz (in this case, this is the name of a parameter and not a value).

Syntax: createListC(list)

Legend:
list - the name of the coordinates participating in a trigonometric network; the list presents one column of to25 formulary

Use:
1. We select a field of size $2 \times (2p+1+1)$ (p columns for the number of network points,1 column for the vector of absolute terms).
2. From the function line, we select UDF, then **createListC**.
3. In the fields opened, we enter the list of point names (taken from to25 formulary). Before closing the window, we confirm the data entered by pressing Ctrl+Shift+Enter.

EllipseW
This function returns a field the contents of which are then imported by AutoCAD, resulting in the depiction of an ellipse.

Syntax: EllipseW(Ycenter,Xcenter,Zcenter, MajorSemi,MinorSemi,Rotation,Ratio)

Legend:
Ycenter - the Y coordinate of the ellipse
Xcenter - the X coordinate of the ellipse
Zcenter - the Z coordinate of the ellipse
MajorSemi - the ellipse major semi-axis
MinorSemi - the ellipse minor semi-axis
Rotation - the azimuth of the major semi-axis
Ratio - the scale at which the ellipse is drawn

Use:
1. Enter the values of the demanded data separately in 7 consecutive fields in one row.
2. Choose one field, open the **EllipseW** function line, enter the data demanded and press Enter.
3. Copy the same field, open an AutoCAD file and paste the data from the selected field. The ellipse gets drawn.

pedaleW
This function returns the values of coordinates for each pedale-forming point. The number of pedale-forming points is recip-

Table 10. Quadratic $n \times n$ matrix and calculated values on its diagonal as a vector of $1 \times n$ dimensions (diagQxx)

Tabela 10. Kvadratna matrika $n \times n$ in izračunane vrednosti na njeni diagonali v obliki vektorja $1 \times n$

M127 fx {=takeDijagWmatrix(M117:V126)}

	K	L	M	N	O	P	Q	R	S	T	U	V
115			MT_1	MT_1	MT_2	MT_2	MT_3	MT_3	T	T	new*	new*
116		Qxx	y	x	y	x	y	x	y	x	y	x
117			0	0	0	0	0	0	0	0	0	0
118			0	0	0	0	0	0	0	0	0	0
119			0	0	0	0	0	0	0	0	0	0
120			0	0	0	0	0	0	0	0	0	0
121			0	0	0	0	0	0	0	0	0	0
122			0	0	0	0	0	0	0	0	0	0
123			0	0	0	0	0	0	0.0002	4.9E-05	0	0
124			0	0	0	0	0	0	5E-05	9.5E-05	0	0
125			0	0	0	0	0	0	0	0	0	0
126			0	0	0	0	0	0	0	0	0	0
127	diagQxx		0	0	0	0	0	0	0.0002	9.5E-05	0	0

Table 11. Table of measurement points and respective coordinate names, expanded with fields for vectors of absolute terms and *Δz*

Tabela 11. Tabela merskih točk in pripadajočih neznank, razširjena s polji za popravek *f* in za orientacijsko smer *Δz*

fx =createListC(A14:A18)

L	M	N	O	P	Q	R	S	T	U	V	W
	point coordinates										
1:A18)	MT_1	MT_1	MT_2	MT_2	MT_3	MT_3	T	T	new*	new*	
z	y	x	y	x	y	x	y	x	y	x	f

Table 12. Calculation of values needed for drawing an ellipse in AutoCAD

Tabela 12. Izračun potrebnih koeficientov za izris elipse v AutoCAD-u (elementi kovariančne matrike neznank, parametri elipse in merilo izrisa)

L	M	N	O	P	Q	R	S	T	U	V
	elements of covariance matrix of unknowns			ellipse parameters						ACAD
mer. tocka	Qyy	Qxy	Qxx	y_cent	x_cent	z_cent	major semi_A	minor semi_B	rotation θ	ratio
T	0.0001651	0.0000489	0.0000948	500.0055	400.0013	500	0.00239178	0.00239165	-54.2739	1000
	ellipse c 500.00554879576,400.00127189378,500 498.063861101369,401.397860096414 2.39164618676024									
	$K=(Q_{xx}-Q_{yy})^2+4*Q_{xy}^2$			$A^2=m_0^{2}*(Q_{xx}+Q_{yy}+K)/2$						
	$\theta=tg^{-1}(2*Q_{xy}/(Q_{xx}-Q_{yy}))$			$B^2=m_0^{2}*(Q_{xx}+Q_{yy}-K)/2$						

rocal to AngleStepH.

Syntax: pedaleW(Ycenter,Xcenter,Zcenter ,MajorSemi,MinorSemi,RotationH, Angel StepH,Ratio)

Legend:
Ycenter, Xcenter, Zcenter, MajorSemi, MinorSemi, Ratio (see previous function)
RotationH - the azimuth of the major semi-axis
AngelStepH - defines how wide an arc is, approximated with the line between two neighbouring pedale-forming points (e.g. the smaller the step, the higher the accuracy of the contour drawn)

Use:

1. Enter the values of the demanded data separately in 8 consecutive fields in one row.
2. Choose 3×*n* fields (*n*….360 º divided by the angle step used, e.g. if you are drawing a circle and the angle step is 10, then you get *n*=36, thus getting the number of chords forming an approximate closed contour of a circle), open the **pedaleW** function line, enter the data demanded and press Enter. (P.S. When changing parameters afterwards, this can be done to all the parameters apart from the angle step, as the decrease in the angle step will cause a gap in the contour).
3. Choose 3×1 fields necessary for adding the coordinate data of the first point beginning the contour, thus forming a closed contour of the curve (this field must be filled manually).
4. Copy all 3×(*n*+1) fields, open an AutoCAD file and paste the data from the selected field. Only the pedale-forming points get drawn. Since it results in better visual conception, it would be reasonable to use the **lineW** function to draw the pedale contour subsequently.

lineW

This function returns the fields the contents of which are then imported by AutoCAD, where they result in the drawing of the contour of the pedale, approximated with the lines defined by this very function.

Syntax: pedaleW(Yfrom,Xfrom,Zfrom, Yto,Xto,Zto)

Legend:
Yfrom - the value for *Y* for the first point of the line
Xfrom - the value for *X* for the first point of the line
Zfrom - the value for *Z* for the first point of the line
Yto - the value for *Y* for the second point of the line
Xto - the value for *X* for the second point of the line
Zto - the value for *Z* for the second point of the line

Use:

1. Choose 1 field, open the **LineW** function line, enter the data demanded and press Enter.
2. Stretch this field to another *n* consecutive fields in the column (*n*….the same number as used in **pedaleW**).
3. Copy all the (*n*+1) fields, open an AutoCAD file and paste the data from the selected field. The contour of the pedale gets drawn.

Table 13. Calculated values of coordinates for each pedale-forming point

Tabela 13. Izračun vrednosti koordinat, ki sestavljajo pedalo (elementi kovariančne matrike neznank, parametri elipse, merilo izrisa, točke pedale in kontur)

L	M	N	O	P	Q	R	S	T	U	V
	elements of covariance matrix of unknowns			ellipse parameters						ACAD
mer. tocka	Qyy	Qxy	Qxx	y_cent	x_cent	z_cent	major semi_A	minor semi_B	rotation θ	ratio
T	0.0001651	0.0000489	0.0000948	500.0055	400.0013	500	0.00239178	0.00239165	-54.2739	1000
	ellipse c 500.00554879576,400.00127189378,500 498.063861101369,401.397860096414 2.39164618676024									
	$K=(Q_{xx}-Q_{yy})^2+4*Q_{xy}^2$			$A^2=m_0^{2*}(Q_{xx}+Q_{yy}+K)/2$						
	$\theta=tg^{-1}(2*Q_{xy}/(Q_{xx}-Q_{yy}))$			$B^2=m_0^{2*}(Q_{xx}+Q_{yy}-K)/2$						

pedale points		z_cent	contour
U9;30;10)	400.0132304	500	
500.011528	400.011628	500	line 500.00554879576,400.013230352175,500 500.011527914547,400.011628031304,500
500.015905	400.0072511	500	line 500.011527914547,400.011628031304,500 500.015905025175,400.00725106562,500
500.017507	400.0012719	500	line 500.015905025175,400.00725106562,500 500.017507466364,400.00127189378,500
500.015905	399.9952924	500	line 500.017507466364,400.00127189378,500 500.015905499528,399.995292448071,500
500.011528	399.9909153	500	line 500.015905499528,399.995292448071,500 500.011528188417,399.990915281898,500
500.005549	399.9893134	500	line 500.011528188417,399.990915281898,500 500.00554879576,399.989313435384,500
499.99957	399.9909158	500	line 500.00554879576,399.989313435384,500 499.999569676972,399.990915756255,500
499.995193	399.9952927	500	line 499.999569676972,399.990915756255,500 499.995192566344,399.995292721939,500
499.99359	400.0012719	500	line 499.995192566344,399.995292721939,500 499.993590125156,400.00127189378,500
499.995192	400.0072513	500	line 499.993590125156,400.00127189378,500 499.995192091992,400.007251339488,500
499.999569	400.0116285	500	line 499.995192091992,400.007251339488,500 499.999569403102,400.011628505661,500
500.005549	400.0132304	500	line 499.999569403102,400.011628505661,500 500.00554879576,400.013230352175,500

Table 14. Calculated values of coordinates for each pedale contour-forming line

Tabela 14. Izračun vrednosti koordinat za linije, ki sestavljajo konturo pedale (točke pedale in linije kontur)

pedale points		z_cent	pedale contour
500.005549	400.0132304	500	
500.011528	400.011628	500	.19;M19;N19)
500.015905	400.0072511	500	line 500.011527914547,400.011628031304,500 500.015905025175,400.00725106562,500
500.017507	400.0012719	500	line 500.015905025175,400.00725106562,500 500.017507466364,400.00127189378,500
500.015905	399.9952924	500	line 500.017507466364,400.00127189378,500 500.015905499528,399.995292448071,500
500.011528	399.9909153	500	line 500.015905499528,399.995292448071,500 500.011528188417,399.990915281898,500
500.005549	399.9893134	500	line 500.011528188417,399.990915281898,500 500.00554879576,399.989313435384,500
499.99957	399.9909158	500	line 500.00554879576,399.989313435384,500 499.999569676972,399.990915756255,500
499.995193	399.9952927	500	line 499.999569676972,399.990915756255,500 499.995192566344,399.995292721939,500
499.99359	400.0012719	500	line 499.995192566344,399.995292721939,500 499.993590125156,400.00127189378,500
499.995192	400.0072513	500	line 499.993590125156,400.00127189378,500 499.995192091992,400.007251339488,500
499.999569	400.0116285	500	line 499.995192091992,400.007251339488,500 499.999569403102,400.011628505661,500
500.005549	400.0132304	500	line 499.999569403102,400.011628505661,500 500.00554879576,400.013230352175,500

Switching the measurement data off/on

Through introducing a switcher (0 or 1; see fields 4F and 4I and subordinary fields B7 to B14 and L7 to L14 of the enclosed case in table 15), we gain the option to improve the final results by excluding bad single or group measurements from the input data set. It also gives us the option of defining the measurement points as either known or unknown. Once the specific data have been switched off/on, this affects all the other subordinate data in the adjustment. In combination with other calculative tools (i.e. the mean square error), we can evaluate the influence of the specific data on the adjustment results and reliability of the trigonometric network, be it either real or simulated.

Conclusions

When adjusting a trigonometric network, a substantial amount of data is treated. In order to achieve better programme performance and easier scanning, UDFs are introduced into Excel. On the basis of the data entered, a UDF can execute algorithms or treat non-numeric data. The optional exporting of UDF derivates to CAD programs is an additional benefit of the Excel environment, thus offering a graphical presentation of the calculated results. UDFs were used considerably in the adjustment model[1], thus saving time and space for the procedure. An additional approach used in this adjustment is switching bad measurements off/on in order to make the model dynamic and consecutively giving us the option to acquire more accurate results.

The case enclosed to this article is a printed small-scale version, and is unfit to reveal the dynamic nature of the referred adjustment, which is another reason why the reader is encouraged to visit the NTF site[1] and download the large-scale adjustment model, which includes all the UDFs presented here.

Povzetek

Pri izravnavi trigonometrične mreže obdelujemo večje količine podatkov. Excelove lastne funkcije (UDF) pripomorejo k večji učinkovitosti programa in omogočajo preglednost izračunov. Z lastnimi funkcijami obdelujemo vnešene numerične ali nenumerične podatke. Dodatna prednost UDF je možnost izvoza nekaterih rezultatov v CAD programe in s tem tudi njihova grafična predstavitev. UDF so bile v precejšnji meri uporabljane v referenčnem modelu izravnave[1], s čimer smo za obdelavo prihranili precej časa in prostora. Dodatno je predstavljen tudi nov pristop, ki omogoča izklop/vklop slabih meritev, kar nam omogoča pridobitev natančnejših rezultatov in hkrati naredi model bolj dinamičen.

Primer, priložen k temu članku, je zgolj poenostavljena verzija referenčnega modela in ne razkriva njegove dinamičnosti, kar je dodaten razlog za obisk NTF strani[1], od koder si lahko prenesete neokrnjeni model z vsemi predstavljenimi lastnimi funkcijami.

	A	B	C	D	E	F	G	H	I	J	K	L	M
1													
2		0/1 switching off/on group of measurements							0/1 defining measurement point as known/unknown				
3													
4		use				1			1			use	A
5						direction			dist [m]				
6			station	visure	o	'	"	o	'	"	md[rad],ml[m]		z
7		1	T	MT_1	0	00	00,0	0	00	05,0	2,42407E-05	1	0
8		1	T	MT_2	270	00	03,0	0	00	05,0	2,42407E-05	1	0
9		0	T	MT_3	216	52	10,0	0	00	05,0	2,42407E-05	0	0
10		1	T	new*	171	52	11,6	0	00	05,0	2,42407E-05	1	0
11		0	T	MT_2					499,99	0,005	0,400008	0	
12		0	T	MT_3					500,01	0,005	0,399992	0	
13		1	T	new*					707,11	0,005	0,282843025	1	
14	5	1	T	MT_1					500,02	0,005	0,399984001	1	

	N	O	P	Q	R	S	T	U	V	W	X	Y
1												
2			offshoot	offshoot								
3					isolated	isolated						
4	0	0	0	0	0	0	1	1	0	0	u=	2
5	MT_1	MT_1	MT_2	MT_2	MT_3	MT_3	T	T	new*	new*		
6	y	x	y	x	y	x	y	x	y	x	f	f[rad]
7	-0,0009	0,0012	0,0004	0,0003	0	0,0005	0,00075	-0,00225	-0,00025	0,00025	0,334237	2E-06
8	0,0003	-0,0004	-0,0012	-0,0009	0	0,0005	0,00115	0,00055	-0,00025	0,00025	-2,665763	-1E-05
9	0,0003	-0,0004	0,0004	0,0003	0	-0,0015	-0,00045	0,00135	-0,00025	0,00025	1,965763	1E-05
10	0,0003	-0,0004	0,0004	0,0003	0	0,0005	-0,00145	0,00035	0,00075	-0,00075	0,365763	2E-06
11	0	0	0,6	-0,8	0	0	-0,6	0,8	0	0	0,01	
12	0	0	0	0	1	0	-1	-0	0	0	-0,01	
13	0	0	0	0	0	0	-0,707107	-0,707107	0,707107	0,70711	0,000781	
14	-0,8	-0,6	0	0	0	0	0,8	0,6	0	0	-0,02	

	B–G	H–Q	R–Y
41			
42	0/1 switching off/on	given input data - field measurments; fields C7 to K14	marked irreg. status of network point-offshoot of traverse; fields N2 to W2
43	single measurement	(podani vhodn podatki - terenske meritve; polja C7 do K14)	(označba iregularnega statusa točke - slepi poligon; polja N2 do W2
44			
45		variables used to switch off/on (0/1) specific data or group of data; for single measurment, for all direction	marked irregular status of network point - isolated point; fields N3 to W3
46	m₀= 0,3277381	measurements, for all distance measurements, defining known points; row 4, columns B and L	(označba iregularnega statusa točke - izolirana točka, polja N3 do W3
47	m₀...mean ponder error	(spremenljivke uporabljene za izklop/vklop posameznega podatka ali skupine podatkov; za posamezno	
48	m₀...srednji pogr. enote uteži	meritev, za vse smerne meritve, za vse meritve dolžin, določanje datumskih točk; vrstica 4, stolpci B in L	
49			
50	X²= 4,057E-05		
51	X²...mean square error		
52	X²...srednji kvadr. pogrešek		

Table 15. Introductory overview of input elements and some control data for simulated case

Tabela 15. Pregledni prikaz vhodnih elementov in nekaterih kontrolnih rezultatov za simulirani primer

REFERENCES

[1] http://www.ntfgeo.uni-lj.si/mvulic/gradiva, last accessed Sept 20th, 2007.

[2] http://www.freedownloadscenter.com/Multimedia_and_Graphics/Screen_Capture_Tools/ CamStudio.html, last accessed Sept 20th, 2007.

[3] http://www.ntfgeo.uni-lj-si/mvulic/gradiva/vule_par_adj4.xla, last accessed Sept 20th, 2007.

[4] http://www.ntfgeo.uni-lj-si/mvulic/gradiva/vule4acad01.xla, last accessed Sept 20th, 2007.

[5] SETNIKAR, D. (2005): *2D adjustment by parameter variation modelling: Bachelor's degree*. Faculty of Natural Science and Technology, Ljubljana, september 2005.

[6] VULIĆ, M. (2005): *User Defined Function*. Faculty of Natural Science and Technology, Ljubljana, 2005.

[7] CASPARY, W. F. (1987): *Concepts of network and deformation analysis*. The University of New South Wales, Kensington, NSW, Australia.

"UDF" for volume calculation with the use of "NTF" method

Lastne Excel funkcije za izračun prostornin po "NTF" metodi

Milivoj Vulić[1], Anes Durgutović[2]

[1]University of Ljubljana, Faculty of Natural sciences and Engineering, Department of Geotechnology and Mining Engineering, Aškerčeva cesta 12, SI-1000 Ljubljana, Slovenia; E-mail: milivoj.vulic@ntf.uni-lj.si
[2]Oikos d.o.o., Jarška cesta 30, SI-1230 Ljubljana, Slovenia; E-mail: anes.durgutovic@oikos.si

Received: September 25, 2007 **Accepted:** October 5, 2007

Abstract: In the article titled Calculation of volume with the use of "NTF" method the idea, of mathematical bases of the mentioned method, is presented. Therefore, we have by consideration of, in the mentioned article, shown results prepared »UDF« add-ins which enable realization of volume calculation with the use of MS Excel program. The preposition for the realization of volume calculation with already mentioned method is already carried out Delaney triangulation of the shape to which we wish to calculate the volume. In the article we wish to represent instructions for the use UDF which we use at volume calculation with the "NTF" method.

Izvleček: V prispevku z naslovom Izračun volumnov z uporabo "NTF" metode je predstavljena zamisel in matematične osnove omenjene metode. Tako smo z upoštevanjem, v omenjenem prispevku, prikazanih ugotovitev pripravili dodatke »UDF«, ki nam omogočijo izvedbo izračuna volumnov z uporabo programa MS Excel. Seveda je predpogoj za izvedbo izračuna po omenjeni metodi izvedena Delaunay-eva triangulacija telesa kateremu prostornino želimo določiti. V prispevku vam želimo prikazati navodila za uporabo UDF-jev, ki jih uporabimo pri izračunu prostornine po metodi "NTF".

Key words: volume calculation, MS Excel, UDF, outline, surface
Ključne besede: izračun volumnov, MS Excel , UDF, kontura, ploskva

Introduction

Today, we can come across many different programs which on the basis of input data give results. However, the results we get with the use of programs (programs, which enable the calculation of the volume) vary among themselves. In order to find out why these particular programs give various results we would be bound to the background of their function. Because this would be difficult we have decided to

Scientific paper

prepare the method of volume calculation in the range of our own capacities. In this way we have made “NTF” method of volume calculation. The basis of this method and the mathematical background of the volume calculation are shown in the article calculation of the volume with the use of “NTF” method.

The basis for the realization of volume calculation with already mentioned method is as in most of the programs already carried out Delaney triangulation of the shape to which we wish to calculate the volume.

In order to carry out the volume calculation with the use of “NTF” method in the most simple way we have, on the basis of finding which is shown in the above mentioned article, prepared our own written functions (UDF) which enable realization of volume calculation with the use of MS Excel program.

What is UDF?

When we see the sign “UDF” we immediately ask ourselves what does it mean? However, we express it in a simple way, that this is “*User Defined Function”,* which functions as add-ins in MS Excel program tools platform. Beside the functions offered by the program itself, we can therefore with the use of Microsoft *Visual Basic for Applications* prepare additional functions which enable faster work. And also possible pooling of resources of some repeated procedures. With “*User Defined Function”* we can solve more complicated mathematical tasks. We can use UDF when working with program on our own as well as other computer.

UDF for volume calculation with the use of “NTF” method

For the realization of Delaney triangulation of the upper and down surface we use software program »Triangel Net«, which is available for free on the internet. When we want to calculate the volume with the use of “NTF” method in MS Excel program we use the next UDF:

- coEntW,
- coVolW3ID,
- linesSortedW3,
- outLineW,
- outPointsW.

In the following, instructions for the use of UDF which we need for the realization of volume calculation with the use of “NTF” method in MS Excel program are presented.

“coEntW”

This function returns the value of elements from two different multitudes. And with it gives the sorted values on the basis of marked element and marked coordinates. Individual values can be a letter or number.

<u>Syntax:</u> coEntW (CoorNames, CoordValues, EntityPointKinds, EntityPoinIDs)

<u>Legend:</u>

- CoorNames names of coordinates (*x, y, z*), which value we wish to find.
- CoordValues values of individual coordinate points, which we have gathered with field measurements.
- EntityPointKinds are marks for the individual points of triangulated net. Marks can be numbers, letters or symbols.
- EntityPoinIDs are identification values

INPUT DATA				RESULT

CoordNames (CoordValues)

x	y	z
115	80	10
116	79	11
115	81	10
118	82	12
120	79	13
119	82	15
121	83	11

EntityPointKinds (EntityPointIDs)

A
4
1
3
0
2

RESULT

A	A	A	A
	x	y	z
4	120	79	13
1	116	79	11
3	118	82	12
0	115	80	10
2	115	81	10

of every triangle edges, which form a triangulated net.

Use:
1. We select two roves more than we have coordinate points.
2. When selecting a column we must add up all the marks of individual set of point and multiply with the number of coordinates (we multiply with 2 if we have *x,y* and with 3 if we have *x,y,z*)
3. We use the function coEntW.
4. We choose the values according to the above written syntax.
5. When finished with the selection, we confirm the realization with a simultaneous press on the key Ctrl-Shift-Enter.
6. The function offers us the wanted result.

"coVolW3ID"

This function returns the value of elements from two different multitudes. And with it gives the sorted values on the basis of marked element and marked coordinates. Individual values can be a letter or number.

Syntax: coVolW3ID (CoordNames, CoordValues, EntityPointKinds, EntityPoinIDs, Z_{Ref})

Legend:
- CoorNames names of coordinates (*x, y, z*), which value we wish to find.
- CoordValues values of individual coordinate points, which we have gathered with field measurements.
- EntityPointKinds are marks for the individual points of triangulated net. Marks can be numbers, letters or symbols.
- EntityPoinIDs are identification values of every triangle edges, which form a triangulated net.
- Z_{Ref} is a reference high.

Use:
1. We select two roves more than we have triangle edges.
2. When selecting a column we must add up all the marks of individual set of point and multiply with the number of coordinates (we multiply with 2 if we have *x, y* and with 3 if we have *x, y, z*) and we add another column to this result for the value of partial volume.
3. We use the function coVolW3ID.
4. We choose the values according to the above written syntax.
5. When finished with the selection, we confirm the realization with a simultaneous press on the key Ctrl-Shift-Enter.

INPUT DATA

CoordNames			
x	y	z	
115	80	10	CoordValues
116	79	11	
115	81	10	
118	82	12	
120	79	13	
119	82	15	
121	83	11	

EntityPointKinds			
A	B	C	
1	2	4	EntityPointIDs
2	3	1	
0	1	3	
3	4	0	
4	0	2	

Z_{ref}	10

RESULT

A	A	A	B	B	B	C	C	C	**24,67**
x	y	z	x	y	z	x	y	z	
116	79	11	115	81	10	120	79	13	*5,33*
115	81	10	118	82	12	116	79	11	*3,50*
115	80	10	116	79	11	118	82	12	*2,50*
118	82	12	120	79	13	115	80	10	*10,83*
120	79	13	115	80	10	115	81	10	*2,50*

6. The function offers us the wanted result.

"linesSortedW3"

The functions offers us, from the individual edges of triangle net, classification of lines between two edges and also mark the ones which occur only once. It marks them with 0 or 1.

Syntax:

linesSortedW3 (Tri) - Tri is the mark of individual edges of triangle net, which we gained by Delaunay triangulation.

Use:

1. We multiply the number of roves individual edges of triangle net with number three. We choose so many roves, which will be equal to the gained result.
2. We choose three columns.
3. We use the function linesSortedW3.
4. We choose the values according to the above written syntax.
5. When finished with the selection, we confirm the realization with a simultaneous press on the key Ctrl-Shift-Enter.
6. The function offers us the wanted result.
7. In the cell above the third column we add up values of the third column. The value we get tells us how many contour lines we have.

"outLineW"

The function, from contour lines between two edges in triangle net, gives us only contour lines.

<u>Syntax:</u> outLineW (OutLineWb, NumOfOutLines)

<u>Legend:</u>

- OutLineWb are the lines between edges of triangle net, which we have gained Delaunay triangulation.
- NumOfOutLines is the number of contour lines. That is the sum of value the third column at the function linesSortedW3.

<u>Use:</u>

1. We choose so many roves, as we have contour lines.
2. We choose two columns.
3. We use the function outLineW.
4. We choose the values according to the above written syntax.
5. When finished with the selection, we confirm the realization with a simultaneous press on the key Ctrl-Shift-Enter.
6. The function offers us the wanted result.

"outPointsW"

The function, from sorted contour lines between two edges in triangle net, gives us only contour point.

<u>Syntax:</u> outPointsW (OutLines)

OutLines is the sorted contour lines between two edges in triangle net.

<u>Use:</u>

1. We choose so many roves, as we have contour lines and we add another roves for the mark of the multitudes.
2. We choose one columns.
3. We use the function outPoints.
4. We choose the values according to the above written syntax.
5. When finished with the selection, we

INPUT DATA			RESULT		
Tri			**From**	**To**	***Mark***
1	2	4	0	1	*1*
2	3	1	0	2	*1*
0	1	3	0	3	*0*
3	4	0	0	3	*0*
4	0	2	0	4	*0*
			0	4	*0*
			1	2	*0*
			1	2	*0*
			1	3	*0*
			1	3	*0*
			1	4	*1*
			2	3	*1*
			2	4	*0*
			2	4	*0*
			3	4	*1*

INPUT DATA				RESULT	
OutLineWb			NumOfOutLines	outLineW	
0	1	1	5	0	1
0	2	1		0	2
0	3	0		1	4
0	3	0		2	3
0	4	0		3	4
0	4	0			
1	2	0			
1	2	0			
1	3	0			
1	3	0			
1	4	1			
2	3	1			
2	4	0			
2	4	0			
3	4	1			

confirm the realization with a simultaneous press on the key Ctrl-Shift-Enter.

6. The function offers us the wanted result.

INPUT DATA		RESULT
OutLinesW		outPointsW
0	1	0
0	2	1
1	4	2
2	3	3
3	4	4

CONCLUSIONS

Presented UDF, which we need for the realization of volume calculation with the use of "NTF" method in MS Excel program, make our work easier. It is important to point out that when there is no definition of down surface it is possible, with the help of UDF (*"linesSortedW3", "outLineW", "outPointsW"*) to pick out Points with which we determine surface which we adopt as down surface. By doing this we must pay attention to the given selection of outpoints and checks the given selection by drawing them in some program for designing. In this way we will check whether we got the actual shape of the outline surface. Visually presented example of the use of UDF is available on the web site: http:/www.geo.ntf.uni-lj.si/mvulic. The example of how we can carry out volume calculation on a practical example with the use of UDF for the volume calculation with the "NTF" method will be given in the next article.

Povzetki

Lastne Excel funkcije za izračun prostornin po "NTF" metodi

Predstavljene Lastne Excelove funkcije (UDF), ki jih potrebujemo za izračun prostornin po "NTF" metodi močno olajšajo naše delo. Pomembno je izpostaviti prednost pri izračunu prostornin teles brez omejitve spodnje ploskve. V takih slučajih je možno z uporabo UDF (*"linesSortedW3", "outLineW", "outPointsW"*) definirati točke, ki določajo spodnjo omejitveno ploskev. Pri tej operaciji moramo točke predhodno določiti in preveriti s CAD programom. Na ta način lahko enostavno preverimo obliko omejitvene ploskve. Vizualizacija primera z uporabo UDF je dostopna na internetnem naslovu: http:/www.geo.ntf.uni-lj.si/mvulic. Prezentacija izračuna prostornine na praktičnem primeru pa bo predstavljena v naslednjem članku.

References

[1] Vulić, M. (2005): *User Defined Function*. Naravoslovnotehniška fakulteta, Ljubljana, 2005.

[2] Vulić, M. (2005): *Matematične osnove določanja prostornin tristranih prizem* (interna predavanja). Naravoslovnotehniška fakulteta, Ljubljana, 2005.

[3] Vulić, M. (2005): *Osnove Delaunay-eve triangulacije in Voronoi diagramov* (interna predavanja). Naravoslovnotehniška fakulteta, Ljubljana, 2005.

[4] Vulić, M., Durgutović, A. (2006): Calculation of volume with the use of "NTF" method. *RMZ - Materials and Geoenvironment.*; Vol. 53, No. 2, pp. 221-228.

Author`s Index

INSTRUCTIONS TO AUTHORS

RMZ-MATERIALS & GEOENVIRONMENT (RMZ- Materiali in geookolje) is a periodical publication with four issues per year (established 1952 and renamed to RMZ-M&G in 1998). The main topics of contents are Mining and Geotechnology, Metallurgy and Materials, Geology and Geoenvironment.
RMZ-M&G publishes original Scientific articles, Review papers, Technical and Expert contributions (also as short papers or letters) **in English**. In addition, evaluations of other publications (books, monographs,...), short letters and comments are welcome. A short summary of the contents in Slovene will be included at the end of each paper. It can be included by the author(s) or will be provided by the referee or the Editorial Office.
**** Additional information and remarks for Slovenian authors:***
English version with extended »Povzetek«, and additional roles (in Template for Slovenian authors) ***can*** *be written. Only exceptionally the articles in the Slovenian language with summary in English will be published. The contributions in English will be considered with priority over those in the Slovenian language in the review process.*

Authorship and originality of the contributions. Authors are responsible for originality of presented data, ideas and conclusions as well as for correct citation of data adopted from other sources. The publication in RMZ-M&G obligate authors that the article will not be published anywhere else in the same form.

Specification of Contributions

Optimal number of pages of full papers is 7 to 15, longer articles should be discussed with Editor, but 20 pages is limit.
Scientific papers represent unpublished results of original research.
Review papers summarize previously published scientific, research and/or expertise articles on the new scientific level and can contain also other cited sources, which are not mainly result of author(s).
Technical and Expert papers are the result of technological research achievements, application research results and information about achievements in practice and industry.
Short papers (Letters) are the contributions that contain mostly very new short reports of advanced investigation. They should be approximately 2 pages long but should not exceed 4 pages.
Evaluations or critics contain author's opinion on new published books, monographs,

textbooks, exhibitions...(up to 2 pages, figure of cover page is expected).
In memoriam (up to 2 pages, a photo is expected).
Professional remarks (Comments) cannot exceed 1 page, and only professional disagreements can be discussed. Normally the source author(s) reply the remarks in the same issue.

Supervision and review of manuscripts. All manuscripts will be supervised. The referees evaluate manuscripts and can ask authors to change particular segments, and propose to the Editor the acceptability of submitted articles. Authors can suggest the referee but Editor has a right to choose another. **The name of the referee remains anonymous.** The technical corrections will be done too and authors can be asked to correct missing items. The final decision whether the manuscript will be published is made by the Editor in Chief.

The Form of the Manuscript

The manuscript should be submitted as a complete hard copy including figures and tables. The figures should also be enclosed separately, both charts and photos in the original version. In addition, all material should also be provided in electronic form on a diskette or a CD. The necessary information can conveniently also be delivered by E-mail.

Composition of manuscript is defined in the attached Template

The original file of Template is temporarily available on E-mail addresses:
peter.fajfar@ntf.uni-lj.si,
barbara.bohar@ntfgeo.uni-lj.si

References - can be arranged in two ways:
- first possibility: alphabetic arrangement of first authors - in text: (Borgne, 1955),
or
- second possibility: [1] numerated in the same order as cited in the text: example[1]

Format of papers in journals:

Le Borgne, E. (1955): Susceptibilite magnetic anomale du sol superficiel. *Annales de Geophysique*, 11, pp. 399-419.

Format of books:

Roberts, J. L. (1989): Geological structures, *MacMillan*, *London*, 250 p.

Text on the hard print copy can be prepared with any text-processor. The electronic version on the diskette, CD or E-mail transfer should be in MS Word or ASCII format.
Captions of figures and tables should be enclosed separately. **Figures (graphs and photos)** and tables should be original and sent separately in addition to text. They can be prepared on paper or computer designed (MSExcel, Corel, Acad).
Format. Electronic figures are recommended to be in CDR, Al, EPS, TIF or JPG formats. Resolution of bitmap graphics (TIF, JPG) should be at least 300 dpi. Text in vector graphics (CDR, Al, EPS) must be in MSWord Times typography or converted in curves.
Color prints. Authors will be charged for color prints of figures and photos.
Labeling of the additionally provided material for the manuscript should be very clear and must contain at least the lead author's name, address, the beginning of the title and the date of delivery of the manuscript. In case of an E-mail transfer the exact message with above asked data must accompany the attachment with the file containing the manuscript.
Information about RMZ-M&G:
Editor in Chief prof. dr. Peter Fajfar (tel. ++386 1 4250-316) or
Secretary Barbara Bohar Bobnar, un. dipl. ing. geol. (++386 1 4704-630),
Aškerčeva 12, Ljubljana, Slovenia

or at E-mail addresses:
peter.fajfar@ntf.uni-lj.si,
barbara.bohar@ntfgeo.uni-lj.si

Sending of manuscripts. Manuscripts can be sent by mail to the **Editorial Office** address:

- RMZ-Materials & Geoenvironment
  Aškerčeva 12,
  1000 Ljubljana, Slovenia

or delivered to:

- **Reception** of the Faculty of Natural Science and Engineering (for RMZ-M&G)
  Aškerčeva 12,
  1000 Ljubljana, Slovenia
- E-mail - addresses of Editor and Secretary
- You can also contact them on their phone numbers.

TEMPLATE

The title of the manuscript should be written in bold letters (Times New Roman, 14, Center)

Name Surname[1], …. , & Name Surname[X]
(Times New Roman, 12, Center)

[x]Faculty of ... , University of ... , Address…, Country, e-mail: ...
(Times New Roman, 11, Center)

THE LENGTH OF FULL PAPER SHOULD NOT EXCEED TWENTY (20, INCLUDING FIGURES AND TABLES) PAGES (OPTIMAL 7 TO 15), SHORT PAPER FOUR (4) AND OTHER TWO (2) WITHOUT TEXT FLOWING BY GRAPHICS AND TABLES.

Abstract (Times New Roman, Normal, 11): The text of the abstract is placed here. The abstract should be concise and should present the aim of the work, essential results and conclusion. It should be typed in font size 11, single-spaced. Except for the first line, the text should be indented from the left margin by 10 mm. The length should not exceed fifteen (15) lines (10 are recommended).

Key words: a list of up to 5 key words (3 to 5) that will be useful for indexing or searching. Use the same styling as for abstract.

Introduction (Times New Roman, Bold, 12)

Two lines below the keywords begin the introduction. Use Times New Roman, font size 12, Justify alignment.
There are two (2) admissible methods of citing references in text:

1. by stating the first author and the year of publication of the reference in the parenthesis at the appropriate place in the text and arranging the reference list in the alphabetic order of first authors; e.g.:
   "Detailed information about geohistorical development of this zone can be found in: Antonijević (1957), Grubić (1962), ..."
   "… the method was described previously (Hoefs, 1996)"

2. by consecutive Arabic numerals in square brackets, superscripted at the appropriate place in the text and arranging the reference list at the end of the text in the like manner; e.g.:
"... while the portal was made in Zope[3] environment."

Materials and methods (Times New Roman, Bold, 12)

This section describes the available data and procedure of work and therefore provides enough information to allow the interpretation of the results, obtained by the used methods.

Results and discussion (Times New Roman, Bold, 12)

Tables, figures, pictures, and schemes should be incorporated in the text at the appropriate place and should fit on one page. Break larger schemes and tables into smaller parts to prevent extending over more than one page.

Conclusions (Times New Roman, Bold, 12)

This paragraph summarizes the results and draws conclusions.

Acknowledgements (Times New Roman, Bold, 12, Center - optional)

This work was supported by the ****.

References (Times New Roman, Bold, 12*)*

In regard to the method used in the text, the styling, punctuation and capitalization should conform to the following:

FIRST OPTION - in alphabetical order

Casati, P., Jadoul, F., Nicora, A., Marinelli, M., Fantini-Sestini, N. & Fois, E. (1981): Geologia della Valle del'Anisici e dei gruppi M. Popera - Tre

Cime di Lavaredo (Dolomiti Orientali). *Riv. Ital. Paleont.*; Vol. 87, No. 3, pp. 391-400, Milano.

Folk, R. L. (1959): Practical petrographic classification of limestones. *Amer. Ass. Petrol. Geol. Bull.;* Vol. 43, No. 1, pp. 1-38, Tulsa.

SECOND OPTION - in numerical order

[1] Trček, B. (2001): *Solute transport monitoring in the unsaturated zone of the karst aquifer by natural tracers.* Ph.D. Thesis. Ljubljana: University of Ljubljana 2001; 125 p.

[2] Higashitani, K., Iseri, H., Okuhara, K., Hatade, S. (1995): Magnetic Effects on Zeta Potential and Diffusivity of Nonmagnetic Particles. *Journal of Colloid and Interface Science 172*, pp. 383-388.

Citing the Internet site:

CASREACT-Chemical reactions database [online]. Chemical Abstracts Service, 2000, updated 2.2.2000 [cited 3.2.2000]. Accessible on Internet: http://www.cas.org/CASFILES/casreact.html.

Povzetek (Times New Roman, 12)

A short summary of the contents in Slovene (up to 400 characters) can be written by the author(s) or will be provided by the referee or by the Editorial Board.

TEMPLATE for Slovenian Authors

The title of the manuscript should be written in bold letters (Times New Roman, 14, Center)

Naslov članka (Times New Roman, 14, Center)

NAME SURNAME[1],…. , & NAME SURNAME[X] (TIMES NEW ROMAN, 12, CENTER)
IME PRIIMEK[1], …, IME PRIIMEK[X] (TIMES NEW ROMAN, 12, CENTER)

[X]Faculty of ... , University of ... , Address…, Country; e-mail: ...
(Times New Roman, 11, Center)
[X]Fakulteta…, Univerza…, Naslov…, Država; e-mail: …
(Times New Roman, 11, Center)

THE LENGTH OF ORIGINAL SCIENTIFIC PAPER SHOULD NOT EXCEED TWENTY (20, INCLUDING FIGURES AND TABLES) PAGES (OPTIMAL 7 TO 15), SHORT PAPER FOUR (4) AND OTHER TWO (2) WITHOUT TEXT FLOWING BY GRAPHICS AND TABLES.
DOLŽINA IZVIRNEGA ZNANSTVENEGA ČLANKA NE SME PRESEGATI DVAJSET (20, VKLJUČNO S SLIKAMI IN TABELAMI), KRATKEGA ČLANKA ŠTIRI (4) IN OSTALIH PRISPEVKOV DVE (2) STRANI.

Abstract (Times New Roman, Normal, 11): The text of the abstract is placed here. The abstract should be concise and should present the aim of the work, essential results and conclusion. It should be typed in font size 11, single-spaced. Except for the first line, the text should be indented from the left margin by 10 mm. The length should not exceed fifteen (15) lines (10 are recommended).

Izvleček (TNR, N, 11): Kratek izvleček namena članka ter ključnih rezultatov in ugotovitev. Razen prve vrstice naj bo tekst zamaknjen z levega roba za 10 mm. Dolžina naj ne presega petnajst (15) vrstic (10 je priporočeno).

Key words: a list of up to 5 key words (3 to 5) that will be useful for indexing or searching. Use the same styling as for abstract.

Ključne besede: seznam največ 5 ključnih besed (3-5) za pomoč pri indeksiranju ali iskanju. Uporabite enako obliko kot za izvleček.

Introduction – Uvod (Times New Roman, Bold, 12)

Two lines below the keywords begin the introduction. Use Times New Roman, font size 12, Justify alignment. All captions of text and tables as well as the text in graphics must be prepared in English and Slovenian language.
Dve vrstici pod ključnimi besedami se začne Uvod. Uporabite pisavo TNR, velikost črk 12, z obojestransko poravnavo. Naslovi slik in tabel (vključno z besedilom v slikah) morajo biti pripravljeni v slovenskem in angleškem jeziku.

Figure (Table) X. Text belonging to figure (table)
Slika (Tabela) X. Pripadajoče besedilo k sliki (tabeli)

There are two (2) admissible methods of citing references – obstajata dve sprejemljivi metodi navajanja referenc:

1. by stating the first author and the year of publication of the reference in the parenthesis at the appropriate place in the text and arranging the reference list in the alphabetic order of first authors; e.g.:
1. z navedbo prvega avtorja in letnice objave reference v oklepaju na ustreznem mestu v tekstu in z ureditvijo seznama referenc po abecednem zaporedju prvih avtorjev; npr.:
   "Detailed information about geohistorical development of this zone can be found in: Antonijević (1957), Grubić (1962), ..."
   "… the method was described previously (Hoefs, 1996)"

or/ali

2. by consecutive Arabic numerals in square brackets, superscripted at the appropriate place in the text and arranging the reference list at the end of the text in the like manner; e.g.:
2. z zaporednimi arabskimi številkami v oglatih oklepajih na ustreznem mestu v tekstu in z ureditvijo seznama referenc v številčnem zaporedju navajanja; npr.;
   "... while the portal was made in Zope[3] environment."

Materials and methods (Times New Roman, Bold, 12)

This section describes the available data and procedure of work and therefore provides enough information to allow the interpretation of the results, obtained by the used methods.
Ta del opisuje razpoložljive podatke, metode in način dela ter omogoča zadostno količino informacij, da lahko z opisanimi metodami delo ponovimo.

Results and discussion – Rezultati in razprava (Times New Roman, Bold, 12)

Tables, figures, pictures, and schemes should be incorporated (inserted, not pasted) in the text at the appropriate place and should fit on one page. Break larger schemes and tables into smaller parts to prevent extending over more than one page.
Tabele, sheme in slike je potrebno vnesti (z ukazom Insert, ne Paste) v tekst na ustreznem mestu. Večje sheme in tabele je potrebno ločiti na manjše dele, da ne presegajo ene strani.

Conclusions – Sklepi (Times New Roman, Bold, 12)

This paragraph summarizes the results and draws conclusions.
Povzetek rezultatov in zaključki.

Acknowledgements – Zahvale (Times New Roman, Bold, 12, Center - optional)

This work was supported by the ………..
Izvedbo tega dela je omogočilo ………

References - Viri (Times New Roman, Bold, 12)

With regard to the method used in the text, the styling, punctuation and capitalization should conform to the following:

Glede na uporabljeno metodo citiranja referenc v tekstu upoštevajte eno od naslednjih oblik:

FIRST OPTION (recommended) – PRVA MOŽNOST (priporočena) – in alphabetical order (v abecednem zaporedju)

Casati, P., Jadoul, F., Nicora, A., Marinelli, M., Fantini-Sestini, N. & Fois, E. (1981): Geologia della Valle del'Anisici e dei gruppi M. Popera – Tre Cime di Lavaredo (Dolomiti Orientali). *Riv. Ital. Paleont.*; Vol. 87, No. 3, pp. 391-400, Milano.

Folk, R. L. (1959): Practical petrographic classification of limestones. *Amer. Ass. Petrol. Geol. Bull.;* Vol. 43, No. 1, pp. 1-38, Tulsa.

SECOND OPTION – DRUGA MOŽNOST - in numerical order (v numeričnem zaporedju)

[1] Trček, B. (2001): *Solute transport monitoring in the unsaturated zone of the karst aquifer by natural tracers.* Ph.D. Thesis. Ljubljana: University of Ljubljana 2001; 125 p.

[2] Higashitani, K., Iseri, H., Okuhara, K., Hatade, S. (1995): Magnetic Effects on Zeta Potential and Diffusivity of Nonmagnetic Particles. *Journal of Colloid and Interface Science 172*, pp. 383-388.

Citing the Internet site:

CASREACT-Chemical reactions database [online]. Chemical Abstracts Service, 2000, updated 2.2.2000 [cited 3.2.2000]. Accessible on Internet: http://www.cas.org/CASFILES/casreact.html.

Citiranje Internetne strani:

CASREACT-Chemical reactions database [online]. Chemical Abstracts Service, 2000, obnovljeno 2.2.2000 [citirano 3.2.2000]. Dostopno na svetovnem spletu: http://www.cas.org/CASFILES/casreact.html.

Povzetek – Summary (Times New Roman, 12)

An extended summary of the contents in Slovene (from one page to approximately $1/3$ of the original article length).

Razširjeni povzetek vsebine prispevka v Angleščini (od ene strani do približno $1/3$ dolžine izvirnega članka).

No. of indexing of RMZ-M&G in singular Databases (Število indeksiranih člankov iz RMZ-M&G v posameznih bazah)

(prepared by Fajfar, P. – from search done by Šercelj, M., CTK Ljubljana, 15.2.2007)

	DATABASE NAME	HITS
1:	Civil Engineering Abstracts	773
2:	CA SEARCH® - Chemical Abstracts® (1967- present)	760
3:	Inside Conferences	313
4:	Materials Business File	253
5:	METADEX®	164
6:	ANTE: Abstracts in New Technologies and Engineering	158
7:	GeoRef	154
8:	Aluminium Industry Abstracts	36
9:	PASCAL	30
10:	Energy Science and Technology	27
11:	TEME - Technology and Management	27
12:	Ei Compendex®	13
13:	CSA Aerospace & High Technology Database	12
14:	Computer and Information Systems	10
15:	Mechanical & Transportation Engineering Abstracts	8
16:	Engineered Materials Abstracts®	3
17:	Corrosion Abstracts	3
18:	Analytical Abstracts	1
19:	FLUIDEX	1
20:	Solid State and Superconductivity Abstracts	1
21:	Electronics and Communications Abstracts	1
		2748


ŠTORE STEEL
155 let
železarska c. 3 3220 štore slovenija
www.store-steel.si